JOURNAL

OF THE PENNSYLVANIA ACADEMY OF SCIENCE

Founded on April 18, 1924

ISSN: 1044-6753

December 2012
Volume 86

Jane E. Huffman, PhD, MPH
Editor
Department of Biological Sciences
East Stroudsburg University
East Stroudsburg, PA 18301

PAS Home Page: http://pennsci.org

Contents

Jane E. Huffman, Editor*
Department of Biological Sciences
East Stroudsburg University, East Stroudsburg, PA 18301
Phone: 570-422-7891
FAX: 570-422-3724
E-Mail: jhuffman@esu.edu

EDITORIAL COMMITTEE MEMBERS*

*Term expires in April 2014

Journal of the Pennsylvania Academy of Science 86(1): 3-4, 2012

COMMENTARY:
THE MARINE SCIENCE CONSORTIUM…HANDS-ON, FEET-WET EDUCATION

THOMAS TAUER

Assistant Provost, East Stroudsburg University, East Stroudsburg, PA 18301

Figure 1. ESU students presenting a poster on CubeSat Development at the 25th Small Satellite Conference at Logan City, Utah students presenting a poster on CubeSat Development at the 25th Small Satellite Conference at Logan City, Utah.

Founded in 1968 by schools in the Pennsylvania State System of Higher Education, The Marine Science Consortium (MSC) is a residential environmental learning center and field station located on the Eastern Shore of Virginia. The Chesapeake Bay and Atlantic Ocean surround this narrow Eastern Shore of Virginia peninsula creating a varied quilt of marshes, tidal creeks, bays, maritime forest, and other coastal and undeveloped barrier island ecosystems. The Eastern Shore is an area of converging species and habitats, where we find organisms at their northern and southern limits, yielding high species diversity. This natural history, combined with the long human history, and unique regional culture makes the Eastern Shore a treasure for educators and scientists.

Throughout its 44 year history, the MSC has realized its mission of providing outstanding multi-disciplinary, educational, and research opportunities that celebrate the rich natural, cultural, economic, and technological resources of the mid-Atlantic Coastal region. This has been accomplished in part via field-based and hands-on learning through its excellent university courses, school field experiences, and adult workshops. The MSC's strength is enhanced by its relationships with leading scientists, as well as, active partnerships and research collaborations with the National Aeronautics and Space Administration (NASA), National Park Service (NPS), National Oceanic and Atmospheric Administration (NOAA), The Nature Conservancy (TNC), and the U.S. Fish and Wildlife Service (FWS).

MSC maintains two campuses. The main campus is located at Wallops Island, VA and is adjacent to the NASA Goddard Space Flight Center Wallops Flight Facility (GSFC WFF) with a second satellite research center located directly on Chincoteague Bay. The main campus offers laboratory and classroom space, dormitory-style student housing, faculty and staff apartments, and complete food services. Research vessels range from 22 foot Boston Whalers and 40 foot monitor barges, to the 47 foot diesel-powered R.V. Phillip N. Parker used for open ocean research cruises. buses and 15 passenger vans are also utilized for transportation around the Eastern Shore. The MSC's staff includes program coordinators and knowledgeable instructors who work collaboratively with faculty from MSC member universities to create truly exceptional educational experiences.

Recently, a $15 million campus revitalization project has provided new accommodations, a Silver LEED Certified education center containing labs, classrooms, meeting spaces, and enhanced services. Strengthening relationships with NASA GSFC WFF and the Chincoteague National Wildlife Refuge (within the FWS) have lead to numerous research collaborations involving faculty and students (partial list provided below) and offer potential for many more collaborative projects. A recent partnership between NASA, FWS, and MSC created a Coastal Zone Research Area that opens the door for a plethora

Figure 2. Anne Armstrong (MSC Program Manager) and Nathan Wright (student) and Jeffrey Sumey (faculty) of California University of Pennsylvania stand near MSC's Silver LEED Certified education center holding kites used during inexpensive tethered aerial data gathering platform testing.

Figure 3. Shippensburg University of Pennsylvania student, Eric McGilliard, holds a reflector rod during a beach survey. A portion of the NASA GSFC WFF launch facilities on Wallops Island, VA are captured in the background.

of multidisciplinary education and collaborative research opportunities ranging from traditional marine science to engineering, cultural history, climate research, art, geophysical studies, and more. Examples of faculty/student research collaborations include:

- Assessing Coastal Environmental Change: Monitoring Storm Response, Sea-Level Rise, and Biodiversity at Wallops Island, Virginia
  - o Dr. Adrienne Oakley, Department of Physical Sciences, Kutztown University of Pennsylvania
  - o Dr. Sean Cornell, Department of Geography-Earth Science, Shippensburg University of Pennsylvania
- Coastal Barrier Island Herpetofauna
  - o Dr. Pablo Delis, Department of Biology, Shippensburg University of Pennsylvania
  - o Dr. Walter Meshaka, The State Museum of Pennsylvania
- Cosmic Ray Detection
  - o Dr. John Elwood, Department of Physics, East Stroudsburg University of Pennsylvania
- CubeSat Development
  - o Dr. Haklin Kimm, Department of Computer Science, East Stroudsburg University of Pennsylvania
- Dwarfism in Barrier Island Fowler's Toads
  - o Dr. John Hranitz, Department of Biological and Allied Health Sciences, Bloomsburg University of Pennsylvania
- Inexpensive Tethered Aerial Data Gathering Platform
  - o Mr. Jeffrey Sumey, Department of Applied Engineering and Technology, California University of Pennsylvania
- LiDAR Data Processing
  - o Dr. Ajoy Kumar, Department of Earth Sciences, Millersville University of Pennsylvania
  - o Dr. Shixiong Hu, Department of Geography, East Stroudsburg University of Pennsylvania
- Soil Moisture Studies
  - o Dr. John Frye, Department of Geography, Kutztown University of Pennsylvania

For more information regarding the Marine Science Consortium and the phenomenal opportunities for faculty and students, please visit their website at http://msconsortium.org/

ACKNOWLEDGEMENT

Special thanks to Amber Parker, MSC Executive Director, for helping prepare this article.

ABOUT THE AUTHOR

Dr. Thomas Tauer is the Assistant Provost at East Stroudsburg University of Pennsylvania and has been the MSC Liaison to NASA since 2009.

Journal of the Pennsylvania Academy of Science 86(1): 5-11, 2012

IONIC DEPENDENCY OF SKIN POTENTIAL, TRANSPORT CURRENT, AND THEIR RELATIONSHIP IN LEOPARD FROG (*RANA SPP.*) VENTRAL EPITHELIA[1]

PAUL M. NEALEN, PHD[2]

[2]*Department of Biology, Indiana University of Pennsylvania, 114 Weyandt Hall, 975 Oakland Ave. Indiana, PA 15705, USA*

ABSTRACT

Amphibian ventral epithelia can perform significant Na^+ transport, as characterized in the now-classic two-membrane model first demonstrated by Ussing and colleagues. This transport is normally demonstrated by using short-circuit current (Isc) to negate transport-generated potentials across epithelia suspended in Ussing chambers. While this model and method have been supported through decades of experimentation, the exact relationship between the transport current and the epithelial potential generated is often ignored, as potentials typically are treated as a factor to be systematically eliminated. Here, leopard frog (*Rana spp.*) ventral epithelium were utilized in Ussing chambers for tests of specifically how the relationship between epithelial potentials and transport currents depends upon external medium ionic content. Stable skin potentials were recorded using 300 mOsm NaCl; potentials were then reduced to 0 mV via Isc in order to estimate the magnitude of the ionic transport current. A subset of the epithelia prepared was then tested in one or more alternative ionic solutions (300 mOsm KCl, $NaHCO_3$, and $CaCl_2$). While identifiable skin potentials were detected in all solutions tested, only in NaCl were the magnitudes of the epithelial potential and short-circuit current statistically significantly related. Detectable skin potentials in non-Na^+-containing solutions indicates the existence of non-Na^+ electrogenic activity in this tissue, whose presence explains the relatively poor ability of transport current magnitudes to explain the magnitudes of observed skin potential. Estimates of molecular transport rates for Na^+ exceed 4 x 10^{14} molec sec^{-1} cm^{-1}, demonstrating the enormous osmoregulatory challenge faced by fresh water amphibians in maintaining ionic homeostasis. [J PA Acad Sci 86(1): 5-11 , 2012]

[1]Submitted for publication January 2012; accepted August 2012.

INTRODUCTION

In any habitat, the specific osmoregulatory problems faced by the organisms within it are functions of the ionic gradients which exist between animal tissues and the external medium as well as the mechanisms of ion gain and loss, including both passive and active forms of uptake and excretion. Osmoregulation is a significant regulatory problem faced by freshwater amphibians, principally due to the efflux (loss) of ions across their external epithelia. In order to function as respiratory exchange surfaces, these epithelia must necessarily be of large surface area, thin, well perfused, and moist, all of which decrease their effectiveness as buffers against environmental ionic flux. In particular, losses of sodium (Na^+) and chloride (Cl^-) ions pose significant regulatory challenges for these organisms. Active recovery of ions from the external medium may consume a substantial portion of an organism's energy budget, given that the costs of active transport have been identified in a variety of tissues to be non-negligible (Al-Bazzaz and Zevin 1984, Edwards et al. 1989, Essig et al. 1978, Labarca et al. 1977, Morgan and Iwama 1999, Welsh 1984).

As a consequence of its role in ion regulation, isolated frog epithelium has long been used as an experimental model for study of the active transport of ions, stemming from the pioneering experiments of Ussing and colleagues (Koefoed-Johnsen and Ussing 1958, Ussing 1949, Ussing and Zerahn 1951). These experiments and much of the work that has followed them focused primarily upon Na^+ transport, leading to the development of the "double membrane" (KJU) model which explains the relationship between Na^+ recovery by passive transport in the epithelial apical membrane followed by active transport of Na^+ (and concomitant K^+ recycling) at the basolateral membrane (reviewed in Reuss 2001). Related experiments have demonstrated the existence and importance of a variety of physiological regulators of this Na^+ uptake process, including dependence upon pH (Palmer 2001) and perfusion (Talbot 2002), and a large body of evidence has been gathered to illustrate the modulatory influences of hormones (Aceves 1977, Uchiyama and Konno 2006, Yamada et al. 2008) and other chemicals (Baba and Smith 1964, Civan et al. 1987, Kelepouris et al. 1985, Nielsen and Larsen 2007, Rabito et al. 1978, Sariban-Sohraby and Benos 1986, Zeiske and Lindemann 1974) on this transport

current, which is largely dependent upon a passive, amiloride-sensitive Na^+ channel at the frog epithelium apical membrane (Cereijido et al. 1974, Rabito et al. 1978, Salako and Smith 1970, Sariban-Sohraby and Benos 1986).

While dissection of transport mechanisms at the molecular and cellular level have proven quite fruitful in this system, study of the global properties of the epithelial tissues involved remain useful, in particular for their ability to provide tests of models of cellular function. Described herein are experiments designed to evaluate the type and magnitude of transport occurring in frog epithelial tissues, specifically with regard to the relationship between transport-generated skin potential magnitudes and the magnitudes of current associated with them, and the degree to which this relationship is influenced by the ionic content of the external media. Data collected from these experiments are also used to estimate the magnitude of the ionic flux conducted in this epithelium.

These experiments, in agreement with prior results, implicate Na^+ as the primary ion of transport in these epithelia. Epithelial transport-generated potentials and associated currents are non-zero in all of the solutions tested, but are of greatest magnitude in Na^+-containing solutions. However, the ability of current magnitudes to explain variation in transport-generated epithelial potentials is generally poor, reaching statistical significance only when measured using NaCl as the external medium. This non-uniformity suggests the existence of other, non-Na^+ associated activity in this tissue. Individual variation in ionic homeostatic condition and epithelial function is considerable, in that the epithelial potentials generated in the various test solutions differed broadly among individuals.

METHODS

Ethical approval

The experiments described here were conducted in accord with the then-current policies of the Indiana University of Pennsylvania regarding animal experimentation.

Study animals

The study subjects were "grass frogs" (n = 48) obtained from Carolina Biological Supply Co. (Burlington, NC), which in practice were North American leopard frogs of the *Rana spp.* complex, including individuals of both *R. pipiens* and *R. sphenocephala utricularia*. Study individuals were unsexed, and varied in size from 7 – 15 cm (SV length). Individuals were maintained en masse in a large indoor terrarium, under conditions of ambient air temperature (15 – 25 °C) with a constant supply of fresh water input to and outflow from the terrarium.

Epithelial tissue preparation

Animals were doubly pithed, after which the ventral epithelium was removed using dissecting scissors. Efforts were made to remove as much of the epithelium as possible, typically resulting in tissue samples 6-12 cm^2 in area. The epithelial samples were then separated from attached connective tissues using forceps.

Ussing chambers and amplification equipment

Epithelial were then suspended between the two halves of custom-designed (A.C. Browe and D. Ramsey) Ussing chambers. Each half of the chambers could accommodate 85 ml of fluid; the fluid within each of the chamber halves was accessible to the epithelial tissue via a circular port 1.5 cm^2 in area. The Ussing chambers were outfitted with custom-designed Ag-AgCl electrodes (silver wire electroplated in NaCl solution to near-zero resistance [mean: 0.42 Ω; range: 0.3 – 0.8 Ω; n = 15]). Electrode leads were connected to oscilloscope inputs (BK Precision, Yorba Linda, CA). Analog oscilloscope output was routed into a PowerLab interface (AD Instruments, Colorado Springs, CO) and visualized via Scope software (AD Instruments) on personal computers. The Scope software was calibrated to a 200 mV test signal incorporated into the oscilloscopes, and was used to measure the magnitude of the electrical potential which existed between electrodes.

Assessment and removal of electrode asymmetry

Because assessment of the ion flow associated with ionic active transport in these tissues requires significant amplification of relatively small signals, it was necessary to first evaluate, and then eliminate, impedance differences between the recording electrodes (which could have contributed to assessed potential differences across the Ussing chambers). To do so, the Ussing chambers (with epithelia in place) were filled with a solution of 300 mOsm NaCl, and the recording electrodes then both placed into the same side of the Ussing chamber. The amplified electrical potential which existed between the electrodes (typically 5 – 15 mV) was then measured via the Scope software, and then eliminated by software removal of "background", to set the potential difference between the electrodes to 0 mV.

Measurements of epithelial skin potential generated by active transport

Having compensated for any potential differences between recording electrodes, measurements of the skin potential generated by active transport across the frog ventral epithelium were now made by locating one electrode on each side of the epithelium, and then measuring via the Scope software the amplified potential (in mV) which existed across the epithelium.

Cancellation of skin potential via short-circuit-current (Isc)

Once a stable skin potential was recorded, a second pair of electrodes were placed into the opposite halves of the Ussing chamber, and connected to a custom (A.C. Browe and T.C. Kirkpatrick) DC current source, adjustable between 0 and 200 μA. Counter-current was applied in order to reduce the observed skin potential to 0 mV, at which time the magnitude of the current delivered was recorded as an indirect estimate of the magnitude of the transport current taking place across the epithelium (Clarke 2009).

Tests of alternate ionic media

In some experiments, the short-circuit current and the original Ringer's solution were then removed from the Ussing chamber, and then chamber then refilled with one or more alternative ionic solutions [300 mOsm KCl (n = 24), 300 mOsm $CaCl_2$ (n = 9), or 300 mOsm $NaHCO_3$ (n = 15)]. For each alternative solution tested, measures of the stable skin potential in the absence of opposing current were again made, followed again by application of counter-current to again estimate the magnitude of the active transport current. For all media tested, data from epithelia whose skin potential could not be measured or negated via counter-current were excluded.

Pharmacological manipulations

To ensure that this experimental preparation retained functional metabolic and transport mechanisms, several epithelia were pharmacologically treated. Stable skin potentials were first measured in 300 mOsm NaCl, and then skin potentials were measured after stabilization following the addition of 2,4-dinotophenol (DNP; n = 3) or vasopressin (n = 3). DNP is a potent proton ionophore which eliminates chemiosmotic production of ATP (Martens 1985, McDonald and MacLeod 1972) and was predicted to dramatically reduce or eliminate transport-generated skin potentials. In contrast, vasopressin is known to enhance the activity of the human kidney Na^+-K^+-2Cl—cotransporter, and was predicted here to stimulate Na^+ transport and transport-generated potentials via its general mechanism of enhancing membrane permeability to Na^+ (Grider et al. 1996, Kudo et al. 1990, Ponec et al. 1989).

Calculations of ion transport magnitude

For each of the solutions tested, the mean magnitude of the short-circuit current (Isc) was determined. Assuming a singular relationship between transport potential and Isc magnitude, it was then possible to calculate a stoichiometric estimate of ion transport magnitude (molec sec^{-1} cm^{-1}) by the epithelia in a given solution, as follows:

$$\text{Transport (molec sec}^{-1}\text{ cm}^{-1}) = (I * N) / (F * A)$$

Where I = mean magnitude of short-circuit current which reduced epithelial potential to 0 mV
N = Avogadro's number (6.023×10^{23})
F = Faraday's constant (9.55×10^4 coulombs mol^{-1})
A = surface area of exposed epithelium (1.5 cm^2)

Statistical comparisons were performed via 1-way ANOVA across group data; relationships among variables were assessed using Pearson's r correlation metric and linear regression (Microsoft Excel, Microsoft Corp, Redmond, WA).

RESULTS

Grass frog ventral epithelium exhibited robust ionic transport as measured in vitro using Ussing chambers. In all test solutions applied, measured skin potentials due to ionic current generally exceeded 10 mV; skin potentials in Na^+ ionic solutions often exceeded 100 mV (Figure 1a). On average, recorded skin potentials were highest in NaCl (84.14 mV, n = 48) and lowest in KCl (19.55 mV; n = 24; Table 1).

Recorded skin potentials due to ionic transport varied significantly across the solutions tested, despite their similar ionic concentrations ($F_{3,92}$, = 7.63, $p < 0.001$). Similar mean values for skin potentials and currents achieved in NaCl and $NaHCO_3$ solutions (Table 1) suggest that these methods at least partially isolated the Na^+ transport current and identified it to be the primary ion of transport. The relatively lower skin potential and current values achieved in KCl and $CaCl_2$ solutions (Table 1) suggest Cl^- to be transported at significantly lower rates over this epithelium.

While Na^+-containing solutions evoked significantly greater skin potentials than did non-Na^+ solutions, the amount of short-circuit current required to negate ionic transport currents did not systematically vary among the solutions tested ($F_{3,92}$, F = 0.25, NS; Figure 1b), in part due to the fact that the relationship between skin potential and the currents which create it is neither singular nor uniform

Table 1. Ionic transport occurring across frog ventral epithelium as a function of external medium.

Solution[1]	n	Skin potential (mV)		Current (μA)		Ionic transport[2]
		Mean	Range	Mean	Range	(molec/sec/ cm^2)
NaCl	48	84.14	3.60 - 345.72	60.81	1.17 - 260.00	$4.24 * 10^{14}$
KCl	24	19.55	1.44 - 78.23	56.21	1.00 - 245.00	--
NaHCO3	15	71.36	2.96 - 212.51	60.04	5.50 - 245.00	--
CaCl2	9	26.18	3.28 - 92.15	41.93	2.40 - 120.00	–

[1]All solutions tested at 300 mOsm. All epithelia were initially tested in NaCl; a subset of these epithelia was then tested in one or more of the alternative solutions.
[2]Only computed for NaCl, as only for this solution were skin potential and current significantly related (see Results).

(see Discussion). Nonetheless, epithelial transport currents (as estimated by short-circuit current magnitudes) were greatest in Na^+-containing solutions (NaCl and $NaHCO_3$) and lower in non-Na^+ ionic solutions (KCl and $CaCl_2$) (Table 1), consistent with the idea that transport of Na^+ ions constitutes the majority of transport in this epithelium.

The relationship between observed skin potential and the current required to negate it was examined for each of the solutions tested (Figure 2). For each solution examined, the relationship between epithelial skin potential and short-circuit current magnitudes was positive (slopes: 0.50 [NaCl], 0.49 [KCl], 0.24 [$NaHCO_3$], 0.64 [$CaCl_2$]). However, only for NaCl did the skin potential explain a significant amount of the variation observed in short-circuit current magnitude ($r = 0.57$, $p < 0.001$). For all other solutions tested, the relationship between epithelial potential and short-circuit current magnitudes, while positive, was not statistically significant (r values: 0.17 – 0.45, all NS).

Because the relationship between skin potential and current magnitude was significant only for NaCl solution, for only this solution was the mean short-circuit current magnitude used to calculate a stoichiometric estimate of molecular transport rates (see Methods). The mean current magnitude for NaCl (60.81 μA, n = 48) suggests that Na^+ ions are transported in this tissue at rates exceeding 4×10^{14} molec sec^{-1} cm^{-1} (Table 1). Using Ohm's law, mean potential and current measurements in NaCl suggest transepithelial resistance (Rt) to be 1.38×10^3 Ω cm^{-2} with a corresponding conductance (Gt) of 7.22×10^{-4} mS cm^{-2}.

Pharmacological manipulations of the epithelia with either DNP or vasopressin had the predicted effect on transport-generated epithelial potentials, indicating that the methods used herein preserved functional transport and metabolic mechanisms. On average, vasopressin enhanced epithelial potentials in 300 mOsm NaCl by 37.79 mV, while DNP reduced potentials by an average of 78.05 mV. DNP was especially effective in that it reduced observed skin potentials by an average of 92.09%.

DISCUSSION

Ventral epithelia of *Rana spp.* are subject to significant amounts of ion flux, due to the combination of ion losses to the environment and concomitant re-uptake from their external medium. The experiments described herein have demonstrated the existence of a significant skin potential resulting from active ionic recovery, and suggest, in accord with prior studies, the principal ion of transport to be sodium (Na^+). Further, the present experiments demonstrate a significant relationship between the magnitudes of the skin potential and the ionic transport short-circuit current, but only in the presence of NaCl. In the other solutions tested, skin potentials and current magnitudes were significantly non-zero but not significantly correlated, suggesting that skin potential and transport current magnitudes are not singularly related and that transport of other (non-Na^+) ions contributed to both.

The amount of transport conducted over individual epithelia (as indicated by epithelial potential magnitude) differed broadly both within and among the ionic solutions tested (Figure 1a). Study animals were tested at variable times (days to weeks) following their local delivery and introduction to common housing, which may have contributed to this variability. That non-Na^+-associated transport (Figure 1a) occurred in some but not all individuals tested further demonstrates the ability of individual homeostatic condition to weaken population-level assessments of these relationships (Figure 2).

That the relationship between epithelial potential and current magnitudes differs among solutions is of particular interest here. Because electrogenic Na^+ transport is the primary determinant of the epithelial potential, it is expected that the magnitude of current necessary to short-circuit this transport current be directly related to the amount of Na^+ transport which occurs. However, the same relationship did not hold true for $NaHCO_3$; one explanation for this difference could lie in the ability of the dissociated bicarbonate ion to

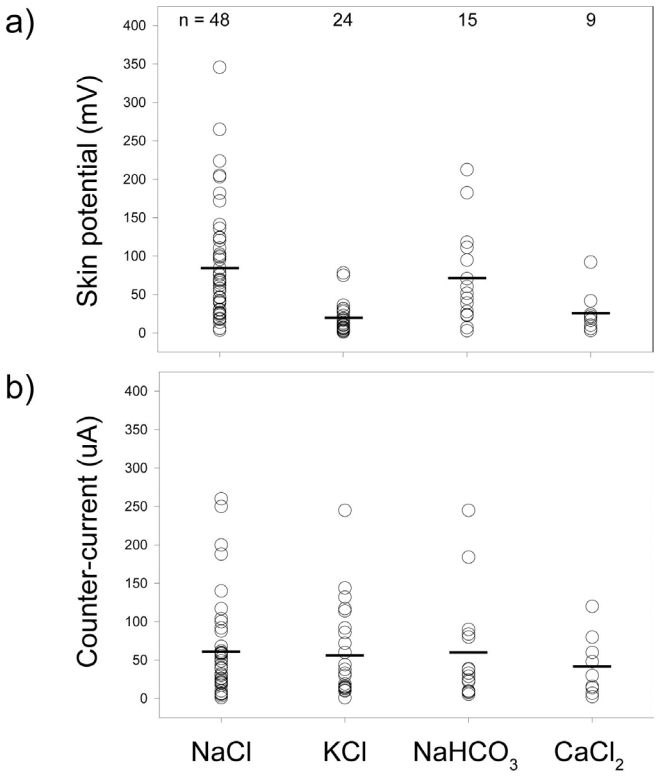

Figure 1. a) Raw data distributions of grass frog ventral epithelium stable skin potentials, as measured via Ussing chamber using the indicated solutions. Skin potentials were robust in all solutions, but differed significantly among solutions (1-way ANOVA, $F_{3,92} = 7.63$, $p < 0.001$). b) Magnitude of the counter-current necessary to reduce observed skin potentials to 0 mV. While current magnitudes exhibited the same general trend as did the skin potentials (relatively high in Na^+-containing solutions, relatively low otherwise), currents did not differ significantly among the solutions tested ($F_{3,92}$, $F = 0.25$, NS). For both panels a) and b), distribution means are indicated by horizontal bars. Sample sizes indicated at Figure top.

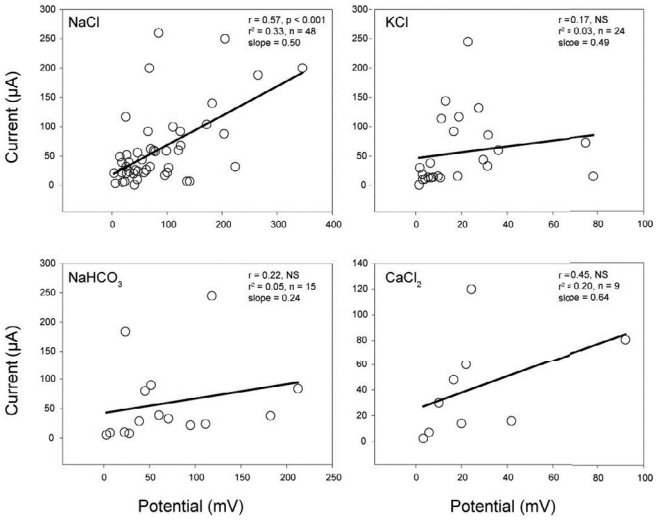

Fig. 2. Relationship between stable skin potential and current magnitude for leopard frog ventral epithelia tested within the four indicated ionic solutions (300 mOsm NaCl, KCl, $NaHCO_3$, and $CaCl_2$). In all solutions, the correlation (Pearson r) between skin potential and current was positive, with slopes ranging from 0.24 to 0.64. However, the amount of variation in current explained by potential (r^2) was significant only for NaCl ($p < 0.001$).

alter solution pH. As expected, the skin potentials generated in both KCl and $CaCl_2$ were modest (Table 1), yet the associated currents were larger than expected.

In theory, application of a counter-current which exactly opposes the epithelial transport current should provide a means of indirectly measuring the exact magnitude of the transport current. In practice, however, several sources of error exist whose effects are difficult to assess. Variability within the study organisms in epithelial capacitance and resistance could de-couple population-level measurements of the potential-current relationship. Further, the lack of capability to assess liquid junction potentials (Clarke 2009) in this simplified experimental preparation suggests that the present measurements of Isc are likely to be overestimates, especially for solutions in which the skin potential amplitude was expected to be minimal (e.g., KCl). Tissue preparations were sufficiently large relative to chamber fluid ports that edge leaks (Clarke 2009, Kottra et al. 1989) should have been minimal.

Potential experimental limitations notwithstanding, two primary conclusions can be drawn from the current study. Firstly, the present experiments confirm Na^+ to be the primary ion of transport across this epithelium, or at least the primary source of electrogenic activity therein, and suggest it to be transported at very high rates. Secondly, tests of this epithelium in solutions other than NaCl reveal the complexity of epithelial transport mechanisms as well as the flexibility with which these organisms can face ionic regulatory challenges. While the relationship between epithelial potential and transport (and thus, short-circuit) currents is theoretically straightforward in this experimental preparation, results from alternative ionic solutions highlight the difficulty in extrapolation from single-cell to whole-tissue models. This is largely due to the diversity of cell types present and routes of ionic passage available (Dorge et al. 1988, Lacaz-Vieira and Procopio 1988, Reuss 2001), which combine to endow these organisms with a broad-spectrum ionic regulatory device, which presumably serves to facilitate their movement within and among local microhabitats (Fellers and Kleeman 2007, Graeter et al. 2008, Regosin et al. 2005, Vos et al. 2007).

ACKNOWLEDGEMENTS

Dr. Andrew Browe conceived of and implemented the experiments as performed herein. I thank Dr. Browe for his assistance.

LITERATURE CITED

Aceves, J. 1977. Sodium pump stimulation by oxytocin and cyclic AMP in the isolated epithelium of the frog skin. Pflugers Arch 371: 211-216.

Al-Bazzaz, F. and R. Zevin. 1984. Ion transport and metabolic effects of amiloride in canine tracheal mucosa. Lung 162: 357-367.

Baba, W.I. and A.J. Smith. 1964. The effect of guanethidine on sodium transport across the isolated frog skin. Q J Exp Physiol Cogn Med Sci 49: 194-198.

Cereijido, M., C.A. Rabito, B.E. Rodriguez, and C.A. Rotunno. 1974. The sodium-transporting compartment of the epithelium of frog skin. J Physiol 237: 555-571.

Civan M.M., K. Peterson-Yantorno, and T.G. O'Brien. 1987. Diacylglycerols stimulate short-circuit current across frog skin by increasing apical Na^+ permeability. J Membr Biol 97: 193-204.

Clarke, L.L. 2009. A guide to Ussing chamber studies of mouse intestine. Am J Physiol Gastrointest Liver Physiol 296: G1151-1166.

Dorge, A., R. Rick, F.X. Beck, and W. Nagel. 1988. Uptake of Br in mitochondria-rich and principal cells of toad skin epithelium. Pflugers Arch 412: 305-313.

Edwards, R.A., P.L. Lutz, and D.G. Baden. 1989. Relationship between energy expenditure and ion channel density in the turtle and rat brain. Am J Physiol 257: R1354-1358.

Essig, A., D. Wolff, S. Rosenthal, M.A. Lang, J.G. King, S.R. Caplan, M. Canessa, P. Labarca, and A. Leaf. 1978. Metabolic cost of sodium transport and the degree of coupling of transport and metabolism in toad urinary bladder. J Membr Biol 41: 189-194.

Fellers, G.M. and P.M. Kleeman. 2007. California red-legged frog (*Rana draytonii*) movement and habitat use: Implications for conservation. J Herpetol 41: 276-286.

Graeter, G.J., B.B. Rothermel, and J.W. Gibbons. 2008. Habitat selection and movement of pond-breeding amphibians in experimentally fragmented pine forests. J Wild Man 72: 473-482.

Grider, J., J. Falcone, E. Kilpatrick, C. Ott, and B. Jackson. 1996. Effect of luminal vasopressin on NaCl transport in the medullary thick ascending limb of the rat. Eur J Pharmacol 313: 115-118.

Kelepouris, E., Z.S. Agus, and M.M. Civan. 1985. Intracellular calcium activity in split frog skin epithelium: effect of cAMP. J Membr Biol 88: 113-121.

Koefoed-Johnsen, V. and H.H. Ussing. 1958. The nature of the frog skin potential. Acta Physiol Scand 42: 298-308.

Kottra, G., G. Weber, and E. Frömter. 1989. A method to quantify and correct for edge leaks in Ussing chambers. Eur J Physiol 415: 235-240.

Kudo, L.H., A.A. van Baak, and A.S. Rocha. 1990. Effect of vasopressin on sodium transport across inner medullary collecting duct. Am J Physiol 258: F1438-1447.

Labarca, P., M. Canessa, and A. Leaf. 1977. Metabolic cost of sodium transport in toad urinary bladder. J Membr Biol 32: 383-401.

Lacaz-Vieira, F. and J. Procopio. 1988. Chloride transport in amphibian skin: a review. Braz J Med Biol Res 21: 1119-1128.

Martens, H. 1985. The effect of dinitrophenol on magnesium transport across an isolated preparation of sheep rumen epithelium. Q J Exp Physiol 70: 567-573.

McDonald, T.F. and D.P. MacLeod. 1972. The effect of 2,4-dinitrophenol on electrical and mechanical activity, metabolism and ion movements in guinea-pig ventricular muscle. Br J Pharmacol 44: 711-722.

Morgan, J.D. and G.K. Iwama. 1999. Energy cost of NaCl transport in isolated gills of cutthroat trout. Am J Physiol Regul Integr Comp Physiol 277: R631-639.

Nielsen, R. and E.H. Larsen. 2007. Beta-adrenergic activation of solute coupled water uptake by toad skin epithelium results in near-isosmotic transport. Comp Bioc Physiol (A): Molec Integ Physiol 148: 64-71.

Palmer, L.G. 2001. Intracellular pH as a regulator of Na^+ transport. J Membr Biol 184: 305-311.

Ponec, J., P. Bakos, and B. Lichardus. 1989. Microelectrode study of insulin effect on apical and basolateral cell membrane of frog skin: comparison with the effect of 1-deamino-8-D-arginine-vasopressin (dDAVP). Gen Physiol Biophys 8: 245-255.

Rabito, C.A., C.A. Rotunno, and M. Cereijido. 1978. Amiloride and calcium effect on the outer barrier of the frog skin. J Membr Biol 42: 169-187.

Regosin, J.V., B.S. Windmiller, R.N. Homan, and J.M. Reed. 2005. Variation in terrestrial habitat use by four poolbreeding amphibian species. J Wild Man 69: 1481-1493.

Reuss, L. 2001. Ussing's two-membrane hypothesis: The model and half a century of progress. J Membr Biol 184: 211-217.

Salako, L.A. and A.J. Smith. 1970. Effects of amiloride on active sodium transport by the isolated frog skin: evidence concerning site of action. Br J Pharmacol 38: 702-718.

Sariban-Sohraby, S. and D.J. Benos. 1986. The amiloride-sensitive sodium channel. Am J Physiol 250: C175-190.

Talbot, C.R. 2002. The effects of perfusion of the cutaneous vasculature on sodium uptake across isolated frog skin. J Comp Physiol (B): Biochem Sytsem Environ Physiol 172: 209-216.

Uchiyama, M. and N. Konno. 2006. Hormonal regulation of ion and water transport in anuran amphibians. Gen Comp Endocrinol 147: 54-61.

Ussing, H.H. 1949. The active ion transport through the isolated frog skin in the light of tracer studies. Acta Physiol Scand 17: 1-37.

Ussing, H.H. and K. Zerahn. 1951. Active transport of sodium as the source of electric current in the short-circuited isolated frog skin. Acta Physiol Scand 23: 110-127.

Vos, C.C., P.W. Goedhart, D.R. Lammertsma, and A.M. Spitzen-Van der Sluijs. 2007. Matrix permeability of agricultural landscapes: an analysis of movements of the common frog (*Rana temporaria*). Herpetol J 17: 174-182.

Welsh, M.J. 1984. Energetics of chloride secretion in canine tracheal epithelium. Comparison of the metabolic cost of chloride transport with the metabolic cost of sodium transport. J Clin Invest 74: 262-268.

Yamada, T., T. Nishio, Y. Sano, K. Kawago, K. Matsuda, and M. Uchiyama. 2008. Effects of arginine vasotocin and vasopressin receptor antagonists on Na^+ and Cl^- transport in the isolated skin of two frog species, *Hyla japonica* and *Rana nigromaculata*. Gen Comp Endocrinol 157: 63-69.

Zeiske, W. and B. Lindemann. 1974. Chemical stimulation of Na^+ current through the outer surface of frog skin epithelium. Biochim Biophys Acta 352: 323-326.

Journal of the Pennsylvania Academy of Science 86(1): 12-23, 2012

LIFE ON THE FRINGE: CHARACTERIZATION OF FRINGE VEGETATION IN ERIE BLUFFS STATE PARK (ERIE COUNTY, PENNSYLVANIA)[1]

MICHAEL T. GANGER, JAMES J. MCGIVERN, LINDSEY BOCIAN, NATHALIE-ANN C. BROWN[2], JOSEPH PERENIC

Department of Biology, Gannon University, 109 University Square, Erie, PA 16541

ABSTRACT

Human activities have resulted in the fragmentation of native habitat. One ubiquitous result of landscape modifications is a narrow strip of vegetation, hereafter referred to as fringe, that occurs between forest and inhospitable habitat like agricultural fields. This study investigated the fringe habitat in the Erie Bluffs State Park in Erie County, Pennsylvania. The park has several agricultural fields that are currently in use and one abandoned field resulting in 67,680 m^2 of fringe. In order to understand the species composition and vegetation structure of the fringe, 1451 m-wide quadrats were established and the number and identity of species occurring within them was determined in both June and August. One hundred sixty-four species from 55 families were observed in the fringe, 39% of which were listed as annuals or biennials, 40% were non-native to Pennsylvania, and six are listed by the Department of Conservation and Natural Resources as exotic invasives or are on their watch list. Sixty-one percent of these species occurred in both the June and August censuses while the remainder were seen in only one of the two censuses. The average number of species per quadrat was greater in August than in June. Agglomerative Hierarchical Cluster Analysis was used to group quadrats in the fringe based on species similarity into three groups in June and five groups in August. Indicator Species Analysis determined 9 species associated with the groups in June and 14 species associated with the groups in August. The fringe is a spatially and temporally complex habitat with high species richness that has the potential to play a role in the stability of the forest habitat and the transition of agricultural fields to native habitat. [J PA Acad Sci 86(1): 12-23, 2012]

[1]Submitted for publication January 2012; accepted August 2012.

[2]Author for communication: Mike Ganger, PMB# 3032 Department of Biology, Gannon University 109 University Square, Erie, PA 16541-0001, (814) 871-7405

INTRODUCTION

Plant species often exist together in large groups or assemblages. For many ecologists, these assemblages have an identity as determined by their spatial extent and the nature and abundance of species within them. These assemblage properties are not static but rather tend to change over time, and in fact a large body of theory has been developed to predict such changes (Wyatt 1947, Keddy 1992, McGill et al. 2006).

Assemblages are arguably artificial constructs (Fauth et al. 1996). Their spatial organization is often determined using complex mathematical models that can establish patterns of species from a large set of quadrat data (Gauch 1982, Greig-Smith 1983). Specific species may then be identified that indicate particular assemblages (Diekmann 2003). This process is likely most effective and useful where the vegetation is established with a high proportion of permanent residents and where the boundaries between assemblages are clearly defined and stable, i.e., an ecotone (Sensu Smith 1996). Where the limit of multiple species vary independently from one another, a transition zone is formed that consists of species shared between the two abutting communities and some that are unique to the transition zone (Malcolm 1994, Risser 1995).

Human activities such as farming, road building, and housing development have resulted in the fragmentation of native habitat (Murcia 1995). This fragmentation of the landscape has resulted in a more spatially complex arrangement of plant assemblages (Saunders et al. 1991, Gustafson & Gardner 1996). A common arrangement is a narrow transition zone (Risser 1995) located between the forest fragment and inhospitable landscape on the other, e.g., road or herbicide treated agricultural field. Hereafter, we refer to this type of transition zone as a "fringe."

Transition zones, including fringe, are not necessarily a uniform assemblage of species but instead may themselves be quite complex spatially and temporally (Jules and Priya 2003). Transition zones can act as boundaries or tunnels to the flow of resources and organisms (Cadenasso et al. 2003; Strayer et al. 2003). Their influence may be felt on forest fragments as higher tree mortality rates closer to the edge

(Cadenasso and Pickett 2000; Godefroid and Koedam 2003), higher recruitment near the edge (Laurance et al. 2007), and the introgression of non-tree species into the forest (Cadenasso and Pickett 2001). In addition to their effects on forest fragments, transition zones may serve as a repository of species that may directly or indirectly affect forest species (Gascon et al. 1999), facilitating dispersal between fragments (Cook et al. 2002) and serving as a source of colonizing species for newly created habitat (e.g., abandoned fields; Gluvna and Ganger 2011). These transition zones are dynamic (Gascon et al. 2000; Laurance et al. 2007) and at various stages in development, may soften, expand, or even function to seal the two assemblages on either side from one another (Harper et al. 2005). The width of this transition zone is important and has been shown to be crucial for the long-term persistence of the fragment (Matlack 1993).

Fringe habitats are ubiquitous in human-modified landscapes. Understanding their composition and pattern is crucial for predicting their stability and role in the larger landscape. The objectives of this study were to determine 1) the species composition and vegetation structure of the fringe and 2) the difference in species composition and vegetation structure of the fringe between two sampling dates within the same season.

STUDY SITE

The Erie Bluffs State Park, a 218.5 hectare property located in Erie County, Pennsylvania, along the southern coast of Lake Erie was officially designated a state park in 2004 (Figure 1). It contains approximately 497 vascular plant species (Ganger et al., unpubl.). In addition to Dry Oak—Mixed Hardwoods Forest, Sugar Maple—Beech Forest and Hemlock Forest, and Great Lakes Region Scarp Woodland (Fike 1999), the park also contains relict dunes and beach ridges formed by depositional processes associated with Lake Whittlesey and Lake Warren, both glacial lakes that occupied the Erie Basin (Thomas et al. 1987, Western Pennsylvania Conservancy 2005).

Nearly one third of the park consists of agricultural fields currently in use and one such field that was allowed to go fallow in 2009 (Gluvna and Ganger 2011). The long-term management goals for the park include converting all of the agricultural fields to native habitat (DCNR 2008). The agricultural fields are bounded by a fringe, which accounts for 3.1% of the total area of the park. In places, the fringe has properties of an abrupt transition zone (i.e., a forest-field ecotone), while in other locations the boundary is distinctly narrow (< 1 m).

MATERIALS AND METHODS

To characterize the vegetation of the fringe, 146 quadrats were established 50 m apart using GPS coordinates. Quadrats were 1 m wide, but the depth of the quadrat varied with location since the fringe was not of uniform width. This meant that the largest quadrat was 41 m^2 while the smallest was 0.5 m^2.

The identity of all vascular plant species within each quadrat was recorded in June 2010 and again in August 2010. This resulted in a presence/absence data set. Vascular plant species were identified following Rhoads and Block (2007) and checked against voucher specimens at the Carnegie Museum of Natural History, Section of Botany (CM; Thiers [continuously updated]).

Species area curves were generated from both June and August census data. EstimateS (Colwell 2005) was used to produce a species accumulation curve to determine whether the observed number of species approximated the number of species in the fringe.

PC-ORD (McCune and Medford 2006) was used to classify the vegetation of the fringe. Only species present in at least 3 quadrats, representing an absolute frequency of > 2%, were included in the analyses. Agglomerative Hierarchical Cluster Analysis, using Sorensen distances and flexible beta linkage with b = -0.25 following McCune and Grace (2002), provided a dendrogram that grouped quadrats based on the presence/absence of plant species. Indicator Species Analysis includes randomization tests that generate p-values for each plant species assuming a different number of quadrat groups (McCune and Grace 2002). The average p-values for all plant species from these individual tests were compared and the lowest average p-value indicated the most meaningful number of quadrat groups (McCune and Grace 2002). Indicator Species Analysis, with 4999 randomizations used in the Monte Carlo test, was also used to determine plant species associated with each of these groups known as indicators (McCune and Grace 2002). These indicators are selected based on their fidelity to a particular group and can be described numerically as a percentage. A species that is 100% faithful is found in only one group,while a species that is 50% faithful would mean that of the quadrats it is present in, half of these are associated with that group. Output from these analyses was used to generate a map of the fringe with quadrat groups designated by indicator species.

In August 2010, the study was repeated using the same quadrats from June 2010. Given the error inherent to the GPS unit, it is likely that the quadrats sampled in August were not exactly those sampled in June. Therefore, the two sets of quadrat samples were treated as independent samples rather than repeated measures of the same quadrats. A t-test was used to assess whether the number of species recorded differed between the two censuses.

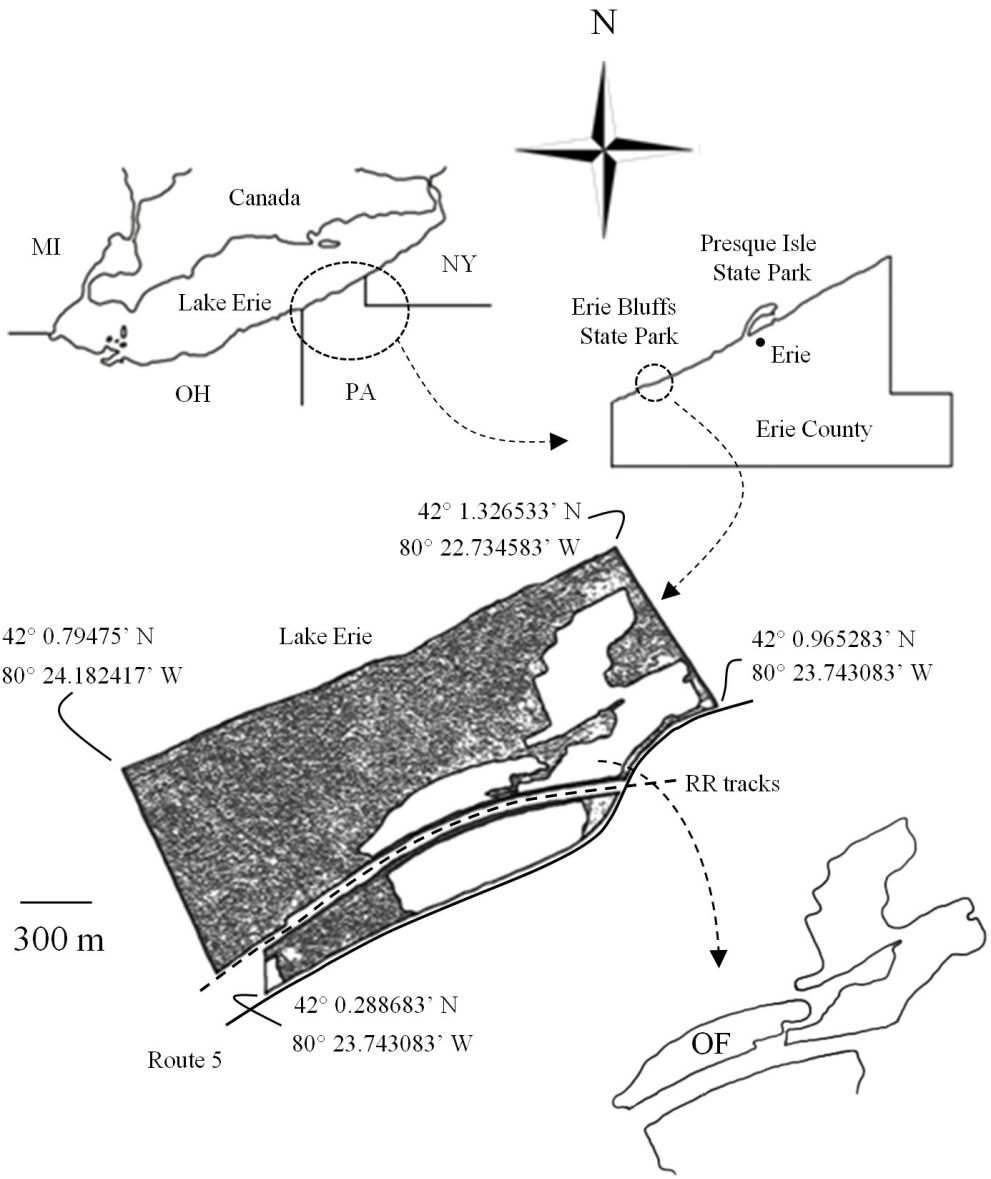

Figure 1. Geographic location and map of the Erie Bluffs State Park. The farmed fields and the old field are in white, while the forested areas are in black. Scale references the Erie Bluffs State Park. The fringing habitat is represented as a dark line in the inset to the park map. The old field (OF) is indicated.

RESULTS

A total of 156 species from 53 families was recorded from the 146 quadrats in the fringe (Table 1). The June census contained 111 species including 17 unique to the June census. The August census contained 138 species including 44 species unique to the August census. EstimateS produced species accumulation curves that asymptoted near the observed number of species for both the June and August censuses. Ninety-five species were observed in both censuses representing 61% of the 156 species seen overall. Eight species were identified in the fringe that were not present in any of the quadrats (Table 1). This increases the total number of species to 164 from 55 families.

Of species seen in the June and August censuses, 39% are listed as annuals or biennials following USDA, NRCS (2011). The remainder are perennials. Of these species, 37% were non-native (Rhoads and Block 2007) and seven appear on either the Exotic Invasive Plants in Pennsylvania list compiled by the Department of Conservation and Natural

Resources (*Aliaria petiolata* (M.Bieb.) Cavara & Grande, *Celastrus orbicularis* Thunb., *Coronilla varia* L., *Lonicera japonica* Thunb., *Lonicera morowii* A.Gray, *Rosa multiflora* Thunb. ex Murray) or their Watch List (*Buddleja davidii* Franch); DCNR (2011).

Quadrat area ranged between 0.5 m^2 and 41 m^2 and averaged 9.5 m^2 (sd = 5.8 m^2). The average number of species observed in quadrats in June was significantly lower than the average number of species observed in quadrats in August ($P < 0.0001$). In June, between 3 and 24 species (mean = 13.7 species; sd = 5.0 species) were present in quadrats. In August, between 5 and 31 species (mean = 10.7 species; sd = 4.5 species) were present in quadrats. There was a positive, albeit very weak, relationship between quadrat size and

Table 1. Vascular plant species observed in the fringe. Species with absolute frequency data occurred in quadrats, while those without were not present in quadrats. J = present in the June census and A = present in August census.

Family	Species	Abs. Freq. (J)	Abs. Freq. (A)
Adoxaceae	*Sambucus canadensis* L.	0.007	0.007
Alliaceae	*Allium vineale* L.	-	0.007
Amaranthaceae	*Amaranthus albus* L.	-	0.021
	Amaranthus powelii S.Watson	-	0.028
	Chenopodium album L.	0.055	0.014
Anacardiaceae	*Rhus typhina* L.	0.370	0.503
	Toxicodendron radicans (L.) Kuntze	0.021	0.048
Apiaceae	*Daucus carota* L.	0.123	0.124
Apocynaceae	*Apocynum cannabinum* L.	0.041	0.034
	Asclepias incarnata L.	-	0.028
	Asclepias syriaca L.	0.055	0.048
Asteraceae	*Achillea millefolium* L.	0.014	-
	Ageratina aromatica (L.) Spach	-	0.028
	Ambrosia artemisiifolia L.	0.247	0.050
	Arctium mimus (Hill) Bernh.	0.007	0.021
	Artemisia vulgaris L.	0.034	0.048
	Centaurea stoebe L.	0.123	0.152
	Cirsium pumilum (Nutt.) Spreng.	-	0.007
	Conyza canadensis (L.) Cronquist	0.315	0.566
	Crepis capillaris (L.) Wallr.	0.123	0.055
	Erechtites hieraciifolia (L.) Raf. ex DC.	-	0.014
	Erigeron annuus (L.) Pers.	0.034	0.048
	Euthamia graminifolia (L.) Nutt	0.027	0.131
	Hieracium pilosella L.	-	0.007
	Lactuca canadensis L.	-	0.007
	Leucanthemum vulgare Lam.	0.048	0.014
	Pseudognaphalium obtusifolium (L.) Hilliard & B. L. Burtt	-	0.014
	Solidago canadensis L.	0.041	0.421
	Solidago gigantea Aiton	0.432	0.317
	Symphyotrichum lateriflorum (L.) Á.Löve & D.Löve	0.075	0.103
	Taraxacum officinale F. H. Wigg.	0.014	0.041
	Tragopogon dubius Scop.	0.034	0.014
Balsaminaceae	*Impatiens capensis* Meerb.	0.048	0.076

Family	Species	Abs. Freq. (J)	Abs. Freq. (A)
Boraginaceae	*Hydrophyllum virginianum* L.	-	0.007
Brassicaceae	*Alliaria petiolata* (M.Bieb.) Cavara & Grande	0.308	0.193
	Arabidopsis thaliana (L.) Heynh. in Holl & Heynh.	0.062	-
	Barbarea vulgaris (L.) R.Br.	-	0.007
	Cardamine hirsuta L.	-	0.021
	Lepidium virginicum L.	0.151	0.172
	Sisymbrium officinale (L.) Scop.	-	0.007
Campanulaceae	*Lobelia inflata* L.	-	0.021
	Triodanis perfoliata (L.) Nieuwl.	0.041	0.007
Caprifoliaceae	*Lonicera japonica* Thunb.	0.021	0.028
	Lonicera morrowii A. Gray	0.281	0.324
Caryophyllaceae	*Arenaria serpyllifolia* L.	0.041	-
	Dianthus armeria L.	0.061	0.028
	Silene latifolia Poir.	0.021	0.007
	Stellaria media (L.) Vill.	0.041	0.034
Celastraceae	*Celastrus orbiculatus* Thunb.	0.192	0.297
Convulvulaceae	*Calystegia silvatica* (Kit.) Griseb.	0.055	0.034
Cornaceae	*Cornus sericea* L.	0.007	0.021
Cucurbitaceae	*Echinocystis lobata* (Michx.) Torr. & A. Gray	-	0.007
Cyperaceae	*Cyperus brevifolioides* Thieret & Delahoussaye	-	0.007
	Cyperus lupulinus (Sprengel) Marcks	0.110	0.048
	Cyperus odoratus L.	-	0.007
Equisetaceae	*Equisetum arvense* L.	0.041	0.041
Ericaceae	*Vaccinium pallidum* Aiton	-	0.007
Euphorbiaceae	*Acalypha rhomboidea* Raf.	-	0.014
	Euphorbia maculata L.	-	0.007
Fabaceae	*Coronilla varia* L.	0.007	0.007
	Desmodium perplexum Schub.	0.288	0.497
	Lespedeza hirta (L.) Hornem	0.021	0.021
	Robinia pseudoacacia L.	0.048	0.028
	Trifolium dubium Sibth.	0.014	-
	Trifolium pratense L.	0.007	-
	Trifolium repens L.	0.055	0.055
Fagaceae	*Quercus rubra* L.	0.102	0.090
	Quercus velutina Lam.	-	0.007
Geraniaceae	*Geranium sp.*	-	0.007
Grossulariaceae	*Ribes americanum* Mill.	0.007	-
Hyperiaceae	*Hypericum punctatum* Lam.	0.041	0.048
Juglandaceae	*Carya cordiformis* (Wang.) K.Koch	-	0.034
Juncaceae	*Juncus tenuis* Willd.	0.068	0.090
Lamiaceae	*Glechoma hederacea* L.	0.021	0.014
	Lamium purpureum L.	-	0.007
	Leonurus cardiaca L.	0.007	0.021

Family	Species	Abs. Freq. (J)	Abs. Freq. (A)
	Teucrium canadense L.	0.116	0.138
	Trichostema dichotomum L.	-	0.007
Lauraceae	*Sassafras albidum* (Nutt.) Nees	-	0.021
Magnoliaceae	*Liriodendron tulipifera* L.	-	0.021
Molluginaceae	*Mollugo verticillata* L.	0.055	0.172
Myrsinaceae	*Lysimachia ciliata* L.	0.007	0.007
Oleaceae	*Fraxinus sp.*	0.034	0.041
	Ligustrum obtusifolium Siebold & Zucc.	0.027	-
Onograceae	*Circaea canadensis* (L.) Hill	0.034	0.014
	Epilobium coloratum Biehler	-	0.007
	Oenothera biennis L.	0.226	0.276
Oxalidaceae	*Oxalis corniculata* L.	0.007	0.028
	Oxalis dillenii Jacq.	0.212	0.166
Phytolaccaceae	*Phytolacca americana* L.	0.158	0.172
Plantaginaceae	*Linaria vulgaris* Hill	0.007	0.021
	Plantago aristata Michx.	0.014	-
	Plantago lanceolata L.	0.137	0.124
	Plantago major L.	0.048	0.041
	Plantago rugelii Decne.	-	0.021
	Veronica arvensis L.	0.068	-
Poaceae	*Agrostis capillaris* L.	-	0.007
	Anthoxanum odoratum L.	0.199	0.124
	Bromus hordeaceus L.	0.021	-
	Bromus inermis Leyss.	0.014	0.021
	Cenchrus tribuloides L.	0.116	0.144
	Dactylis glomerata L.	0.144	0.110
	Dichanthelium acuminatum (Sw.) Gould and C. A. Clark	-	0.007
	Digitaria cognatum (Schult.) Pilg.	0.096	0.166
	Digitaria ischaemum (Schreb ex Schweigg.) Schreb. ex Muhl.	0.089	0.331
	Digitaria sanguinalis (L.) Scop.	0.014	0.097
	Elymus repens (L.) Desv. ex Nevski	0.137	0.131
	Eragrostis minor Host; Lovegrass	0.014	0.028
	Eragrostis spectabilis (Pursh) Steud.	0.014	0.124
	Muhlenbergia mexicana (L.) Trin.	-	0.014
	Panicum dichotomiflorum Michx.	0.027	0.544
	Phleum pratense L.	0.089	0.097
	Poa annua L.	0.041	-
	Poa palustris L.	0.096	0.166
	Poa pratensis L.	-	0.021
	Setaria faberi Herrm.	-	0.262
Polygonaceae	*Fallopia cilinodis* (Michx.) Holob	-	0.310
	Persicaria pensylvanica (L.) M.Gómez	-	0.021
	Persicaria virginiana (L.) Gaertner	0.075	0.124

Family	Species	Abs. Freq. (J)	Abs. Freq. (A)
	Polygonum aviculare L.	0.075	0.055
	Rumex acetosella L.	0.267	0.145
	Rumex crispus L.	-	0.007
	Rumex obtusifolius L.	0.192	0.172
Polypodiaceae	*Onoclea sensibilis* L.	0.007	0.007
Portulacaceae	*Portulaca oleracea* L.	0.041	0.083
Ranunculaceae	*Clematis terniflora* DC	-	0.007
Rosaceae	*Agrimonia pubescens* Wallr.	-	0.007
	Crataegus sp.	0.007	-
	Fragaria vesca L.	0.007	0.014
	Fragaria virginiana Duchesne	0.404	0.462
	Geum canadense Jacq.	0.164	0.110
	Malus pumila Mill.	-	0.007
	Potentilla recta L.	0.014	-
	Prunus serotina Ehrh.	0.137	0.083
	Rosa multiflora Thunb. ex Murray	0.178	0.159
	Rubus allegheniensis	0.185	0.200
	Rubus flagellaris Willd.	0.425	0.538
	Rubus idaeus L.	0.308	0.421
	Rubus odoratus L.	-	0.007
	Rubus pensilvanicus Poir.	0.089	0.138
Rubiaceae	*Galium aparine* L.	0.048	-
Salicaceae	*Populus deltoides* Bantram ex Marsh.	-	0.007
	Populus tremuloides Michx.	0.007	-
Sapindaceae	*Acer rubrum* L.	0.027	0.021
Scrophulariaceae	*Verbascum thapsus* L.	0.144	0.145
Solanaceae	*Physalis heterophylla* Nees	0.014	0.007
	Solanum carolinense L.	0.260	0.214
	Solanum dulcamara L.	-	-
	Solanum nigrum L.	0.034	0.041
Urticaceae	*Pilea pumila* (L.) A. Gray	-	0.007
Verbenaceae	*Verbena urticifolia* L.	-	0.007
Violaceae	*Viola arvensis* Murray	0.034	-
	Viola blanda Willd.	-	0.007
Vitaceae	*Parthenocissus quinquefolia* (L.) Planch.	0.192	0.241
	Vitis aestivalis Michx.	0.041	0.069
	Vitis riparia Michx.	0.398	0.517
Asteraceae	*Eupatorium perfoliatum* L.	-	-
Balsaminanceae	*Impatiens pallida* Nutt.	-	-
Fabaceae	*Desmodium paniculatum* (L.) DC	-	-
Malvaceae	*Abutilon theophrastii* Medik.	-	-
Phrymaceae	*Mimulus ringens* L.	-	-
Polygonaceae	*Persicaria glabra* (Willd.) M.Gómez	-	-

Family	Species	Abs. Freq. (J)	Abs. Freq. (A)
Rosaceae	*Rubus occidentalis* L.	-	-
Scrophulariaceae	*Buddleja davidii* Franch.	-	-

species richness for June ($P < 0.01$; adjusted $R^2 = 0.051$), but not for August ($p = 0.210$). In June, an additional species was predicted for every 0.11 m^2 increase in quadrat area.

Of the 111 species recorded in June quadrats, 56 had a low absolute frequency, present in less than 5% of quadrats, while 5 had a high absolute frequency, present in greater than 33% of quadrats. Of the 140 species recorded in August quadrats, 83 had a low absolute frequency, present in less than 5% of quadrats, while 8 species had a high absolute frequency, present in greater than 33% of quadrats. Of the 61 species that only occurred in one census, 32 were present in only one quadrat, 50 were present in one or two quadrats, and 59 had absolute frequencies of less than 5%.

For the June census, Hierarchical Agglomerative Cluster Analysis produced low chaining, 0.71%. Indicator Species Analysis recommended three assemblages of species within the fringe (Figure 2) that were defined by the following species: 1) *A. petiolata* ($P < 0.001$), *C. orbicularis* ($P < 0.001$), and *Geum canadense* Jacq. ($P < 0.001$); 2) *Cenchrus tribuloides* L. ($P < 0.001$); and 3) *Conyza canadensis* (L.) Cronquist ($P < 0.001$), *Desmodium perplexum* Schub. ($P < 0.001$), *Fragaria virginiana* Duchesne ($P < 0.001$), *Rubus flagellaris* Willd. ($P < 0.001$), and *Rumex acetosella* L. ($P < 0.001$).

For the August census, Hierarchical Agglomerative Cluster Analysis produced low chaining, 1.55%. Indicator Species Analysis recommended five assemblages of species within the fringe (Figure 3) that were defined by the following species: 1) *C. canadensis* ($P < 0.05$), *F. virginiana* ($P < 0.01$), and *R. multiflora* ($P < 0.001$); 2) *Panicum dichotomiflorum* Michx. ($P < 0.001$); 3) *Rubus idaeus* L. ($P < 0.01$); 4) *Mollugo verticilata* L. ($P < 0.01$), *Oenothera bienis* L. ($P < 0.01$), *Portulacca oleracea* L. ($P < 0.001$), and *Rhus typhina* L. ($P < 0.01$); and 5) *Anthoxanum odoratum* L. ($P < 0.001$), *Ambrosia artemisiifolia* L. ($P < 0.001$), *C. tribuloides* ($P < 0.01$), *Centaurea stoebe* L. ($P < 0.001$), and *Eragrostis spectibilis* (Pursh) Steud. ($P < 0.001$).

DISCUSSION

That this narrow strip of fringe contains so many of the park's plant species attests to its potential ecological importance and its relevance to any management plan. Despite the small area of the fringe (67,680 m^2 = 3.1% of the park overall), it contains roughly 31% of the species present in the park overall and 93% of the species occurring in the old field (Gluvna and Ganger 2011). This suggests that in addition to serving as a source of colonists for the forest (Gascon et al. 1999), the fringe may also serve as a source of colonists for the start and maintenance of old field succession.

The fringe of the park is an assemblage composed of both long-term and short-term residents. The high proportion of annuals and biennials suggests a dynamic habitat with a set of species continuously re-colonizing the fringe.

Fringe habitats are known to be highly variable with respect to microenvironmental variables such as light, humidity, and shrub cover (Matlack 1993). The results here suggest a dynamic assemblage that exhibits both spatial and temporal variability. This variability was evident as a difference in species composition between the June and August censuses, especially among species that occurred at low frequency. Of the 61 species that only occurred in one census, 52.5% were present in only one quadrat, 82% were present in one or two quadrats, and 96.7% had absolute frequency values of less than 5%. Subtle differences in quadrat placement in August, using the GPS coordinates established in June, could have resulted in a slightly different impression of species composition based on whether low frequency species were present in a particular quadrat.

Alternatively, the differences in species composition between June and August may be due to seasonal species turnover from the spring to late summer where over 25% of the species in August were unique to that census. Given the extent of the fringe and the likelihood of different environmental conditions—e.g., there is fringe with both northern and southern exposures—the species turnover is likely to progress over different time scales in different locations.

Differences in species number and species transition likely explain why the Indicator Species Analysis organized the vegetation into three main groups in June versus five main groups in August. The spatial organization of the fringe in June is much more simple than it is in August owing in part to fewer species present in June. The fringe overall accumulates more species throughout the season than disappear from it during the same time interval. As this transition is occurring at different rates in different locations, this leads to an increase in the variation in spatial structure of the fringe vegetation.

Despite the large number of species in the fringe (164), only 9 species served as indicators for the June groupings, while

14 species served as indicators for the August groupings. Three species, *Cenchrus tribuloides* L., *Conyza canadensis* (L.) Cronquist, and *Fragaria virginiana* Duchesna, served as indicators for both the June and August groupings. Unfortunately, their association is not spatially consistent between the two censuses. For example, *C. tribuloides* indicates the southern field fringe in June (K-L in Figure 2) but different fringe habitat in August (notably A-B in Figure 3). Similarly *C. canadensis* is associated with different fringe habitats in June versus August. This is probably best explained by the dynamic nature of the fringe itself. Early in June, with fewer species present, certain species serve as indicators. As seasonal changes in species occur, these same species have less predictive ability (lower indicator values) of the same fringe in August.

This is not to say that there are not underlying vegetation

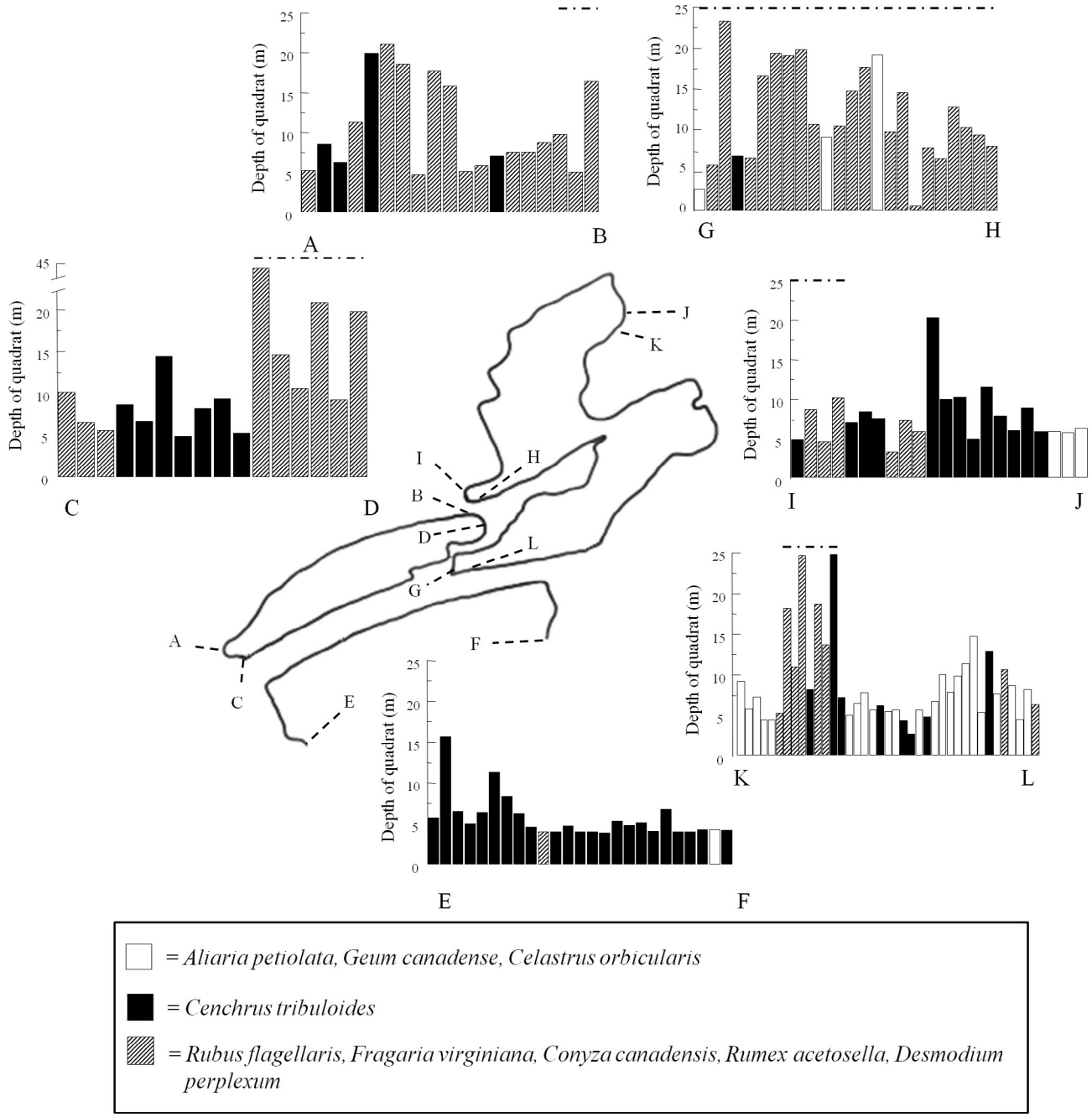

Figure 2. Vegetation map of the June fringe habitat showing three species assemblages generated by Agglomerative Hierarchical Cluster Analysis and Indicator Species Analysis output. Bars on the histograms represent quadrats between two lettered points along the fringe. Dot-dashed lines above histograms represent quadrats occurring within either dune ridge or relict dune habitat.

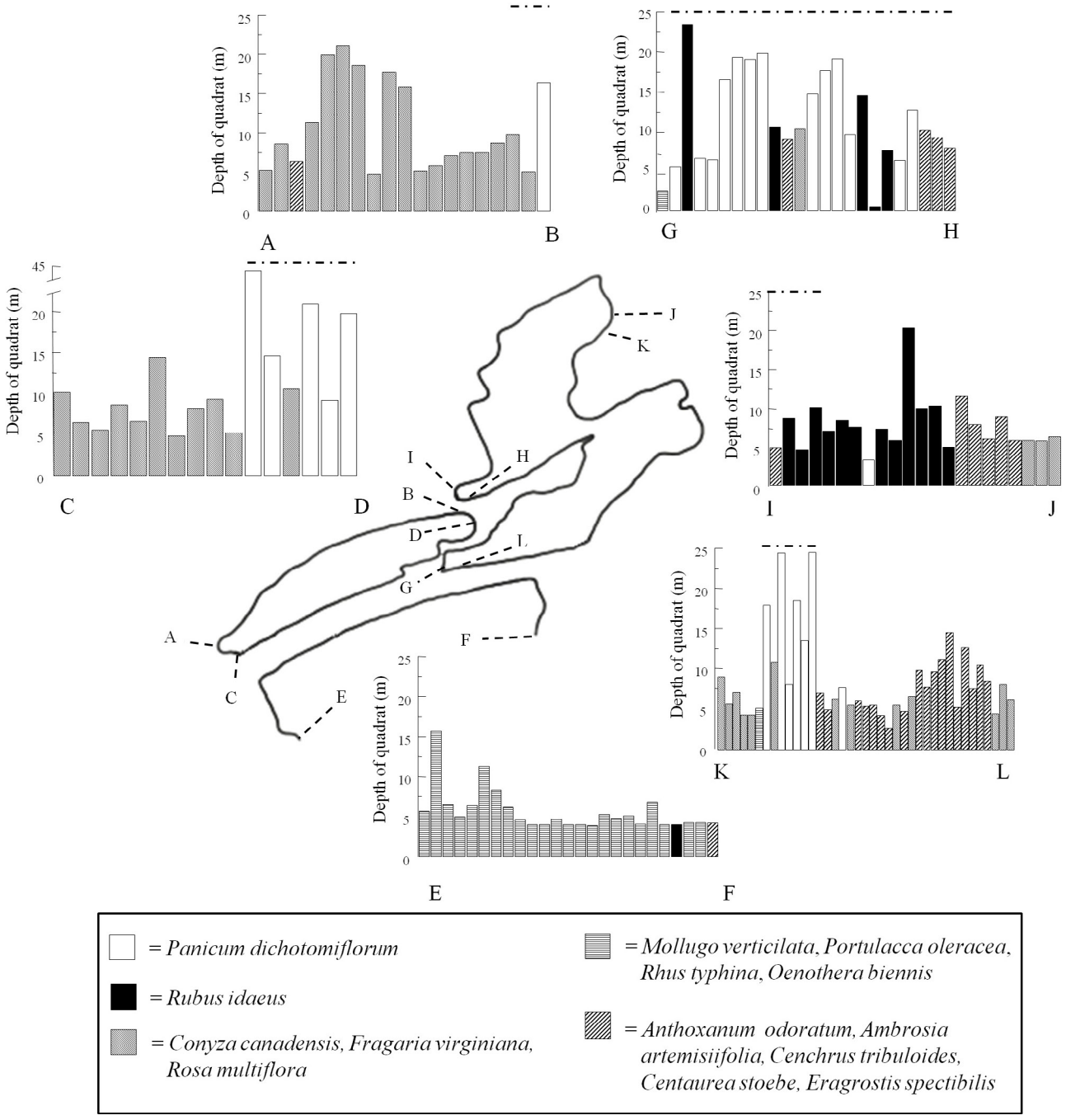

Figure 3. Vegetation map of the August fringe habitat showing three species assemblages generated by Agglomerative Hierarchical Cluster Analysis and Indicator Species Analysis output. Bars on the histograms represent quadrats between two lettered points along the fringe. Dot-dashed lines above histograms represent quadrats occurring within either dune ridge or relict dune habitat.

patterns explained by factors other than spatial differences in quadrat placement or temporal patterns in vegetation development. The park itself is notable for the bluffs and as one of the largest contiguous forested areas along the Lake Erie shoreline (Western Pennsylvania Conservancy 2005). In addition, a relict dune runs northeast—southwest through the agricultural fields (Western Pennsylvania Conservancy 2005). The influence of this dune ridge is evident in the vegetation classification of both the June and August census despite different species serving as indicators. In June the indicators of this dune ridge were *Rubus flagellaris* Willd., *F. virginiana*, *C. canadensis*, *Rumex acetosella* L., and *Desmodium perplexum* Schub., while in August they were *Panicum dichotomiflorum* Michx., *Anthoxanum odoratum*

L., *Ambrosia artemisiifolia* L., *C. tribuloides*, *Centaurea stoebe* L., and *Eragrostis spectibilis* (Pursh) Steud. The fringe associated with the southernmost agricultural field is basically one grouping for both June and August. In both cases, the species that indicate this grouping are weedy, prostrate herbs: *C. tribuloides*, *Mollugo verticilata* L., and *Portulacca oleracea* L. and the fringe is much narrower in this location. In addition to the relict dune and the southernmost agricultural field, a third grouping includes narrow fringe adjacent to established forest of *Quercus rubra* L., *Acer rubrum* L., *Liriodendron tulipifera* L., and *Populus deltoides* Bantram ex Marsh. The indicators of this habitat include species consistent with forested habitats: *Rosa multiflora* Thunb. ex Murray, *D. perplexum*, *R. flagellaris*, and *F. virginiana*.

Implicit in the definition of an ecotone is the notion of a steep environmental gradient that underlies vegetation transition between more homogeneous communities (van der Maarel 1990, Risser 1995). Since the fringe is a transition zone, a type of ecotone, it would be expected to be defined by an environmental gradient. In the case of the fringe at Erie Bluffs State Park, the fringe is not one homogeneous ecotone but rather a mixture of distinct transition zones that could potentially be based on either distinct environmental gradients in unique locations or the combination of several gradients whose intensity varies with fringe location. The fringe is a very complex, heterogeneous community that resists classification. It exists rather as a patchwork of communities that each have ecotone-like properties.

The lack of a relationship between quadrat area and species richness for August, and the presence of an extremely weak relationship for June, coupled with the large number of species present in quadrats overall suggests species packing within the fringe. With the abandonment of the agricultural fields, it is expected that the fringe will begin to expand and play a large role in colonization and influence the subsequent succession of the old fields. It will be interesting to see whether the groupings of species within the fringe are ultimately reflected as groupings within the subsequent old fields as succession occurs. These baseline data should be useful in answering this long-term question.

ACKNOWLEDGMENTS

The authors thank B. Isaac of CM as well as E. Zimmerman of the Western Pennsylvania Conservancy for plant identification assistance. We also thank B. Isaac and C. Morton for their help with herbarium specimens at CM. G Andraso and J Sacco provided helpful comments on the manuscript. Funding for this project was generously provided by a MiniGrant from the Presque Isle Partnership Environmental Research Committee, PA Sea Grant, and the Regional Science Consortium; a Faculty Research grant to M. Ganger; and the Biology Department at Gannon University.

LITERATURE CITED

Cadenasso, M.L. and Pickett, S.T.A. 2000. Linking forest edge structure to edge function: mediation of herbivore damage. Journal of Ecology 88:31-44.

Cadenasso, M.L. and Pickett, S.T.A. 2001. Effect of edge structure on the flux of species into forest interiors. Conservation Biology 15:91-97.

Cadenasso, M.L., Pickett, S.T.A., Weathers, K.C. and Jones, C.G. 2003. A framework for a theory of ecological boundaries. BioScience 53:750-758.

Colwell, R.K. 2005. EstimateS: Statistical estimation of species richness and shared species from samples. Version 7.5. Retrieved from a persistant URL <purl.oclc.org/estimates>.

Cook, W.M., Lane, K.T., Foster, B.L. and Holt, R.D. 2002. Island theory, matrix effects and species richness in habitat fragments. Ecology Letters 5:619-623.

Diekmann, M. 2003. Species indicator values as an important tool in applied plant ecology—a review. Basic and Applied Ecology 6:493-508.

DCNR. 2008. Master plan for Erie Bluffs State Park. http://www.dcnr.state.pa.us/stateparks/parks/eriebluffs/eriebluffs_masterplan_pdf.pdf. (Accessed November 8, 2011)

DCNR. 2011. DCNR invasive exotic plant tutorial for land managers. http://www.dcnr.state.pa.us/forestry/invasivetutorial/List.htm. (Accessed October 22, 2011)

Fauth, J.E., Bernardo, J., Camara, M., Resetarits, Jr., W.J., Van Buskirk, J. and McCollum, S.A. 1996. Simplifying the jargon of community ecology: a conceptual approach. American Naturalist 147:282-286.

Fike, J. 1999. Terrestrial and Palustrine Plant Communities of Pennsylvania. Pennsylvania Department of Conservation and Natural Resources. Harrisburg, PA.

Gascon, C., Lovejoy, T.E., Bierregaard, Jr., R.O., Malcolm, J.R., Stouffer, P.C., Vasconcelos, H.L., Laurance, W.F., Zimmerman, B., Toucher, M. and Borges, S. 1999. Matrix habitat and species richness in tropical forest remnants. Biological Conservation 91:223-229.

Gascon, C., Williamson, G.B. and da Fonseca, G.A.B. 2000. Receding forest edges and vanishing reserves. Science 288:1356-1358.

Gauch, Jr, H.G. 1982. Multivariate Analysis in Community Ecology. Cambridge University Press, Cambridge.

Gluvna, J. E. and Ganger, M.T. 2011. First-year colonization of an old field within the Erie Bluffs State Park in northwestern Pennsylvania. Journal of the Pennsylvania Academy of Science 85:81-87.

Godefroid, S. and Koedam, N. 2003. Distribution pattern of the flora in a peri-urban forest: an effect of the city—forest ecotone. Landscape and Urban Planning 65:169-185.

Greig-Smith, P. 1983. Studies in Ecology, Volume 9: Quantitative Plant Ecology, 3rd edition. Blackwell Scientific Publications, Great Britain.

Gustafson, E.J. and Gardner, R.H. 1996. The effect of landscape heterogeneity on the probability of patch colonization. Ecology 77:94-107.

Harper, K.A., MacDonald, E., Burton, P., Chen, J., Brosofske, K.D., Saunders, S.C., Euskirchen, E.S., Robers, D., Jaiteh, M.S. and Esseen, P.-A. 2005. Edge influence on forest structure and composition in fragmented landscapes. Conservation Biology 19:768-782.

Jules, E.S. and Priya, S. 2003. A broader ecological context to habitat fragmentation: why matrix habitat is more important than we thought. Journal of Vegetation Science 14:459-464.

Keddy, P.A. 1992. Assembly and response rules: two goals for predictive community ecology. Journal of Vegetation Science 3:157-164.

Laurance, W.F., Nascimento, H.E.M., Laurance, S.G., Andrade, A., Ewers, R.M., Harms, K.E., Luizão, R.C.C. and Ribeiro, J.E. 2007. Habitat fragmentation, variable edge effects, and the landscape-divergence hypothesis. PLoS ONE 2(10):e1017.

Malcolm, J. 1994. Edge effects in central Amazonian forest fragments. Ecology 75:2438-2445.

van der Maarel, E. 1990. Ecotones and ecoclines are different. Journal of Vegetation Science 1:135-138.

Matlack, G.R. 1993. Microenvironment variation within and among forest edge sites in the eastern United States. Biological Conservation 66:185-194.

McCune, B. and Grace, J.B. 2002. Analysis of Ecological Communities. MJM Software Design, Gleneden Beach, Oregon.

McCune B. and Medford M.J. 2006. Multivariate Analysis of Ecological Data. Version 5.31. MJM Software Design, Gleneden Beach, Oregon.

McGill, B.J., Enquist, B.J., Weiher, E. and Westoby, M. 2006. Rebuilding community ecology from functional traits. Trends in Ecology & Evolution 21:178-185.

Murcia, C. 1995. Edge effects in fragmented forests: implications for conservation. Trends in Ecology and Evolution 10:58-62.

Rhoads, A. F. & Block, T.A. 2007. The Plants of Pennsylvania: an Illustrated Manual, 2nd edition. University of Pennsylvania Press, Philadelphia.

Risser, P.G. 1995. The status of the science examining ecotones. BioScience 45:318-325.

Saunders, D.A., Hobbs, R.J. and Margules, C.R. 1991. Biological consequences of ecosystem fragmentation: a review. Conservation Biology 5:18-32.

Smith, R.L. 1996. Ecology and Field Biology, 5th edition. HarperCollins College Publishers. New York, NY.

Strayer, D.L., Power, M.E., Fagan, W.F., Pickett, S.T.A. and Belnap, J. 2003. A classification of ecological boundaries. BioScience 53:723-729.

Thiers, B. continuously updated. Index Herbariorum: A global directory of public herbaria and associated staff. New York Botanical Garden's Virtual Herbarium. http://sweetgum.nybg.org/ih. (Accessed November 8, 2011)

Thomas, D.J., Delano, H.L., Buyce, M.R. and Carter, C.H. 1987. Pleistocene and Holocene Geology of a Dynamic Coast. Guidebook for the 52nd Annual Field Conference of Pennsylvania Geologists. Bureau of Topographic and Geologic Survey. Fourth Series. Harrisburg, PA.

USDA, NRCS. 2011. The PLANTS Database (http://plants.usda.gov). National Plant Data Team, Greensboro, NC 27401-4901 USA. (Accessed June 20, 2011)

Western Pennsylvania Conservancy. 2005. Rapid Inventory and Assessment of Landscape, Ecological and Biodiversity Resources Relative to Management Options for Erie Bluffs State Park. Erie County Pennsylvania. Report to the Pennsylvania Department of Natural Resources, Office of Conservation Science.

Wyatt, S.W. 1947. Pattern and process in the plant community. Journal of Ecology 35:1-

Journal of the Pennsylvania Academy of Science 86(1): 24-29, 2012

LIPID HYDROPEROXIDE LEVELS, OXIDATIVE STATUS AND GLUCOSE ABSORPTION IN RODENTS FOLLOWING BDE-85 EXPOSURE[1]

MARY C VAGULA[2], NATHAN R KUBELDIS[2], CHARLES NELATURY[3]

[2]Biology Department, Gannon University, 109 University Square, Erie, PA 16541
[3]Biology Department, Penn State Behrend, 5091 Station Rd, Erie, PA

ABSTRACT

The Polybrominated Diphenyl Ethers (PBDEs) are a class of synthetic flame retardant compounds which are available in three commercial forms, penta BDEs, octa BDEs, and deca BDEs. Because of their extensive commercial use they have become widespread environmental contaminants. BDE-85 is a congener of the penta variety; to the best of the authors' knowledge there are no studies reported on the toxicity potential of this compound. This study reports the effects of BDE-85 on the oxidative stress and glucose absorption in rodents. Oxidative stress was measured using oxidative stress markers, lipid hydroperoxides in conjunction with activities of antioxidant enzymes, superoxide dismutase (SOD), glutathione peroxidase (GPx), glutathione-S-transferase (GST), and catalase in mice kidney and intestine tissues after exposure to 0.25 mg/kg body weight of BDE-85 via intraperitoneal route for four days. Mice tissues showed significant alterations ($p<0.05$) in the oxidative stress markers. Lipid hydroperoxide levels were elevated, indicating increased lipid peroxidation, while the activities of GPx, SOD, catalase and GST were reduced despite increased lipid peroxidation pointing to disruption in oxidant/antioxidant equilibrium. In addition to this, glucose absorption and Na^+/K^+ ATPase activities were studied in rats using isolated small intestinal segments exposed to 5 µg/mL of BDE-85 in vitro. The results showed a significant reduction (-63.97%) in the absorption of glucose through the small intestine along with decreased Na^+/K^+ ATPase activity, indicating significant disruption in the sodium-dependant glucose absorption process in the small intestine. [J PA Acad Sci 86(1): 24-29, 2012]

[1]Submitted for publication July 2012, accepted December 2012.
[2]Corresponding Author: Mary Vagula, Biology Department, Gannon University, 109 University Square, Erie, PA 16541, Telephone # 814-871-7572

INTRODUCTION

Polybrominated Dipenyl Ethers (PBDEs) are a class of organic flame retardant compounds used in various consumer products ranging from electronics to foam mattresses and upholstery. Due to their persistent nature they have become wide-spread environmental contaminants. These compounds are now present in detectable levels in the human population (Sjödin et al. 2008) as well as in soil, sediment, household dust, birds, fish and other terrestrial organisms (Belles et al. 2010). Although many congeners of PBDEs have now been banned, humans are currently still at risk of exposure to these compounds through existing consumer products through inhalation (Julander et al. 2005) or ingestion (Hayward et al. 2007).

PBDEs are available in three commercial forms namely, penta-BDEs, octa-BDEs, and deca-BDEs. Of the 46 possible congeners of penta-BDE, six are used extensively in commercial products including BDE-85 (Figure 1). Although there are some reports on the adverse effects of several congeners of PBDEs in experimental animals (Branchi et al. 2003, Giordano et al. 2008) there are none on the toxicity of BDE-85. BDE-85 has greater binding affinity to AhR (aryl hydrocarbon receptor) indicating a higher potential for toxicity than other PBDE compounds (Chen et al. 2001). Congener specific distribution and metabolism of PBDEs makes it even more important to consider differential toxicities when assessing the risk to human health. In addition, the exact mechanism of PBDE toxicity is currently

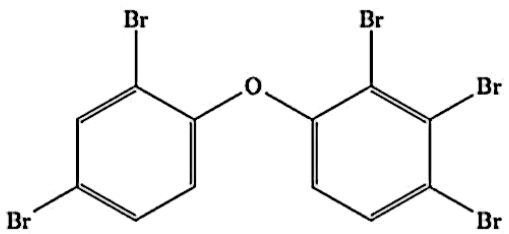

Figure 1. Chemical structure of BDE-85

unknown although it has been conjectured that PBDEs favor free radical formation by virtue of their electron-affinity (Zhao et al. 2008). In light of this, we have surmised oxidative stress induction following BDE-85 exposure in the mice. This is also based on a recent study showing the induction of oxidative stress in rat neurons exposed to BDE-47, which is another congener of penta BDE mixture (He et al. 2008).

In this in vivo study, the oxidative stress indicators such as lipid hydroperoxides (LOOHs), activities of superoxide dismutase (SOD), glutathione peroxidase (GPx), glutathione S-transferase (GST), and catalase (CAT) were analyzed in the kidney and intestines of BDE-85 treated mice. The intestines and kidney tissues were selected for this study due to their significant role in determining the body burdens of toxicants.

The second objective of this study is to examine the effects of BDE-85 on glucose absorption across the small intestine. Since the primary route of entry of PBDEs into the body is through ingestion, the authors intend to investigate the effects of BDE-85 on glucose absorption by looking into the in vitro intestinal transport of glucose and the activity of Na^+ K^+ APTase in the mucosal membranes of rat small intestine. The Na^+ K^+ ATPase is an enzyme known for its role in maintaining low intracellular sodium levels which in turn facilitate sodium-dependent glucose transport into the enterocytes.

MATERIALS AND METHODS

For this study, BDE-85 (purity 98%, certified standard) was procured from Cambridge Isotope Laboratories, Inc. Andover, MA, USA. Assay kits for determination of LOOH, SOD, GPx, GST, catalase, and glucose were obtained from Cayman Chemical Company, Ann Arbor, Michigan and BCA protein assay kits were purchased from Peirce Biotechnology, Rockford, IL, USA; all other chemicals were obtained from Sigma Aldrich Company, USA.

In this study, mice were used for studying oxidative stress and rats for glucose absorption. The gross intestinal structure of mice rendered a reliable glucose absorption assay infeasible and therefore precluded their use for glucose absorption study.

Male Swiss Webster mice were obtained from Taconic, Inc., Hudson, NY,USA. The mice weighing 33±3 grams were maintained at 23±2° C in a 12 hour light/12 hour dark photoperiods and were provided food pellets and water ad libitum. The care and use of the animals in the experiments was according to the guidelines set forth by the Institutional Animal Care and Use Committee (IACUC). Mice were acclimated to laboratory conditions for a period of 15 days before being randomly assigned into two experimental groups (n=9). Group 1 received intraperitoneal injections of 0.25 mg/kg body weight of BDE-85 for a period of four consecutive days. Group 2 was used as the control and received the same volume of corn oil. Oral route of administration was not considered for this part of the study as the aim of this study is to report the biochemical alterations induced at this particular concentration and administering via oral route results in elimination of some fraction of this chemical through feces. The dosage in this study was selected based on previous reports of other BDE studies in rodents (Belles et al. 2010, Albina et al. 2010, Cheng et al. 2009) and is commensurate with the average levels of PBDEs (excluding BDE-209) found in household dust (Toms et al. 2009). On the fifth day, mice were sacrificed; kidney and intestinal tissues were excised and washed in a phosphate buffer solution, and a 5% tissue homogenate was prepared using appropriate buffers.

All the assays (LOOHs, SOD, GPx, GST, catalase) were performed according to the protocols that were provided along with the assay kits (the protocols are also available at: www.caymanchem.com/app/template/productQualifiers,Home.vm). The protein content of the enzyme samples was assayed using Pierce® BCA Protein Assay Kit. Bovine serum albumin was used as the standard.

For the second part of the study, adult male Holtzman rats purchased from Harlan Laboratories Inc, Madison, Wisconsin, USA, were used. They were maintained in the same conditions as previously outlined for mice. To determine glucose absorption across the small intestinal wall, the everted sac technique was utilized. Rats (n=9) weighing 200±20 g were sacrificed and 15-20 cm duodenal segments were isolated and flushed using mammalian Ringer's solution. The segments were then everted and cut into two segments of equal length measuring between 6 and 8 centimeters each and randomly assigned one segment as control and the other as experimental. Experimental segments were submerged in 3 mL of mammalian Ringer's solution containing 5 µg/mL of BDE-85 and received constant aeration for 30 minutes. The dosage and exposure duration were based on study by Kodavanti and Ward (2005). The control segment was treated in the same manner in mammalian Ringer's solution without BDE-85.

To test for glucose absorption, control and experimental segments were removed from the Ringer's solution and ligated on one end; the other end was slid over a cannula attached to a stopper. The intestinal segments were then filled with a choline chloride buffer solution, placed in a muscle warmer containing 1% glucose, and incubated for 20 minutes at 37° C. Following incubation, the choline chloride solution is extracted and tested for glucose concentration.

The Na^+/K^+ ATPase activity was assayed in control and exposed (5 µg/mL of BDE-85 for 30 minutes) intestinal mucosal membranes. The intestinal segments were prepared in a manner similar to that used for glucose determination. The intestinal mucosa was scraped into a watch glass and rinsed with phosphate buffer solution and a 5% homogenate was prepared using SEID buffer. The homogenate was

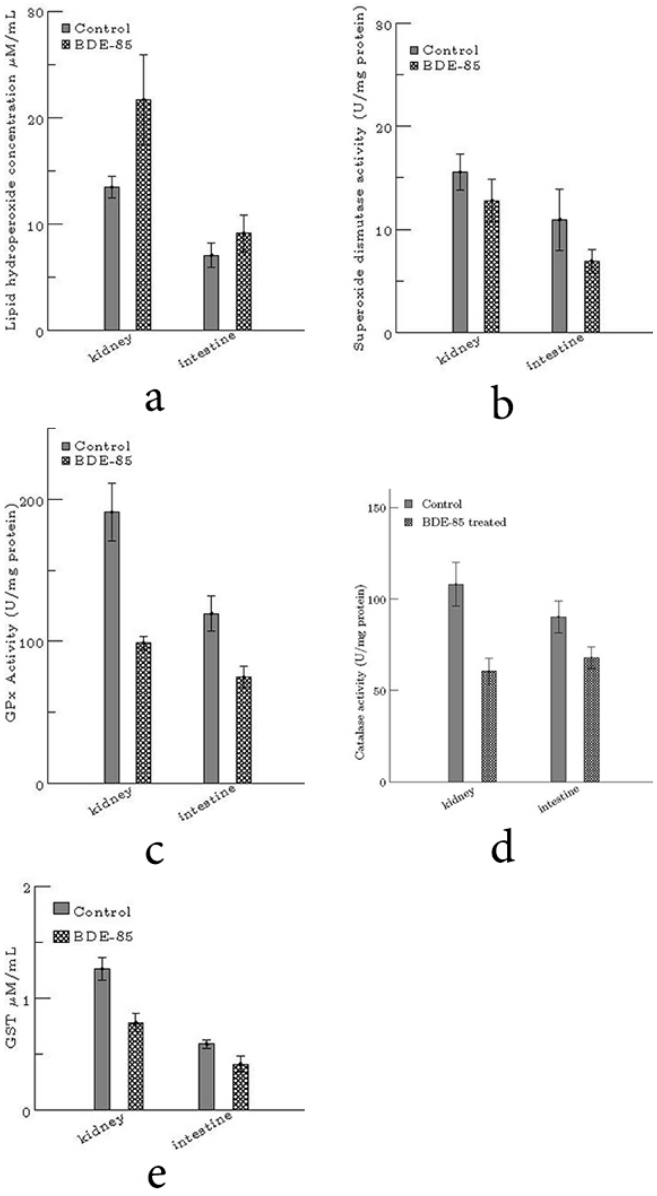

Figure 2. Oxidative stress markers in the kidney and small intestine of control and BDE-85 treated mice. Values are mean ±SD (n=9) and all the values are significant at p<0.05. (a) Lipid hydroperoxides (b) Superoxide dismutase (c) Glutathione peroxidase (d) Catalase (e) Glutathione S-transferase.

cold centrifuged at 4700xg and 4°C for 20 minutes, the supernatant was used as the enzyme source and the enzyme activity was assayed as described by Zaugg and McLain (1972) and modified by Finstad et al. (1989). The well known Fiske and Subbarow method (1925) was used to determine the inorganic phosphate released. The activity of the enzyme is given in µmol inorganic phosphate hydrolyzed from ATP per hour per mg protein. The protein content of the enzyme samples was assayed using Pierce® BCA Protein Assay Kit. Bovine serum albumin was used as the standard.

Data are presented in Figure 2a-e and Figure 3 as the mean ± SD of the nine animals in each group. The data was subjected to ANOVA; significantly different means were subjected to the Tukey test. A value of $p<0.05$ was considered significant.

RESULTS

Exposure of mice to BDE-85 at 0.25mg/kg bw for four days has resulted in a significant ($p < 0.05$) increase in LOOHs (Figure 2a) in both the tissues. The levels of LOOHs were increased by 61.02 % in the exposed kidney and 29.18% in the exposed intestines. The activities of all the enzymes studied in this work were significantly reduced ($p<0.05$) following exposure (Figure 2b-e). SOD was reduced by 17.91% in exposed kidney tissue, and by 36.62% decline in exposed intestinal tissue (Figure 2b). Similarly, GPx, which catalyzes the reduction of hydroperoxides, was lowered by 48.27% activity in exposed kidney tissue, whereas a decline of 39.5% activity is observed in exposed intestinal tissue (Figure 2c). CAT enzyme was also reduced, 44% in kidney and 24.71% in intestine (Figure 2d). Lastly, GST enzyme activity also was reduced; a 38.10% decline in exposed kidney tissue and a 30.51% decline in exposed intestinal tissue were noted (Figure 2e).

The glucose absorption in the exposed intestinal segments was reduced ($p<0.05$) by 63.97% (Figure 4a). To the best of the authors' knowledge there are no reports on PBDEs role in nutrient transport or absorption. The present study also observed a decrease (-37.93%) in the small intestine's mucosal Na^+ K^+ ATPase activity (4b).

DISCUSSION

Exposing mice to BDE-85 at 0.25mg/kg bw for four days has resulted in a significant ($p < 0.05$) increase in LOOHs (Figure 2a) in both the tissues. As LOOHs are the primary intermediates of lipid peroxidation process, their increase signifies increased lipid peroxidation process. Though both kidney and intestinal tissues showed a significant increase ($p<0.05$) in the levels of lipid hydroperoxides, the percent increase in kidney was doubly greater than that in intestine. This could be due to higher susceptibility of kidney or due to elevated levels of toxicant in kidney possibly due to its excretory role. Above all, this observation could be due to the intrinsic biochemical and functional differences between these organs. Similar results of increased free radicals and lipid peroxidation were noted in rat hippocampal neurons following BDE-47 exposure (He et al. 2008). In addition, reactive oxygen species (ROS) were detected in rats following exposure to BDE-99 (Belles et al. 2010, Albina et al. 2010) and BDE-71 (Giordano et al. 2008). The exact mechanism

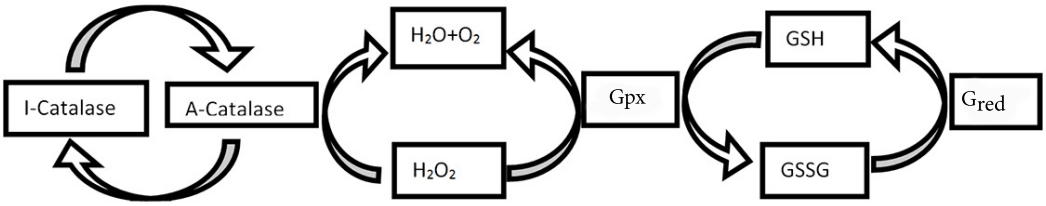

Figure 3: H_2O_2 is disposed by Catalase and GPx. Glutathione acts as an electron donor and is recycled by glutathione reductase (Gred). Auto-inactivation of catalase (I-catalase) by H_2O_2 is prevented by GPx, which maintains catalase in active form (A-catalase).

underlying ROS generation during PBDEs is not clear, but it is suggested that they act as electron acceptors in biological systems under standard conditions (Zhao et al 2008). Reports on PBDE exposure and their involvement in the release of [3H] arachidonic acid, protein kinase-C translocation and disruption in calcium homeostasis (Kodavanti and Derr-Yellin 2002, Kodavanti and Ward 2005) could further explicate the mechanism of ROS formation (He et al. 2008).

Although an increased lipid hydroperoxides and lipid peroxidation is noted in the tissues after BDE-85 exposure, there was no corresponding increase in the antioxidant enzymes to protect against the oxidative stress. Contrary to what could be reasonably expected of a healthy tissue, our observations showed a significant reduction of these enzyme activities (Figure 2b-e) following BDE-85 exposure. Significantly diminished activities of SOD, GPx, GST, and catalase enzyme indicated a decreased ability of both tissues to quench free radicals and alleviate oxidative stress.

SODs catalyze the dismutation of the superoxide anion to O_2 and H_2O_2 and GPx catalyzes the reduction of hydroperoxides and serves to protect the cell from the hostile free radicals. These two enzymes, which are indispensable in the cellular antioxidant defense mechanism, are reduced following BDE-85 exposure indicating the disruption in balance between oxidant and antioxidant forces in the cells and setting in severe oxidative stress. CAT enzyme was also reduced reflecting an inability of these tissues to eliminate hydrogen peroxide (Figure 2d). CAT and GPx exhibit a degree of cooperativity in their actions (Baud et al. 2004). Generally, during increased hydroperoxide formation catalase activity depends on GPx activity from being inactivated (Figure 3). In the face of decreased GPx activity in BDE-85 exposed tissue, the catalase might be inactivated by higher concentration of hydroperoxides. Lipid hydroperoxides act as "suicide substrates" at moderate to high concentrations and cause irreversible inactivation of catalase (Lardinois 1996). An example of this manner of catalase inactivation was seen in astrocytes with a deteriorated glutathione system (Sokolova et al. 2001). PBDEs are reported to perturb glutathione system (Belles et al. 2010, He et al. 2008). In the light of reduced GPx activity and disturbed glutathione system it is not surprising to see reduced catalase activity in exposed animal tissues.

Lastly, GST enzyme activity also was reduced (Figure 2e). Similar response of decreased antioxidant enzymes at 0.6mg/kg body weight was observed after BDE-99 exposure in rats (Belles et al. 2010). In another report on BDE-99, rat liver and kidney showed an upsurge of lipid peroxidation and unstable antioxidant system (Albina et al 2010) rendering support to our observations.

Another objective of this work is to observe the effect of BDE-85 on glucose transportation across the small intestines. The results of this study indicate a significant ($p<0.05$) decrease (-63.97%) in the transport of glucose (Figure 4a) across the small intestine. The present study also observed a decrease (-37.93%) in the small intestine's mucosal Na^+ K^+ ATPase activity (Figure 4b). Normally, glucose transportation from the intestinal lumen into the enterocyte is coupled with the transportation of sodium ions via SGLT (sodium dependent glucose transporters) transporters. A low intracellular sodium ion concentration is necessary for this transport which is achieved by the action of Na^+K^+ATPase. Any disruption in Na^+ K^+ activity leads to

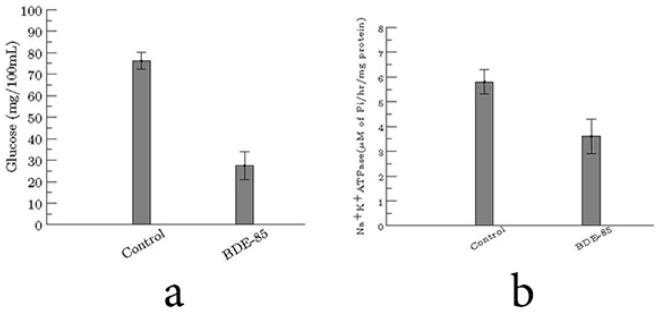

Figure 4. a) Glucose concentration in the control and BDE-85 treated small intestine segments of rats. Values are mean ±SD (n=9) and are significant at $p<0.05$. b) Na+K+ATPase activity in the control and treated small intestine mucosae. Values are mean ± SD (n=9) and are significant at $p<0.05$.

disruption in the sodium gradient across the intestinal lumen and enterocyte, leading to decreased glucose absorption. BDE-85 has resulted in decreased in Na^+ K^+ activity which might be the reason for observed reduction in glucose absorption. Similar inhibition in the intestinal Na^+K^+ ATPase was noted after CU, Zn, Cd and Pb exposure (Atli and Canli 2007). PCBs are reported to disrupt the Na^+K^+ ATPase activity by inducing oxidative stress (Sreedevi et al 2007). Based on the structural similarities of BDE-85 with PCBs and along with the observation of oxidative stress in mice intestinal tissue (Figure 2) in the first part of this study, we assume that the reduction in Na^+K^+ATPase might be due to oxidative stress in exposed rats intestinal segments. This study is first of its kind in reporting the impact of BDE-85 on nutrient absorption. Studies on toxicant impact on nutrient absorption are important as many of the developmental abnormalities noted in exposed neonatal animals could be due to impairment in nutrient absorption.

In summary, BDE-85 has a significant potential to bring about a severe oxidative stress in mice. When compared to the work of other researchers on the toxic effects of BDE-47 and BDE-99 (other penta BDE congeners), the present findings on the profile of BDE-85 stand consistent and appear to resonate the same theme that these fire retardants subject organisms to oxidative stress. Glucose transportation across the intestine and Na^+K^+ ATPase activity was significantly reduced. This observation is not reported for other BDEs. Further studies on ATP levels, absorption of amino acids and other nutrients and histological examinations during BDE-85 are warranted to explain the extent of disruption in absorptive process.

ACKNOWLEDGEMENTS

Mary Vagula thanks Gannon University for the award of faculty research grant. The authors also thank Dr. Michael Rutter, Penn State Behrend, for his help in the data analysis.

LITERATURE CITED

Albina ML, Alonso V, Linares V, et al. 2010. Effects of exposure to BDE-99 on oxidative status of liver and kidney in adult rats. Toxicology 271:(1-2)51-56.

Atli G, Canli M. 2007. Enzymatic responses to metal exposures in a freshwater fish *Oreochromis niloticus*. Comparative Biochemistry and Physiology Part C: Toxicology & Pharmacology 145(2):282-287.

Baud O, Greene AE, Li J, Wang H, Volpe JJ, Rosenberg PA. 2004. Glutathione Peroxidase–Catalase Cooperativity Is Required for Resistance to Hydrogen Peroxide by Mature Rat Oligodendrocytes. The Journal of Neuroscience 24(7):1531-1540.

Belles M, Alonso V, Linares V, Albina M, Sirvent JJ, DomingoJL, et al. 2010. Behavioral effects and oxidative status in brain regions of adult rats exposed to BDE- 99. Toxicology Letters 194(1-2):1-7.

Branchi I, Capone F, Alleva E, Costa LG. 2003. Polybrominated diphenyl ethers: neurobehavioral effects following developmental exposure. Neurotoxicology 24:449-462.

Chen G, Konstantinov AD, Chittim BG, Joyce EM, Bols NC, Bunce NJ. 2001. Synthesis of Polybrominated diphenyl ethers and their capacity to induce CYP1A by the Ah receptor mediated pathway. Environmental Science & Technology 35: 3749-3756.

Cheng J, Gu J, Ma J, Chen X, Zhang M, Wang W. 2009. Neurobehavioral effects, redox responses and tissue distribution in rat offspring developmental to BDE-99. Chemosphere. 75:963-968

Finstad B, Nilssen KJ, Arnesen AM. 1989. Seasonal chang es in the sea water tolerance of Archtic charr (Salvilinus alpinus). Journal of Comparative Physiology 159:371-378.

Fiske CH, Subbarow Y. 1925. The calorimetric determination of phosphorus. Journal of Biological Chemistry 66:375-400

Giordano G, Kavanagh TJ, Costa LG. 2008. Neurotoxicity of a polybrominated diphenyl ether mixture (DE-71) in mouse neurons and astrocytes is modulated by intracellular glutathione levels. Toxicology and Applied Pharmacology 232:161-168.

Hayward D, Wong J, Krynitsky AJ. 2007. Polybrominated diphenyl ethers and polychlorinated biphenyls in commercially wild caught and farm raised fish fillets in the United States. Environmental Research 103(1):46-54.

He P, He W, Wang A, Xia T, Xu B, Zhang M et.al. 2008. PBDE-47 induced oxidative stress, DNA damage and apoptosis in primary cultured rat hippocampal neurons. Neuro Toxicology 29(1):124-129

Julander A, Karlsson M, Hagstrom K, Ohlson CG, Engwall M, Bryngelsson IL, et al. 2005. Polybrominated diphenyl ethers--plasma levels and thyroid status of workers at an electronic recycling facility. International Archives of Occupational and Evironmental Health 78(7):584-592.

Kodavanti PR, Derr-Yellin, EC. 2002. Differential effects of polybrominated diphenyl ethers and polychlorinated biphenyl on [3 H] arachidonic acid release in rat cerebellar granule neurons. Toxicological Sciences 68:451-457.

Kodavanti PR, Ward TR. 2005. Differential effects of commercial polybrominated diphenyl and polychlorinated biphenyl mixtures on intracellular signaling in rat brain in vitro. Toxicological Sciences 85:952-962.

Lardinois OM, Mestdagh MM, Rouxhet PG. 1996. Reversible inhibition and irreversible inactivation of catalase in presence of hydrogen peroxide. Biochimica et Biophysica Acta 1295:222-238.

Sjödin A, Wong LY, Jones RS, Park A, Zhang Y, Hodge C, et al. 2008. Serum concentrations of polybrominated diphenylethers and polybrominated biphenyl in the United States population. Environmental Science & Technology 42(4): 1377-1384.

Sokolova T, Gutterer JM, Hirrlinger J, Hamprecht B, Dringen R. 2001. Catalase in astroglia-rich primary cultures from rat brain: immunocytochemical localization and inactivation during the disposal of hydrogen peroxide. Neuroscience Letters 297:129-132.

Sridevi N, Venkataraman P, Senthilkumar K, Krishnamoorthy G, Arunakaran J. 2007. Oxidative stress modulates membrane bound ATPases in brain regions of PCB (Aroclor 1254) exposed rats: protective role of alpha-tocopherol. Biomedicine and Pharmacotherapy 61(7):435-440.

Toms LL, Hearn L, Kennedy K, Harden F, Bartkow M, Temme C, Mueller JF. 2009. Concentrations of polybrominated diphenyl ethers in the matched samples of human milk, duct and indoor air. Environment International 35(6): 864-869.

Zaugg WS, Mclain LR. 1972. Changes in gill adenosine triphosphatase activity associated with parr-smolt transformation in steelhead trout, coho and spring Chinook salmon. Journal of the Fisheries Research Board of Canada 29:167-171.

Zhao YY, Tao FM, Zeng EY. 2008. Theoretical study on the chemical properties of polybrominated diphenyl ethers. Chemosphere 70:901–907.

Journal of the Pennsylvania Academy of Science 86(1): 30-35, 2012

LIGHT AND SCANNING ELECTRON MICROSCOPIC OBSERVATIONS OF THE CERCARIAE AND REDIAE OF *RIBEIROIA ONDATRAE*[1].

SHAMUS P. KEELER[2,4], BERNARD FRIED,[3] AND JANE E. HUFFMAN[2]

[2]*Fish & Wildlife Microbiology Laboratory, Department of Biological Sciences, East Stroudsburg University of Pennsylvania, East Stroudsburg, PA 18301*
[3]*Department of Biology, Lafayette College, Easton, PA 18042*

ABSTRACT

***Ribeiroia ondatrae* (Price, 1931) is a digenetic trematode occurring in lentic aquatic systems throughout North and South America and has been identified as a cause of limb malformations in numerous species of amphibians. Several questions still remain related to basic morphology of the various life stages of *R. ondotrae*. The purpose of this study was to describe the daughter rediae and cercariae of *R. ondatrae* using light and scanning electron microscopy. *Helisoma trivolvis* snails infected with *R. ondatrae* were collected from Delaware Lake, NJ. Daughter rediae and cercariae were collected from the infected snails, and light and scanning electron microscopy were used to describe the life stages with particular focus on the tegumentary surface. The tegument of *R. ondatrae* rediae and cercariae is aspinose despite reports in the literature describing a spinose tegument in the cercariae. The rediae and cercariae were observed to be much simpler in tegumentary structure than various species of Echinostoma that have been studied recently with scanning electron microscopy.**
KEYWORDS: *Ribeiroia ondatrae*, scanning electron microscopy, light microscopy, cercariae, rediae, tegument
[J PA Acad Sci 86(1): 30-35, 2012]

INTRODUCTION

Ribeiroia ondatrae (Price 1931) is a digenetic trematode of the family Psilostomidae, which occurs in lentic aquatic systems throughout North and South America (Johnson et al. 2004; Wilson et al. 2005). The life cycle of *R. ondatrae* includes planorbid snails as the first intermediate host, amphibians and fish as the second intermediate host, and birds and mammals as the definitive host (Beaver 1939; Johnson et al. 2004). *Helisoma trivolvis* has been reported to serve as the first intermediate host for *R. ondatrae* in Pennsylvania, USA (Schmidt and Fried 1997; Klockars et al. 2007).

Beginning in 1990, *R. ondatrae* infection has been implicated as a cause of limb malformations in numerous species of amphibians (Sessions and Ruth 1990; Johnson et al. 1999, 2001, 2002; Sessions et al. 1999). Other potential causes for the deformities include chemical toxins such as pesticides and hormone mimics, and UV-B radiation (Blaustein and Johnson 2003; Kiesecker 2002; Taylor et al. 2005). Several mass malformation events have been linked to trematode infections and many experimental infections have produced significant frequencies of deformities and mortality (Sessions and Ruth 1990; Johnson et al. 1999, 2001, 2002). Since the discovery of the potential link between *R. ondatrae* and limb malformations in amphibians, extensive research has been done on the ecological and environmental factors contributing to these deformities and to the mechanism of action of the parasite. Despite this increase in research, some questions still remain related to basic morphology of the cercariae of *R. ondatrae.*

The cercariae of *R. ondatrae* have been described extensively in previous literature but no one has reported the dimensions of the cercariae and conflicting reports exist about the tegumentary surface (Beaver 1939; Johnson et al. 2004). The tegument of *R. ondatrae* has been reported as lacking spines (Faust and Hoffman 1934; Fain 1953) but Ostrowski de Núñez et al. (1991) reported *R. ondatrae* as having a spined tegument. Additionally, spines have been described along the margin of the ventral sucker and this feature has been proposed as a diagnostic feature to differentiate *R. ondatrae* from *R. marini* (Basch and Sturrock 1969) but Johnson et al. (2004) reported a lack of spines along the margin of the ventral sucker and instead observed papillae. The purpose of this study was to describe the cercariae of *R. ondatrae* using light and scanning electron microscopy with particular focus on the tegument.

[1]Submitted for pulication June 2012; accepted October 2012.
[4]Corresponding author: Southeastern Cooperative Wildlife Disease Study (SCWDS), Department of Population Health, 589 D.W. Brooks Drive, College of Veterinary Medicine, University of Georgia, Athens, GA 30602, Phone 706-542-1741, Fax 706-542-5865, email: skeeler@uga.edu

MATERIALS AND METHODS

Helisoma trivolvis were collected from Delaware Lake (40°55′19.1 N; 75°03′49.5 W) located in Warren County, New Jersey from April 2006 to May 2007. Snails were collected by hand and transported back to the lab in coolers. Infected snails were identified and cercariae collected following previously described methods within 24hrs of collection (Klockars et al. 2007). All cercariae were examined using a compound microscope at 100x and 400x. Cercariae of *R. ondatrae* were identified using the genus specific characteristics defined by Johnson et al. (2004). Five of the snails suspected of being infected with *R. ondatrae* were crushed and the rediae were isolated for DNA extraction. Free swimming psilostome cercariae were also collected for DNA extraction.

DNA was extracted from the cercariae and rediae using the MoBio Ultraclean Tissue DNA Isolation Kit (MoBio Laboratories Inc, Carlsbad, CA). The intertranscribed spacer region 2 (ITS2) of the ribosomal gene complex was targeted using the primer set 3S (5' GGT ACC GGT GGA TCA CGT GGC TAG TG 3'; Bowles et al. 1995) and ITS2.2 (5' CCT GGT TAG TTT CTT TTC CTC CGC 3'; Hugall et al. 1999). Promega Master Mix (Promega Corporation, Madison WI) was used for all PCR reactions at 25µL reaction volume with template and primer concentrations based on manufactures recommendations. PCR was performed using the following thermocycler protocol: initial denaturation at 95ºC for 5 min, then 30 cycles of 95ºC for 30 sec, 57.6ºC for 30 sec, and 72ºC for 1.5 min, with a final extension of 72ºC for 7 min. PCR product was visualized using a 3% agarose gel for the presence of a 429bp. The PCR products were purified using the DyeEx 2.0 Spin Kit (Qiagen Inc., Valencia, CA) following the manufactures protocol. The purified product was sequenced using Big Dye Terminator v3.1 Cycle Sequencing Kit (Applied Biosystems, Forest City, CA) on an AB 3130 Genetic Analyzer (Applied Biosystems, Forest City, CA) following the manufactures protocol. The sequences were compared to GenBank sequences using the basic local alignment tool (BLAST) (Altschul et al. 1990) based on the nucleotide-nucleotide BLAST search (blastn) with the default settings. BioEdit Sequence Alignment Editor was used to directly compare the project sequences to *R. ondatrae* ITS2 sequences from GenBank (Hall 1999).

Ribeiroia ondatrae cercariae were fixed in 10% neutral buffered formalin for 1-2 hours. Fixed cercariae were mounted onto slides and measured under a compound microscope at 100x using an ocular micrometer. For the rediae the total length, total width, and the pharyngeal width were measured, and the number of cercariae was recorded. For the cercaria, the body length, body width, tail length, and tail width at base were measured. The average, standard deviation, and range were determined for each measurement using Microsoft Excel.

Free swimming *R. ondatrae* cercariae and daughter rediae were collected and fixed in 3% gluteraldehyde in 0.2M phosphate buffer (pH 7) for 24 hours. The samples were dehydrated in a graded ethanol series (70%, 85%, 90%, and 100%) and post fixed with 1% osmium tetraoxide for 1-2 hours. The samples were again dehydrated in a graded ethanol series (70%, 85%, 90%, and 100%). The samples were immersed into examethyldisilazane (HMDS) (Polysciences, Inc, Warrington, PA) for 15 minutes and then allowed to air dry. Samples were attached to stainless steel stubs using double sided tape and sputter coated with gold palladium. All samples were examined with an Amray 1810 Scanning Electron Microscope at an acceleration of 20kV at varying magnifications.

Table 1. Average length, width, pharyngeal diameter, and number of cercariae for 60 *Ribeiroia ondatrae* rediae from Delaware Lake, Warren County, NJ.

	Length (µm)	Width (µm)	Pharyngeal Diameter (µm)	Number of Cercaria
Average	1068.7	191.5	40.8	4.2
Standard Deviation	279.5	46.2	9.9	1.6
Range	495 - 1680	120 - 305.7	23.1 - 60	2.0 - 8.0

Table 2. Average body length, body width, tail length, and tail width at base for 50 *Ribeiroia ondatrae* cercariae from Delaware Lake, Warren County, NJ.

	Body Length (µm)	Body Width (µm)	Tail Length (µm)	Tail Width at Base (µm)
Average	252.3	153.1	521.3	35.5
Standard Deviation	24.8	12.3	49.7	9.0
Range	219.2 - 311.5	121.2 - 173.1	392.3 - 605.8	23.1 - 59.1

RESULTS

The ITS2 region of *R. ondatrae* was successfully sequenced for the rediae collected from the 5 psilostome infected snails. All five sequences were a 100% match to a *R. ondatrae* ITS2 sequence (Accession Number AY761142) from GenBank.

Sixty daughter rediae and fifty cercariae were isolated from *R. ondatrae* infected *H. trivolvis* and measured. The results are summarized in Tables 1 and 2. Many of the redial measurements have been performed on members of the closely related trematode family Echinostomatidae, which has a morphologically similar redia. The redial length of *R. ondatrae* (1069 ± 280µm) is larger than that reported for *Echinostoma trivolvis* (701 ± 19µm) and *E. caproni* (992 ± 300µm) (Krejei and Fried 1994; Fried and Awatramani 1992). The redial widths of both *E. trivolvis* (221 ± 6µm) and *E. caproni* (278 ± 51µm) are larger than that of *R. ondatrae* (192 ± 46µm) (Krejei and Fried 1994; Fried and Awatramani 1992). The pharyngeal diameter of *R. ondatrae* (41 ± 10µm) is smaller than *E. caproni* (56 ± 10µm) but consistent with *E. trivolvis* (40.2 ± 1.1µm) (Krejei and Fried 1994; Fried and Awatramani 1992). A similar number of mature cercariae were reported in *E. caproni* (4.8 ± 1.4) compared to *R. ondatrae* (4.2 ± 1.6) but *E. trivolvis* (3.2 ± 1.1) is reported to have less cercaria (Krejei and Fried 1994; Fried and Awatramani 1992). The cercaria of *R. ondatrae* are morphologically distinct from the Echinostomatidae and based on our results, larger in length and width (Toledo et al. 2000).

As previously reported, the daughter rediae of *R. ondatrae* had a mouth at the anterior followed by a four-lobbed collar with a birth papilla and two ambulatory buds, and the papilliform process at the posterior (Figure 1A). The mouth of the daughter rediae was observed to be surrounded by tegumentary ciliated papillae (Figure 1B). Longitudinal ridges were observed inside the mouth at the anterior portion of the pharynx (Figure 1B). Posterior to the mouth, the tegument was folded into transverse rings (Figure 1C). The characteristic four-lobbed collar was observed slightly posterior to the mouth (Figure 1C). Transverse rings were observed anterior and posterior to the lobed collar (Figure 1D). The transverse ring pattern did not continue over the surface of the lobes (Figure 1D-E). The tegument of the lobes had a series of folds with no distinct pattern (Figure 1D). A birth papilla was observed directly posterior to the four-lobbed collar (Figure 1C). The surface of the birth papilla was not folded but spherical structures and microvilli-like structures were observed on the surface of the birth papilla (Figure 1E). A pair of ventral ambulatory buds was observed (Figures 1F). The base of the ambulatory buds was covered in transverse folds and the remaining portions had a ridged tegument (Figure 1F). The transverse folds extended the length of the redia to the base of the papilliform process (Figure 1G). The surface of the papilliform process was folded (Figure 1G).

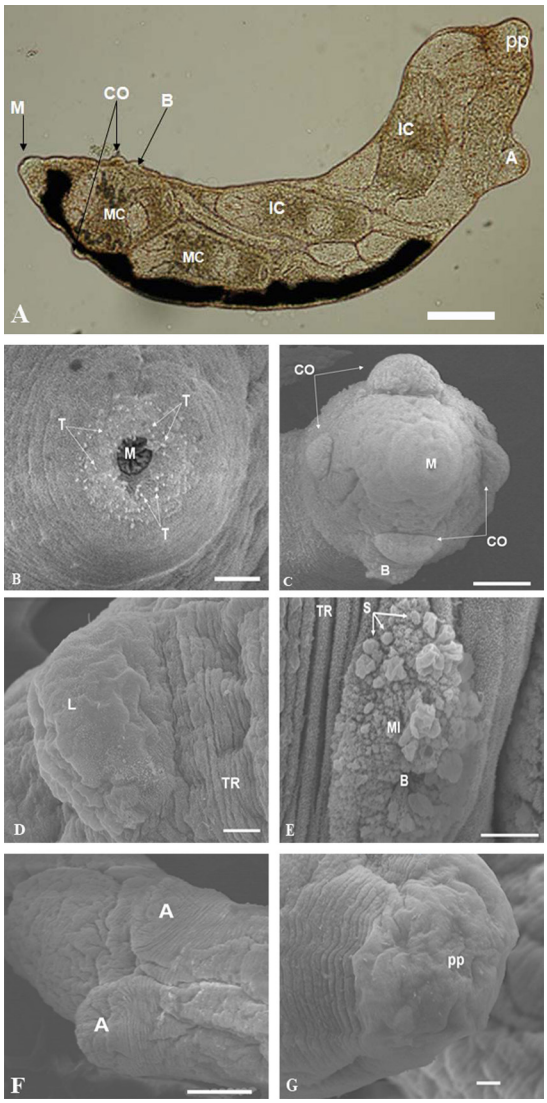

Figure 1. A.) Light micrograph of daughter redia of *Ribeiroia ondatrae* showing mouth (M), lobed collar (CO), birth papillae (B), ambulatory buds (A), posterior papillary process (pp), mature cercaria (MC), and immature cercaria (IC). Bar = 100µm. B.) Scanning electron micrograph of the anterior portion of the daughter redia. The mouth (M) surrounded by integumentary ciliated papillae (T). Longitudinal ridges (LR) are clearly visible at the anterior portion of the pharynx. Bar = 10µm. C.) Scanning electron micrograph of the anterior portion of the daughter redia. The collar (CO) of the daughter redia has a four-lobbed shape. The collar (CO) is slightly posterior to the mouth (M) and directly anterior to the birth papilla (B). Transverse rings are visible across the body of the rediae posterior to the mouth. Bar = 50µm. D.) Scanning electron micrograph of a lobe (L) of the collar of the daughter redia. The transverse ring (TR) pattern of the tegument is clearly visible. Bar = 10µm. E.) Scanning electron micrograph of the birth papilla (B). Spherical structures (S) and microvilli-like structures (MI) can be observed on the surface of the birth papilla. The transverse rings (TR) of the tegument surface are clearly visible. Bar = 10µm. F.) Scanning electron micrograph of the ventral portion of the redia showing the ambulatory buds (A) with the transverse ring pattern continuing onto buds. Bar = 50µm. G.) Scanning electron micrograph showing the posterior papilliform process (pp) of the daughter redia. Bar = 10µm.

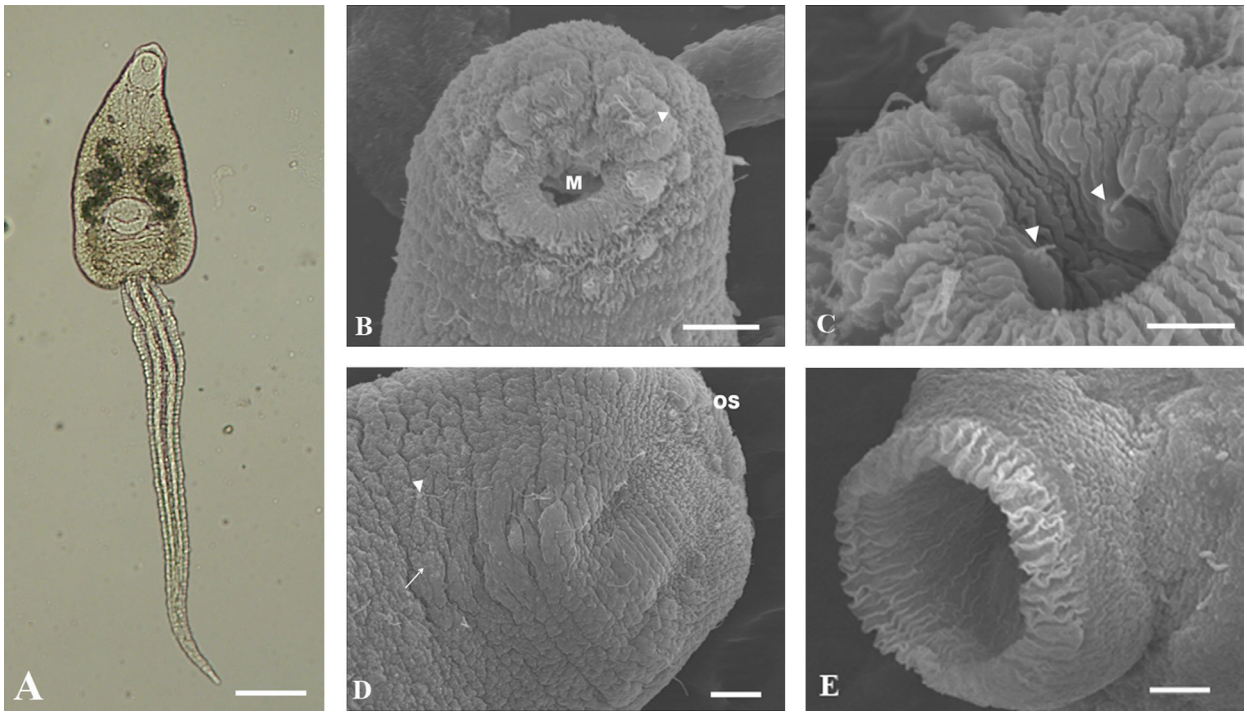

Figure 2. A.) Light micrograph of the *Ribeiroia ondatrae* cercaria. Bar = 100µm. B.) Scanning electron micrograph of the anterior portion of the cercaria (1,880x). Unicilliated papillae (arrow head) were observed surrounding the mouth (M). A large concentration was observed at the anterior margin of the mouth. Bar = 10µm. C.) Scanning electron micrograph of the anterior portion of the oral sucker (4,160x). Paired unicilliated papillae (arrow head) were observed on longitudinal ridges running into the mouth of the cercaria. Bar = 5µm. D.) Scanning electron micrograph of the anterior-dorsal portion of the cercarial body (1,210x) with the oral sucker (OS) labeled for reference. Very broad ridges were observed along the dorsal body with numerous unicilliated papillae (arrow head) and spherical bodies (arrow). Bar = 10µm. E.) Scanning electron micrograph of the acetabulum (1,300x). Bar = 10µm.

SEM observations of the oral sucker, ventral sucker, body and tail of *R. ondatrae* cercariae were performed. No spines were observed anywhere on the cercariae. Uniciliated papillae were observed surrounding the mouth with a large concentration at the anterior portion of the mouth (Figure 1A). The outer margin of the oral sucker has a transverse ridged pattern (Figure 1A). Two sets of paired uniciliated papillae were observed on longitudinal ridges running into the mouth of the cercariae (Figure 1B). The tegument surrounding the outer margin, directly anterior to the oral sucker had spherical structures. Uniciliated papillae and spherical bodies were observed over the length of the cercariae (Figure 1C). The body of the cercariae was observed to be relatively smooth with very broad ridges (Figure 1C). No multiciliated papillae were observed anywhere on the cercariae. No ciliated papillae were observed around the acetabulum (Figure 1D). Longitudinal ridges were observed on the lip and the inner portion of the acetabulum (Figure 1D). Fin folds were observed on the tail of the cercaria starting at the base and running almost to the tip. The tail was covered in transverse ridges with no ciliated papillae and fin folds extending along both sides of the anterior three quarters of the tail.

DISCUSSION

The tegumentary structure of the rediae of *R. ondatrae* has not been previously described. The tegument is similar to other trematode species; transverse folds were seen along the entire length of the rediae (Fujino and Ichikawa 2000). Uniciliated papillae were seen only around the mouth of the rediae. The uniciliated papillae are sensory structures and have been seen in other trematode species (Fujino and Ichikawa 2000). The function of the spherical bodies seen surrounding the birth papillae is unknown but it has been proposed they are involved in the expulsion of waste material (Fujino and Ichikawa 2000). Microvilli-like structures have been reported from the entire length of other species of trematode (Fujino and Ichikawa 2000). In *R. ondatrae*, microvilli-like structures were only seen on the birth papillae. The microvilli-like structures may allow for expansion of the birth papillae during the release of cercariae. The distal portion of the lobed collars and the ambulatory buds was observed to have a ridged tegumentary structure, which was devoid of other structural features. The lack of transverse folds at the distal portion of these structures may relate to use of these structures for locomotion and positioning within

the snail.

The tegument of *R. ondatrae* cercariae has been reported to be spinose (Ostrowski de Núñez et al. 1991) but other authors have also described the tegument as aspinous (Faust and Hoffman 1934; Fain 1953). Spines or papillae have been reported around the margin of the ventral sucker (Basch and Sturrock 1969). The SEM observations during this study found no spines over the length of cercarial body or along the margin of the ventral sucker consistent with reports by Faust and Hoffman (1930) and Fain (1953). Additionally, no papillae were observed around the margin of the ventral sucker as reported by Johnson et al. (2004). Longitudinal ridges were observed along the outer lip of the ventral sucker and may look similar to spines when observed with light microscopy. Very broad, and smooth transverse ridges or folds were observed along the body of the cercariae. No multiciliated papillae were observed anywhere on the cercariae. Uniciliated papillae were observed over the entire cercarial body with a dense concentration found around the oral sucker. The cilia observed on the cercariae were much longer than those observed around the mouth of the rediae. The two sets of paired uniciliated papillae were on longitudinal ridges running into the mouth of the cercariae. The uniciliated papillae have a sensory function and aide the cercariae as it actively quests for a second intermediate host and for an encystment site on that host. Very small spherical bodies were also observed on the tegument of the cercariae. These spherical bodies have been observed in other species of trematode but the exact function is unknown (Fujino and Ichikawa 2000).

The measurements of the rediae and cercariae presented in this study represent the average values for the *R. ondatrae* found in Delaware Lake. These measurements are a step toward a greater understanding of *R. ondatrae* and may be beneficial for differentiating between species of *Ribeiroia* or for identifying potential geographic differences within the different *Ribeiroia* species. The tegument of *R. ondatrae* rediae and cercariae is aspinose despite reports in the literature describing a spinose tegument in the cercariae. The rediae and cercariae were observed to be much simpler in tegumentary structure than trematodes of the family Echinostomatidae.

LITERATURE CITED

Altschul, S.F., W. Gish, W. Miller, E.W. Myers, and D.J. Lipman. 1990. Basic local alignment search tool. J. Mol. Bio. 215: 403-410.

Basch, P.F., and R.F. Sturrock. 1969. Life history of Ribeiroia marini (Faust and Hoffman, 1934) comb. n. (Trematoda: Cathaemasiidae). J. Parasitol. 55: 1180-1184.

Beaver, P.C. 1939. The morphology and life history of Psilostomum ondatrae Price 1939 (Trematoda: Psilostomidae). J. Parasitol. 25: 383-393.

Blaustein, A.R. and P.T.J. Johnson. 2003. The complexity of deformed amphibians. Front. Ecol. Environ. 1:87-94.

Bowles, J, D. Blair, and D.P. McManus. 1995. A molecular phylogeny of the human schistosomes. Mol. Phylogenet. Evol. 4:103-109.

Fain, A. 1953. Contribution a l'etude des formes larvaires des Trematodes au Congo belge et specialement de la larve de Schistosoma mansoni, Memoires, Institute Royal Colonial Belge. Section des Sciences Naturelles et Medicales 22:1-312.

Faust, E.C., and W.A. Hoffman. 1934. Studies on schistosomiasis mansoni in Puerto Rico. J. Pub. Health Trop. Med. 10:1-47.

Fried, B. and R. Awatramani. 1992. Light and scanning electron microscopical observations of the daughter rediae of Echinostoma trivolvis (Trematoda). Parasitol. Res. 78: 257-259.

Fujino, T., and H. Ichikawa. 2000. Ultrastructural studies on echinostomes. In: Fried B., Graczyk, T.K. (eds).Echinstomes as Experimental Models for Biological Research. Springer, New York. pp. 119-136.

Hall, T.A. 1999. BioEdit: a user-friendly biological sequence alignment editor and analysis program for Windows 95/98/NT. Nucl. Acids Sympos. Ser. 41:95-98.

Hugall, A., J. Stanton, and C. Moritz. 1999. Reticulate evolution and the origins of ribosomal internal transcribed spacer diversity in apomictic Meloidogyne. Mol. Biol. Evol. 16: 157-164.

Johnson, P.T.J., K.B. Lunde, E.G. Ritchie, and A.E. Launer. 1999. The effect of trematode infection on amphibian limb development and survivorship. Science 284: 802-804.

Johnson, P.T.J., K.B. Lunde, R.W. Haight, J. Bowermannm, and A.R. Blaustein. 2001. Ribeiroia ondatrae (Trematoda: Digenea) infection induces severe limb malformations in western toads (Bufo boreas). Can. J. Zoolog. 79: 370-379.

Johnson, P.T.J., K.B. Lunde, E.M. Thurman, E.G. Ritchie, S.W. Wray, S.R. Sutherland, J.M. Kapfer, T.J. Frest, J. Bowerman, and A.R. Blaustein. 2002. Parasite (R. ondatrae) infection linked to amphibian malformations in the western US Ecolog. Mongraphs 72: 151-168.

Johnson, P.T.J., D.S. Sutherland, J.M. Kinsella, and K.B. Lunde. 2004. Review of the trematode genus Ribeiroia (Psilostomidae): Ecology, life history, and pathogenesis with special emphasis on the amphibian malformation problem. Adv. Parasitol. 57: 191-253.

Kiesecker, J.M. 2002. Synergism between trematode infection and pesticide exposure: A link to amphibian deformities in nature? Proc. Natl. Acad. Sci. 99:9900-9904.

Klockars, J.L., J.E. Huffman, and B. Fried. 2007. Survey of Seasonal Trematode Infections in Helisoma trivolvis (Gastropoda) from Lentic Ecosystems in New Jersey, U.S.A. Comp. Parasitol. 74:75-80.

Krejei, K.G., and B. Fried. 1994. Light and scanning electron microscopic observations of the eggs, daughter rediae, cercariae, and encysted metacercariae of Echinostoma trivolvis and E. caproni. Parasitol. Res. 80:42-47.

Ostrowski de Núñez, M., M.I. Hamann, and A. Rumi. 1991. Population dynamics of planorbid snails from lentic biotope in northeastern Argentina. Larval trematodes of Biomphalaria occidentalis and analysis of their prevalence and seasonality. Acta Parasitol. Polonica 36:159-166.

Price, E.W. 1931. Four new species of trematode worms from the muskrat, Ondrata zibethica with a key to the trematode parasites of the muskrat. Proc. US Natl. Mus. 79: 1-13.

Schmidt, K.A., and B. Fried. 1997 Prevlance of larval trematodes in Helisoma trivolvis (Gastropoda) from a farm pond in Northampton, County, Pennsylvania with special emphasis on Echinostoma trivolvis (Trematoda) cercariae. J. Helminthol. Soc. Wash. 64: 157-159.

Sessions, S.K., and S.B. Ruth. 1990. Explanation for naturally occurring supernumerary limbs in amphibians. J. Exper. Zoolog. 254:38-47.

Sessions, S.K., R.A. Franssen, and V.L. Horner. 1999. Morphological clues from multilegged frogs: are retinoids to blame? Science 284: 800-802.

Taylor, B., D. Skelly, L.K. Demarchis, M.D. Slade, D. Galusha, and P.M. Rabinowitz. 2005. Environmental Health Perspectives 113: 1497-1501.

Toledo, R., C. Munoz-Antoli, and J.G. Esteban. 2000. The life-cycle of Echinostoma friedi n. sp. (Trematoda: Echinostomatidae) in Spain and a discussion on the relationships within the `revolutum' group based on cercarial chaetotaxy. Syst. Parasitol. 45: 199-217.

Wilson, W.D., P.T.J. Johnson, D.R. Sutherland, H. Mone, and E.S. Loker. 2005. A molecular phylogenetic study of the genus Ribeiroia (Digenea): Trematodes known to cause limb malformations in amphibians. J. Parasitol. 91: 1040-1045.

Journal of the Pennsylvania Academy of Science 86(1): 36-40, 2012

THE IMPACT OF WOOD TYPE, SEASON, AND REPELLENT USE ON NORTH AMERICAN PORCUPINE DAMAGE[1]

ANDIE S. GRAHAM, KEELY TOLLEY ROEN[2]

The Pennsylvania State University, DuBois Campus, 1 College Place, DuBois, PA 15801

ABSTRACT

We evaluated the impact of wood type, season, and repellent use on North American Porcupine damage to forty installed posts along Rails-to-Trails property in Brockway, Pennsylvania, USA. Treatments were (1) pressure-treated Pine posts with Ro-Pel (a liquid repellent), (2) pressure-treated Pine posts without Ro-Pel, (3) Black Locust posts with Ro-Pel, and (4) Black Locust posts without Ro-Pel. We assessed new damage to posts 1 – 4 times per month from June 2007 – January 2009. All damage was to Pine posts ($\bar{x}$ = 12.9 cm2, SE = 3.70 cm2) and no damage was observed to Black Locust posts. Observed damage to untreated posts ($\bar{x}$ = 9.93 cm^2, SE = 2.10 cm^2) was 3.3 times greater than damage to posts treated with Ro-Pel ($\bar{x}$ = 2.99 cm^2, SE = 2.86 cm^2). Total monthly damage to Pine posts was greatest in August ($\bar{x}$ = 2.31 cm^2, SE = 1.51 cm^2) and there was no observed damage in February, October, and November. When examining damage by season, damage to Pine posts was 54 times greater in summer (June – August; $\bar{x}$ = 1.62 cm^2, SE = 0.567 cm^2) than in fall (September – November; $\bar{x}$ = 0.030 cm^2, SE = 0.030 cm^2). We suspect the seasonality observed may be related to salt loss and salt-seeking behavior. We suggest that landowners and managers who anticipate Porcupine damage consider using alternatives to pressure-treated Pine for their wooden structures. In addition, repellent applications could be timed to correspond with the peak of damage to reduce cost. [J PA Acad Sci 86(1): 36-40, 2012]

INTRODUCTION

Erethizon dorsatum Linnaeus (North American Porcupines) chew and consume wooden structures and unconventional items such as bottles, automobile tires, aluminum kettles, plastic tubing (Merritt 1987), and tool handles (especially those that have come in contact with human perspiration) (Whitaker 1996). Traditional Porcupine damage management has focused on lethal methods (Schemnitz 1994, Witmer and Pipas 1998), which may not be desirable or tolerated, especially on recreational land. Witmer and Pipas (1998) called for more research on the development of effective, non-lethal methods to reduce Porcupine damage and Wagner and Nolte (2000) suggested that chemical repellents may be a practical alternative.

There are no registered repellents labeled to deter Porcupine damage in the United States. Although multiple home remedies (e.g., capsaicin or thiram) and commercial repellents are available, few studies evaluate their efficacy in deterring Porcupine damage (Witmer and Pipas 1998). We chose to test the efficacy of Ro-Pel Liquid Repellent™ (Ro-Pel, Nixalite of America, Inc., East Moline, Illinois) because it is advertised as a non-toxic, odorless way to deter animal, rodent, and bird damage. Ro-Pel contains 0.065% denatonium and 0.035% thymol and has a strong bitter taste (Nixalite of America 2009).

Porcupines caused significant damage to wooden bridges and signs along the Brockway, Pennsylvania, USA, portion of Rails-to-Trails (RTT). At the request of RTT, we initiated a study to evaluate the impact of wood type and repellent use on Porcupine damage. We contrasted *Pinus spp.* Linnaeus (Pine) and *Robinia pseudoacacia* Linnaeus (Black Locust) because of visible existing damage to Pine structures used by RTT, the documented damage to Pine in several North American studies (as reviewed by Witmer and Pipas 1998), the presence of several undamaged fences constructed of Black Locust near the bridges, and Black Locust's rot resistant properties and relative hardness (McAlister 1971).

In April 2007, we assessed an 8 km portion of RTT in Brockway, Jefferson County, Pennsylvania, USA, for Porcupine damage. Suspected Porcupine damage was confirmed through the examination of teeth and claw marks on bridges and signs, as well as a large number of Porcupine tracks, quills, and feces. The highest concentration of damage was around two bridges, approximately 1 km apart, constructed of pressure-treated Pine in the early 1990s (J. Farr, Rails-to-Trails, pers. comm., 2007). The bridges, appropriate for foot and bicycle traffic, spanned Toby Creek which intersects the Brockway portion of RTT. The trail

[1]Submitted for publication April 2012; accepted August 2012.
[2]Corresponding author – kat175@psu.edu; 814-372-3003

is bordered by mixed deciduous-coniferous forest with large stands of *Pinus strobus* Linnaeus (White Pine), *Tsuga canadensis* Linnaeus (Eastern Hemlock), *Acer saccharum* Marsh (Sugar Maple), *Prunus serotina* Ehrh. (Black Cherry), *Fagus grandifolia* Ehrh. (American Beech), *Quercus spp.* Linnaeus (Oak), and *Populus spp.* Linnaeus (Aspen), as well as large rocky outcrops, making the area suitable Porcupine habitat (Whitaker 1996).

MATERIALS AND METHODS

Our experiment had two factors (wood type and repellent use) and each factor had two levels. Treatments were (1) pressure-treated Pine posts with Ro-Pel, (2) pressure-treated Pine posts without Ro-Pel, (3) Black Locust posts with Ro-Pel, and (4) Black Locust posts without Ro-Pel. Forty wood posts 10 cm x 10 cm x 120 cm in size were experimental units.

We purchased the twenty pressure-treated Pine posts at a local home improvement store. The Pine posts were treated with Alkaline Copper Quaternary (AQC) (C.M. Tucker Lumber Corporation 2008), a water-type wood preservative that is widely used to treat timbers, fence posts, and other wooden structures (USEPA 2011, Lebow and Tippie 2001). Chemical composition of AQC may include monoethanolamine, copper oxides, alkyl dimethyl benzyl ammonium chloride (ADBAC), didecyl dimethyl ammonium chloride, dialkyl dimethyl ammonium carbonate/ bicarbonate, and/or boric acid (Viance Treated Wood Solutions 2009). ADBAC is composed of 24 compounds, some of which contain salts (USEPA 2006). The active ingredients in boric acid are its sodium salts (USEPA 1993). The twenty Black Locust posts were milled locally from trees grown in Jefferson County, Pennsylvania, to the same dimensions as the pressure treated posts. Black Locust posts were not pressure treated.

We installed all posts in June 2007 near the two bridges that exhibited severe Porcupine damage. We placed five posts one meter apart in a linear fashion along the trail at each of the four bridge corners, for a total of twenty posts per bridge. We used a randomized block design, in which the four treatments were randomly assigned and replicated five times at each bridge (Fig. 1). We buried each post approximately 0.6 m in the ground leaving 0.6 m exposed. On the posts that were randomly assigned repellent application, Ro-Pel was applied every four weeks or after heavy rain or snowfall according to the product's label.

We identified Porcupine damage by the characteristic shape and width of the tooth marks (Spencer 1964) and linear stripping of the wood. We frequently observed Porcupines, as well as Porcupine tracks, quills and feces at the study site. On 4 August 2007 we directly observed a Porcupine damaging one of the posts. In addition, we examined damage to trees and wooden structures in close proximity to the posts. Teeth marks were often visible and many of the damaged trees exhibited the oval feeding scars distinctive to Porcupine damage (Spencer 1964). *Sciurus niger* Linnaeus (Fox Squirrels) and *Marmota monax* Linnaeus (Woodchucks) may cause similar damage (Weeks and Kirkpatrick 1978). However, they were excluded as candidates due to the width of the tooth marks (Spencer 1964) and the lack of observed individuals and habitat of either species at our field site (Derge and Yahner 2000, Weeks and Kilpatrick 1978).

We monitored the posts 1 – 4 times per month for new damage from June 2007 to January 2009. We calculated the damage by overlaying 4 x 4 square (4 squares per inch) graph paper on the damaged area. The damage was traced onto the paper and then the total number of squares within the margin was counted. We compared cumulative damage over the study period to each post using 3-way ANOVA (using SPSS version 16.0) to test for effects due to wood type, repellent application, and bridge location. In addition, we used 1-way ANOVA to compare monthly and seasonal damage to Pine posts to test for effects due to month and season, respectively. Seasons were defined as winter (December – February), spring (March – May), summer (June – August), and fall (September – November). Black Locust posts were excluded from these analyses due to the observed lack of damage to these posts.

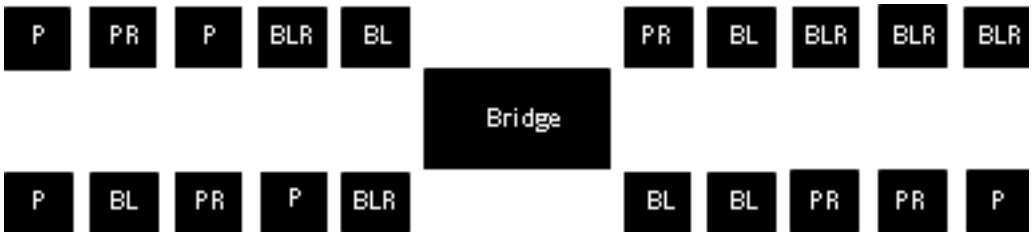

Figure 1. Layout of posts at bridges along Rails-to-Trails in Pennsylvania, USA. BL= Black Locust; BLR=Black Locust with Ro-pel; P= Pine; PR= Pine with Ro-pel. Figure not to scale.

RESULTS

We observed thirty-one areas of Porcupine damage on eleven different posts, totaling 258 cm^2, between June 2007 and January 2009. Five of the damaged posts ($\bar{x}$ = 7.53 cm^2, SE = 3.47 cm^2, n = 20) were located adjacent to one bridge and six of the damaged posts ($\bar{x}$ = 5.39 cm^2, SE = 2.43 cm^2, n = 20) were located adjacent to the other bridge (P = 0.546). All damage was to Pine posts ($\bar{x}$ = 12.9 cm^2, SE = 3.70 cm^2, n = 20) and there was no observable damage to Black Locust posts (n = 20) (P = 0.001).

Posts treated with Ro-Pel sustained 59.8 cm^2 of damage on two Pine posts, whereas eleven Pine posts that were not treated with Ro-Pel exhibited 198 cm^2 of damage. Observed damage to untreated posts ($\bar{x}$ = 9.93 cm^2, SE = 2.10 cm^2, n = 20) was over 3 times greater than damage to posts treated with Ro-Pel ($\bar{x}$ = 2.99 cm^2, SE = 2.86 cm^2, n = 20) (P = 0.056). One hundred percent of the wood stripped from posts without Ro-Pel was missing and therefore assumed to be consumed. In contrast, only 3.8% (2.60 cm^2) of wood stripped from posts with Ro-Pel was missing. The remaining 96.2% (57.2 cm^2) of wood stripped from posts with Ro-Pel was found on the ground next to the posts. The strips that were remaining at the study site fit directly into the depressions on the posts where damage occurred.

The apparent peak of damage at our study site occurred between May and August, whereas minimal damage occurred between September and February (Fig. 2). Total monthly damage to Pine posts was greatest in August ($\bar{x}$ = 2.31 cm^2, SE = 1.51 cm^2, n = 40) and there was no observed damage in February (n = 20), October (n = 40), and November (n = 40) (P = 0.099; Fig. 3). When examining damage by season, damage to Pine posts was 54 times greater in summer (June – August; $\bar{x}$ = 1.62 cm^2, SE = 0.567 cm^2, n = 120) than in fall (September – November; $\bar{x}$ = 0.030 cm^2, SE = 0.030 cm^2, n = 120) (P = 0.002; Fig. 4).

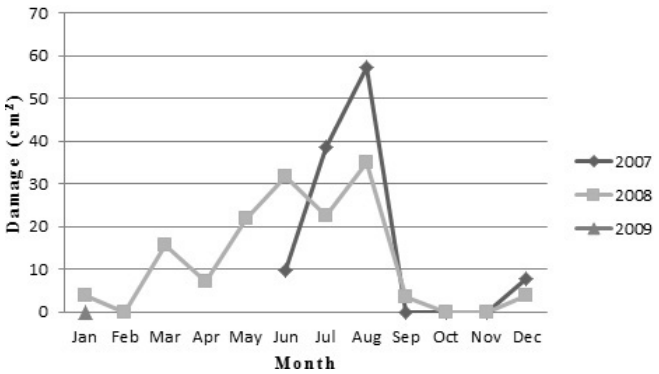

Figure 2. Porcupine damage observed to all posts (cm^2), June 2007 – January 2009, Pennsylvania, USA.

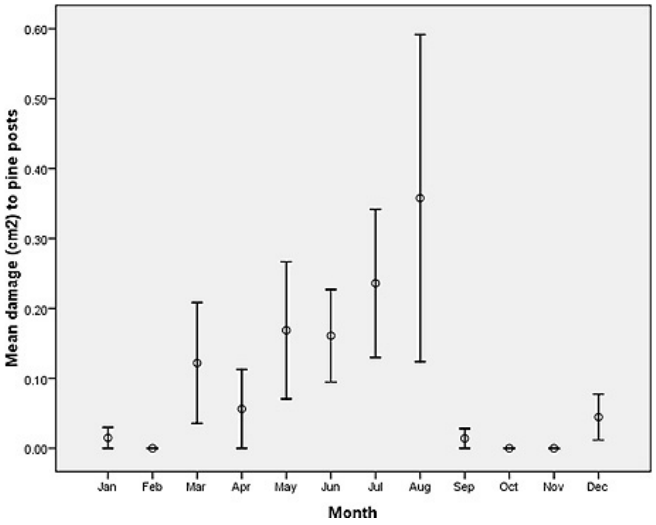

Figure 3. Mean Porcupine damage to Pine posts (cm^2) by month, June 2007 – January 2009, Pennsylvania, USA. Error bars represent +/- 1 SE from the mean.

DISCUSSION

Ro-Pel may deter some damage and more specifically consumption; however, it may not be cost-effective. The total cost to apply Ro-Pel from June 2007 to January 2009 over our forty posts was $235.80. Moreover, whether the stripped wood is consumed may not be of concern for landowners or managers. Witmer and Pipas (1998) reported that eight of eleven repellents tested gave promising results in reducing Porcupine damage. However, they also noted that 0.065% denatonium saccharide, the same ingredient and concentration in Ro-Pel™, did not deter Porcupine feeding in a 24-hour test period.

In the northeastern United States, Porcupine winter diet consists mainly of evergreen bark and needles, with a strong preference for eastern hemlock (Curtis and Kozicky 1944, Griesemer et al. 1998, Roze 1989, Woods 1973). In spring and summer, diet changes to graminoids, *Viola spp.* Linnaeus (Violet), *Taraxacum spp.* F. H. Wigg (Dandelion), *Rubus spp.* Linnaeus (Raspberry), *Fraxinus americana* Linnaeus (White Ash), Sugar Maple buds (Roze 1989), *P. tremuloides* Linnaeus (Trembling Aspen) (Bertreaux et al. 2005, Griesemer et al. 1998, Roze 1989) and White Pine (Griesemer et al. 1998, Tenneson and Oring 1985). Porcupines also eat acorns, beechnuts, and Black Locust leaves (Curtis and Kozicky 1944). This rich diet causes rapid weight gain (Bertreaux et. al 2005) and the molting of their winter fur; however it also leads to sodium loss (Roze 1989).

Roze (1989) found a strong seasonal pattern to Porcupine salt intake at a study site in the Catskill Mountains of New York referred to as the "salthouse". Visits to the salthouse stopped almost completely between the months of November

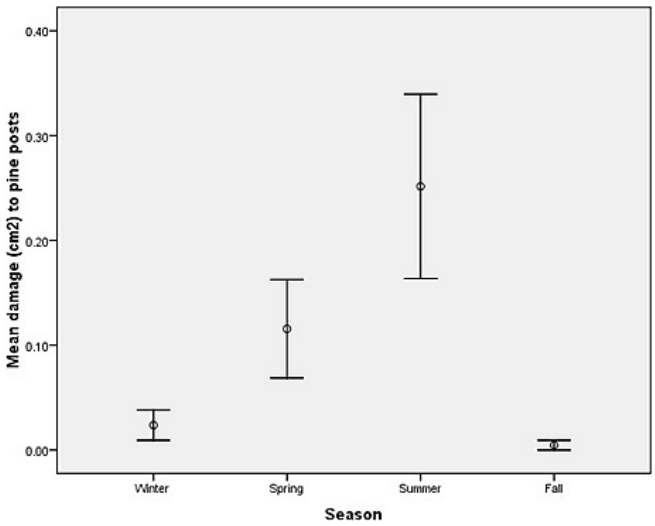

Figure 4. Mean Porcupine damage to Pine posts (cm^2) by season (winter = Dec – Feb, spring = Mar – May, summer = Jun – Aug, fall = Sep – Nov), June 2007 – January 2009, Pennsylvania, USA. Error bars represent +/- 1 SE from the mean.

and March. This is consistent with our findings that damage was minimal during these months. This suggests that attraction to our posts were a result of salt-seeking behavior which may be reduced in these months. The Pine posts used by RTT and in our study were treated with sodium based preservatives and these metal-salt solutions may attract Porcupines (Schemnitz 1994).

Porcupines breed in the fall, which involves searching for mates, elaborate courtship displays, and searching for den sites (Merritt 1987). Porcupines use winter den sites from November to April and may reduce activity in the winter months (Griesemer et al. 1998). Breeding, followed by this decline in activity, may also partially explain the minimal damage observed during fall and winter.

Similarly, sodium loss may be related to the observed increase in damage after March. Roze (1989) reported the majority of salt intake occurred in April with a secondary peak in August and September. We similarly observed a peak in August, although there was very little damage in April. This could be attributed to the short duration of our study or the presence of other sodium-rich material in the area. There are wooden structures (i.e. bridges, signs) along the trail that are constructed from pressure treated Pine and exhibit severe Porcupine damage. Weeks and Kirkpatrick (1978) showed a similar seasonal salt preference in Fox Squirrels and Woodchucks, with salt intake peaks in spring and a secondary peak in fall for Fox Squirrels. If landowners chose to use a repellent, applications could be made in the summer months which corresponded with the peak of damage in our study. This would significantly reduce the cost of repellent use.

The observed preference for Pine over Black Locust could be a result of the presence of pressure-treatment chemicals, a natural preference for Pine, or a combination of both. We suggest that landowners and recreation managers who anticipate Porcupine damage consider using alternatives (e.g., Black Locust) to pressure-treated Pine for their wooden structures. Black Locust is a very durable hardwood (McAlister 1971) and has a history of being favored for outdoor uses (Pollet et al. 2008). Because of its durability, stability, and the ability to hold nails, it is a very common wood used for fence construction. With its natural rot resistance, wood preservatives are not needed (McAlister 1971).

ACKNOWLEDGEMENTS

This work was supported by the DuBois Educational Foundation, DuBois Undergraduate Professional Development Fund, the Penn State Office of Undergraduate Education, and Penn State DuBois.

RTT, J. Farr, G. Gilmore, G. A. Bartholomay, S. McGough, and R. Graham were helpful in the design and implementation of the study. The manuscript was reviewed prior to submission by A. Stottlemyer.

LITERATURE CITED

Bertreaux, D., I. Klvana, and C. Trudeau. 2005. Spring-to-fall mass gain in a northern population of North American Porcupines. Journal of Mammalogy 86:514-519.

C.M. Tucker Lumber Corporation. 2008. ACQ Preserve® - C.M. Tucker Lumber. Available online at http://www.cmtuckerlumber.com/woodtreatment/preserve.html. Accessed on 10 March 2011.

Curtis, J. D. and E. L. Kozicky. 1944. Observations on the eastern Porcupine. Journal of Mammalogy 25: 137-146.

Derge, K.L. and R.H. Yahner. 2000. Ecology of sympatric fox squirrels (*Sciurus niger*) and gray squirrels (*S. carolinensis*) at forest-farmland interfaces of Pennsylvania. American Midland Naturalist 143(2):355-369.

Griesemer, S. J., T. K. Fuller, and R. M. Degraaf. 1998. Habitat use by porcupines (*Erethizon dorsatum*) in central Massachusetts: Effects of topography and forest composition. American Midland Naturalist 140:271-279.

Lebow, S.T. and M. Tippie. 2001. Guide for minimizing the effect of preservative-treated wood on sensitive environments. Gen. Tech. Rep. FPL GTR 122. U.S. Department of Agriculture, Forest Service, Forest Products Laboratory, Madison, WI. 18 pp.

McAlister, R.H. 1971. Black locust. U.S. Forest Service, American Woods – FS 244. Washington, D.C.

Merritt, J.F. 1987. Guide to the Mammals of Pennsylvania. University of Pittsburgh Press. Pittsburgh, PA, 236-240.

Nixalite of America, Inc. 2009. Ropel animal, rodent and bird repellent. Available online at http://www.nixalite.com/PDFs/ropelrepellent.pdf. Accessed 1 July 2010.

Pollet, C., B. Jourez, and J. Hebert. 2008. Natural durability of black locust (*Robinia pseudoacacia* L.) wood grown in Wallonia, Belgium. Canadian Journal of Forest Research 38:1366-1372.

Roze, U. 1989. The North American Porcupine. Smithsonian Institution Press. Washington, D.C., xix + 282 pp.

Schemnitz, S. 1994. Porcupines. Pages B-81 – B-84 in Prevention and control of wildlife damage. Edited by S. Hygnstrom, R. Timm, and G. Larsen. Cooperative Extension Division, University of Nebraska – Lincoln, Nebraska.

Spencer, D.A. 1964. Porcupine population fluctuations in past centuries revealed by dendrochronology. Journal of Applied Ecology 1(1):127-149.

Tenneson, C. and L. W. Oring. 1985. Winter food preferences of porcupines. Journal of Wildlife Management 49:28-33.

USEPA. 1993. R.E.D. Facts. Boric acid. United States Environmental Protection Agency (USEPA). USEPA Report EPA-738-F-93-006. Washington, DC. 8 pp.

USEPA. 2006. Reregistration Eligibility Decision for Alkyl Dimethyl Benzyl Ammonium Chloride (ADBAC). United States Environmental Protection Agency (USEPA). USEPA Report EPA-739-R-06-009. Washington, DC. 126 pp.

USEPA. 2011. Chromated Copper Arsenate (CCA): ACQ-An Alternative to CCA. Pesticides: Regulating Pesticides. United States Environmental Protection Agency (USEPA). Available online at http://www.epa.gov/oppad001/reregistration/cca/acq.htm. Accessed on 11 March 2011.

Viance Treated Wood Solutions. 2009. Material safety data sheet: ACQ preserve and preserve plus pressure treated wood. MSDS ID: VIA-142.

Wagner, K. K., and D. L. Nolte. 2000. Evaluation of hot sauce® as a repellent for forest mammals. Wildlife Society Bulletin 28:76-83.

Weeks, H.P., Jr. & C.M. Kirkpatrick. 1978. Salt preferences and sodium drive phenology in fox squirrels and woodchucks. Journal of Mammalogy 59(3):531-532.

Whitaker, J. O. 1996. National Audubon Society Field Guide to Mammals. Second Edition. Alfred A. Knopf Inc. New York, NY, 672-676.

Witmer, G. W. and M. J. Pipas. 1998. Porcupine damage and repellent research in the interior Pacific Northwest. Proceedings of the 18th Vertebrate Pesticide Conference 18: 203-207.

Woods, C. A. 1973. *Erethizon dorsatum*. Mammalian Species 29:1-6.

Journal of the Pennsylvania Academy of Science 86(1): 41-45, 2012

QUANTIFYING WING DAMAGE OF SUMMER BATS IN THE NORTHEASTERN UNITED STATES[1]

KAREN E. FRANCL[2]*, TESSA K. CANNIFF[2], R. CRAIG BLAND[2,4], DALE W. SPARKS[3], VIRGIL BRACK, JR.[2]

[2] *Biology Department, Radford University, Radford, VA 24142*
[3]*Environmental Solutions & Innovations, Inc., Cincinnati, OH 45233*

ABSTRACT

While conducting mist net surveys for the federally endangered Indiana bat (*Myotis sodalis*) in West Virginia, New York, and Pennsylvania, we quantified wing damage on 422 bats of four species: big brown (*Eptesicus fuscus*, N = 190), eastern red (*Lasiurus borealis*, N = 82), little brown (*M. lucifugus*, N = 55), and northern myotis (*M. septentrionalis*, N = 95) bats. From 15 May – 15 August 2010, we photographed back-lit wings to reveal damage such as scars, holes, and blotching (non-uniform pigmentation). After quantifying the percent cover of these damage types using image-analysis software, we used generalized non-linear mixed models to determine if percent area of damage differed among scores associated with the categorical wing damage index (WDI) developed by Reichard and Kunz (2009). Although quantified damage did generally increase with WDI score across all species, statistical separation by WDI was only documented for the big brown bat (blotching, scars, blotching + scars combined) and northern myotis (blotching, blotching + scars). We suggest that studies like ours can provide quantitative species-specific datasets that can be examined in a more precise manner than a categorical index. [J PA Acad Sci 86(1): 41-45, 2012]

INTRODUCTION

Since its discovery in 2006 in New York, White-Nose Syndrome (WNS) and its definitive cause, the fungal pathogen *Geomyces destructans* (Lorch et al. 2011), is linked to the catastrophic decline of some bat populations in the northeastern United States (e.g., Blehert et al. 2009, Frick et al. 2010, Turner et al. 2011). Visible effects of *G. destructans* infection include necrosis of wing membranes, resulting in scars and "irregular areas of pallor" (Cryan et al. 2010) or depigmented spotting on the membrane (hereafter, "blotching"). Because of this acknowledged wing damage, Reichard and Kunz (2009) developed a 4-point scale, coined the "Wing-Damage Index" (WDI), which is based on the percent cover of membrane-darkened scars, blotching, necrotic tissue, and holes or tears. To summarize, a WDI score of 0 indicates little to no damage (<5 small spots on the membrane, typically visible only when the wing is transilluminated, and no holes or necrotic tissue), a WDI of 1 indicates light damage (blotching on <50% of wings), a WDI of 2 indicates moderate damage (blotching on >50% of wings, few necrotic spots and small holes), and a WDI score of 3 indicates severe damage, with blotching on >90% of the membrane and the presence or abundance of necrotic tissue. The WDI is now widely used in the eastern United States to document damage on bats potentially infected with WNS.

The utility of the WDI was tested by Francl et al. (2011) on a regional scale, examining trends in the WDI for multiple species across five states. The lack of large-scale geographic trends coupled with a lack of strong relationships between a body mass index (weight[g]/ forearm length; Chappell and Titman 1983) and the WDI suggested that aspects of the index required additional study. One concern of Francl et al. (2011) was that of subjective scoring method, rather than an objective one. We suggested that this could be addressed by statistically comparing qualitative wing scores to quantitative wing damage. Based on continuing research suggestions by Francl et al. (2011), we continue to study the utility of the WDI. We first asked whether the WDI as reported by our field staff accurately assessed wing damage on free-ranging bats. That is, did bats with a greater percentage of wing damage score higher on the WDI? Second, we questioned if one or more types of wing damage (blotching, scars, holes) was strongly correlated to an individual bat's assessed score for WDI. Third, we asked whether our quantitative level of damage corresponded with the damage levels described for the WDI (Reichard and Kunz 2009).

[1]Submitted for publication March 2012; accepted August 2012.
[2]Corresponding author: Karen E. Francl, Department of Biology, Box 6931, Radford, VA 24142 email: kfrancl@radford.edu; Phone: (540) 831-6537; Fax: (540) 831-51293
[4]Current address: Warnell School of Forestry and Natural Resources, University of Georgia, Athens, GA 30602

MATERIALS AND METHODS

Field Methods

Between 15 May and 15 August 2010, we conducted mist-netting surveys for bats at 125 sites in New York, Pennsylvania, and West Virginia that were selected primarily to investigate the presence/probable absence of the Indiana bat (*Myotis sodalis* Miller and Allen), an endangered species (USFWS 2007). Assessment of wing damage was completed in conjuction with these field efforts. Netting procedures followed the protocol for summer surveys of Indiana bats (USFWS 2007) and included standard WNS decontamination procedures (2010 protocol: http://www.fws.gov/whitenosesyndrome/pdf/WNS1pageDecontaminationProtocol_073110.pdf).

We identified captured bats to species and recorded sex and age (juvenile vs. adult; Anthony 1988). We scored damage to the wings using the WDI of Reichard and Kunz (2009), and photographed one or (typically) both wings of individuals using backlighting by incandescent sources.

Analytical Methods and Statistics

We quantified wing damage from 770 photos of 443 bats of eight species captured. Because we did not investigate trends in species with less than 50 wing samples, we limited our study to four species (682 photos of 422 bats): big brown (*Eptesicus fuscus* Palisot de Beauvois; N = 190 individuals, 304 photos), northern myotis (*Myotis septentrionalis* Trouessart; N = 95 individuals, 157 photos), eastern red (*Lasiurus borealis* Müller; N = 82, 138 photos), and little brown (*Myotis lucifugus* LeConte; N = 55 individuals, 83 photos; Table 1) bats.

We quantified wing damage by digital image analysis with ImageJ v. 1.37a (Fuller et al. 2011, Rasband 2011). Following Reichard and Kunz (2009), we defined wing damage as visible holes or tears, necrotic tissue, membrane-darkened scars, and blotching. Although boundaries of holes, tears, and darkened scars were consistently clear, boundaries of blotching were less discernable. We conservatively estimated blotching on wing photographs, including depigmented or lightened spots on wings, rather than the combined mottling of light and "normal" dark portions across the wing. For this reason, our estimates of blotching may be low by Reichard and Kunz (2009) standards. We opted to provide precise quantification of damage by using boundaries that were most distinct.

Handlers stretched bat wings during photography, so tips of wings were always obscured, although in nearly all cases, ≥75% of the wing was visible. Therefore, damage estimates were calculated as a proportion of the area of the visible wing membrane. These estimates were created by tracing polygons around damaged areas in ImageJ, and using the software to calculate damaged areas relative to the total visible wing area. This method allowed us to account for variation in color, image quality, and image size, which could not be standardized across photographers. Digital images of poor quality, due to irregular background color, insufficient backlighting, or image clarity were discarded. These photos were not included in the total number of wings we reported. When both wings of a bat were photographed, we averaged the percent damage for the two wings.

For each species, we compared WDI scores with percent cover of scars, percent cover of holes, percent cover of blotching, and total damage, i.e., the combined percent damage by blotching and scars. Although holes are a part of the published documentation by Reichard and Kunz (2009), holes were not included in the original WDI numerical assignment in the widely-distributed white paper of Reichard and Kunz (unpublished data) in summer 2009. Because our original assignment of WDI followed this white paper, we considered total damage to include just blotching and scars.

For each species, we used generalized non-linear mixed models to see if the area of different kinds of damage was significantly different among categorical WDI values, followed by post-hoc Scheffe's tests (if $P < 0.1$) to determine which pairs of WDI scores differed from one another. We used these methods because our data could not be normalized through standard transformations, and these procedures do not require an assumption of normality. This post-hoc analysis provides robust control of Type I experimental error, but often overlooks differences between groups that other statistical analyses might detect (Littell et al. 2006).

RESULTS

Of the four species examined, 255 scored 0 (no visible damage), 154 scored 1 (minor visible damage), and 13 scored 2 (moderate visible damage) and no bats exhibited severe damage (WDI = 3; Table 1). Of the 422 bats, 323 (76.5%) exhibited blotching on wing membranes. Just 28 (6.6%) had holes in one or both wings, while 184 (43.6%) had scars. For all species, blotching accounted for most wing damage (Table 1).

The percent coverage by holes was never significantly different among WDI scores for any species (Table 1), and trends in scars, blotching, and the combination of the two factors yielded variable results among species. For the big brown bat, individuals with different WDI scores had significantly different amounts of blotching ($F = 7.95$, $p = 0.0005$), scarring ($F = 4.12$, $p = 0.0178$) and blotching + scarring combined ($F = 7.82$, $p = 0.0005$; Table 1). Post-hoc Scheffe's tests separated quantitative measures for WDI = 2 bats from the lower WDI scores (Table 1). For the northern myotis, we detected differences in individuals with different WDI scores for blotching ($F = 21.32$, $p < 0.0001$), scars ($F =$

Table 1. Damage class (blotching, scarring, holes, or combination of blotching + scars) versus Wing Damage Index (WDI) scores for four bat species (422 bats, 682 wings) from West Virginia, Pennsylvania, and New York in summer 2010. We report F-statistics and p-values for generalized non-linear mixed models, which examined differences among WDI score (0, 1, 2) and relative damage by category (average [standard error in parentheses]) reported for each damage category, WDI score, and species. Within each row, WDI scores that statistically differ from one another (Post-hoc Scheffe's tests performed when P < 0.1) have different superscripts.

				WDI Score		
	Variable	F	P	0	1	2
Eptesicus fuscus	N			100	84	6
	Blotching	7.95	0.0005	0.0097 (0.0017)^{A}	0.0104 (0.0015)^{A}	0.0299 (0.0121)^{B}
	Scars	4.12	0.0178	0.0007 (0.0003)^{A}	0.0007 (0.0001)^{AB}	0.0034 (0.0022)^{B}
	Holes	0.76	0.4697	0.0001 (0.0001)	0.00002 (0.00001)	0.00007 (0.00007)
	Blotching + Scars	7.82	0.0005	0.0105 (0.0018)^{A}	0.0111 (0.0016)^{A}	0.0334 (0.0121)^{B}
Lasiurus borealis	N			63	17	2
	Blotching	8.91	0.0003	0.0026 (0.0008)^{A}	0.0105 (0.0048)^{A}	0.0077 (0.0077)^{A}
	Scars	2.11	0.1283	0.00004 (0.00001)	0.000001 (0.000001)	0.0005 (0.0005)
	Holes	0.07	0.9306	0.000009 (0.000005)	0.000001 (0.000001)	0 (0)
	Blotching + Scars	9.63	0.0002	0.0026 (0.0008)^{A}	0.0105 (0.0048)^{A}	0.0081 (0.0073)^{A}
Myotis lucifugus	N			36	17	2
	Blotching	2.8	0.0699	0.0026 (0.0008)^{A}	0.0083 (0.0027)^{A}	0.0080 (0.0047)^{A}
	Scars	0.42	0.6561	0.0003 (0.00007)	0.0005 (0.0002)	0.0003 (0.0002)
	Holes	2.39	0.1012	0 (0)	0.0003 (0.0002)	0 (0)
	Blotching + Scars	4.01	0.0241	0.0029 (0.0008)^{A}	0.0091 (0.0027)^{A}	0.0083 (0.0050)^{A}
Myotis septentrionalis	N			56	36	3
	Blotching	21.32	<0.0001	0.0011 (0.0002)^{A}	0.0058 (0.0010)^{AB}	0.0107 (0.0029)^{B}
	Scars	3.34	0.0398	0.0003 (0.0001)^{A}	0.0007 (0.0002)^{A}	0.0039 (0.0039)^{A}
	Holes	0.73	0.4865	0.00005 (0.00003)	0.00007 (0.00007)	0.00001 (0.00001)
	Blotching + Scars	25.51	<0.0001	0.0015 (0.0002)^{A}	0.0065 (0.0010)^{B}	0.0146 (0.0001)^{B}

3.34, p = 0.0398), and the combination of the two (F = 25.51, p < 0.0001; Table 1). However, post-hoc analyses did not detect differences among individuals with differing WDI values for scarring. For blotching, only WDI = 2 and WDI = 1 were definitively separated in this species, whereas blotching + scarring separated WDI = 0 from higher damage categories (Table 1). For the eastern red bat, we found discernible differences among individuals with different WDI scores for blotching (F = 8.91, p = 0.0003) and blotching + scarring (F = 9.63, p = 0.0002; Table 1). However, post-hoc analyses failed to indicate significant differences among categories, and quantified damage for bats with WDI = 1 actually was numerically greater than WDI = 2 (Table 1). Similarly, for the little brown bat, we discovered statistically significant differences in individuals with different WDI scores for only blotching (F = 2.80, p = 0.0699) and blotching + scarring (F = 4.01, p = 0.0241; Table 1). Post-hoc analyses again failed to find differences among categories, and quantified damage for bats with WDI = 1 was marginally greater than WDI = 2 (Table 1).

DISCUSSION

For the four species analyzed, quantitative measurements of blotching and total damage (with blotching most common) showed significant separation among WDI scores, suggesting that observers were basing wing damage on an

accurate assessment of this type of wing damage. Generally, bats with more damage scored a higher WDI value. A few exceptions were documented: eastern red and little brown bats had damage values marginally higher in WDI = 1 than in WDI = 2. With only two individuals of each species with a WDI score of 2, it is difficult to obtain an accurate estimate of the population. Indeed, the lack of moderate-to-severe wing damage among all captured bats limited our investigation of WDI.

When we questioned if one or more types of wing damage (blotching, scars, holes) was strongly correlated to an individual bat's assessed score for WDI, in no cases were quantitative damages from holes related to WDI. However, conservative post-hoc analyses did not always detect clear differences between pairs of WDI scores. For two species, big brown and northern myotis, individuals with a moderate WDI score (2) also showed significantly more scarring than those with lower scores, but scarring differences were less differentiated for lower WDI scores.

We questioned whether the level of damage corresponds with the scale proposed by Reichard and Kunz (2009). Damage to wings (on a percent scale) scored a 1 or a 2 were markedly lower than the percentage of damage proposed by the WDI authors. For example, while the WDI scale might suggest blotching over 50% of the wing membrane, our big brown bats only averaged damage over 3% of the area; other species averaged just 1% or 2% damage for WDI scores of 2 (Table 1).

Perhaps the most important question to ask, therefore, is why are bat surveyors over-scoring these summer populations? The amount of difference between the damage we measured and the damage reported by biologists in the field may represent systematic error in the application of the WDI. Specifically, we suggest that because biologists rarely see the type of damage considered "moderate" by Reichard and Kunz (2009; WDI = 2, >50% of a wing blotched and necrotic tissue visible), surveyors are "upgrading" those wings that they perceive as more severe.

The WDI has widespread use as a component for assessing bat health (Reichard et al. 2011), but questions remain over its functionality on a large scale (e.g., Sparks et al. 2011). As shown by evidence of wing-healing in little brown bats (Fuller et al. 2011) and big brown bats (Faure et al. 2009), the rarity of bats with WDI of 2 or 3 across the summer months limits the utility of this index to the hibernation period and at the time of spring emergence. Because just 13 of 422 bats scored a WDI = 2, our analyses essentially were limited to a dichotomous assessment of damage (comparing WDI = 0 to WDI = 1). In two species, each with just two individuals with WDI = 2, the utility of these comparisons (WDI = 2 to lower scores) was severely limited. Because statistical trends differed among species and among damage types, we suggest that quantifiable damage studies like ours can be helpful by providing data that can be examined in a more precise manner than a categorical index.

ACKNOWLEDGMENTS

We thank employees of Environmental Solutions & Innovations, Inc., who participated in data collection in summer 2010, and the U.S. Army Garrison at Fort Drum, New York, for sharing data from ongoing research. W. Mark Ford assisted with statistical analyses.

LITERATURE CITED

Anthony, E.L.P. 1988. Age determination. Pages 47–57 in Kunz, T.H. (ed.) Ecological and Behavioral Methods for the Study of Bats. Smithsonian Institution Press, Washington, DC, USA. 556 pp.

Blehert, D.S., A.C. Hicks, M. Behr, C.U. Meteyer, B.M. Berlowski-Zier, E.L. Buckles, J.T.H. Coleman, S.R. Darling, A. Gargas, R. Niver, J.C. Okoniewski, R.J. Rudd, and W. B. Stone. 2009. Bat white-nose syndrome: an emerging fungal pathogen? Science 323:227.

Chappell, W.A., and R.D. Titman 1983. Estimating reserve lipids in greater scaup (*Aythya marila*) and lesser scaup (*A. affinis*). Can. J. Zool. 61:35-38.

Cryan, P.M, C.U. Meteyer, J.G. Boyles, and D.S. Blehert. 2010. Wing pathology of white-nose syndrome in bats suggests life-threatening disruption of physiology. BMC Biology 8:135.

Faure, P.A., D.E. Re, and E.L. Clare. 2009. Wound healing in the flight membranes of big brown bats. J.Mammal. 90:1148–1156.

Francl, K.E., D.W. Sparks, V. Brack, Jr., and J. Timpone. 2011. White-nose syndrome and wing index scores among summer bats in the northeastern United States. J. Wildl. Dis. 47(1):41-48.

Frick, W.F., J.F. Pollock, A.C. Hicks, K.E. Langwig, D.S. Reynolds, G.G. Turner, C.M. Butchkoski, and T.H. Kunz. 2010. An emerging disease causes regional population collapse of a common North American bat species. Science 329:679–682.

Fuller, N.W., J.D. Reichard, M.L. Nabhan, S.R. Fellows, L.C. Pepin and T.H. Kunz. 2011. Free-ranging little brown myotis (*Myotis lucifugus*) heal from wing damage associated with White-Nose Syndrome. EcoHealth 8(2):154-62.

Littell, R.C., G.A. Milliken, W.W. Stroup, R.D. Wolfinger, and O. Schabenberber. 2006. SAS for Mixed Models, 2nd ed. SAS Publishing, Inc. 840 pp.

Lorch, J.M., C.U. Meteyer, M.J. Behr, J.G. Boyles, P.M. Cryan, A.C. Hicks, A.E. Ballmann, J.T.H. Coleman, D.N. Redell, D.M. Reeder, and D.S. Blehert. 2011. Experimental infection of bats with *Geomyces destructans* causes white-nose syndrome. Nature 480:376–378.

Rasband, W.S. 2011. ImageJ. U. S. National Institutes of Health, Bethesda, Maryland, http://imagej.nih.gov/ij/, 1997–2011.

Reichard, J.D., N.W. Fuller, and T.H. Kunz. 2011. Condition of wings is an important criterion of bat health: a response to Francl et al. J. Wildl. Dis. 47:1050–1051.

Reichard, J.D., and T.H. Kunz. 2009. White-nose syndrome inflicts lasting injuries to the wings of little brown myotis (*Myotis lucifugus*). Acta Chiropterologica 11:457–464.

Sparks, D.W., K.E. Francl, and V. Brack, Jr. 2011. Indexing at different scales: a response to Reichard et al. J. Wildl. Dis. 47:1052–1053.

Turner, G., D.M. Reeder, and J.T.H. Coleman. 2011. A five-year assessment of mortality and geographic spread of White-nose Syndrome in North American bats and a look to the future. Bat Res. News 52:13–27.

U.S. Fish and Wildlife Service (USFWS). 2007. Indiana Bat (*Myotis sodalis*) Draft Recovery Plan: First Revision. U.S. Fish and Wildlife Service, Fort Snelling, MN, 258 pp.

Journal of the Pennsylvania Academy of Science 86(1): 46-53, 2012

STREET TREE INVENTORY OF SELINSGROVE, PENNSYLVANIA[1]

DANIEL E. RESSLER AND JOHN A. KILMER

Susquehanna University, Earth and Environmental Sciences Department, Selinsgrove, PA 17870 and University of Florida, Department of Biology, Gainesville, FL 32611

ABSTRACT

Street trees provide a number of social and environmental benefits to their communities. A street tree inventory was conducted in Selinsgrove, Pennsylvania to quantify the number of trees, the species present, tree characteristics, and sidewalk characteristics. The field data collected was combined with historical aerial photographs to evaluate the sustainability of the street tree community over time, as well as determine diversity and ecology statistics of the community by neighborhood. The analysis determined that more than half of the 1974 community existed in 2009, and that five of the eight neighborhoods lost nearly two-thirds of their trees. The street tree community is dominated by only three species and is not appropriately diverse to withstand potential threats from invasive boring insects that threaten the region's trees. Selinsgrove needs to find ways to limit tree losses and diversify the street tree community. [J PA Acad Sci 86(1): 46-53, 2012]

INTRODUCTION

Street trees are unique biological resources of urbanized communities because of their position between the street curb and the sidewalk and their important role providing environmental services for nearby landowners as well as the larger benefits of defining community aesthetics. The environmental services provided by street trees include trapping carbon and filtering air pollution (Brack 2002; McHale et al. 2009), reducing heating and cooling requirements due to shading and wind breaks (Akbari et al. 1992, Donovan and Butry, 2009), reducing the "heat-island" effect in the summer (Georgi and Zafiriadis, 2006), providing improved wildlife habitat and aesthetic quality to their communities (Schwaab et al. 1995), and extending the useful life of paved streets (McPherson and Muchnick 2005). For a community to understand its urban tree resources it must have information about the trees on private property (over which municipalities have no jurisdiction), and trees within roadway right of way, the street trees, where the municipality may exert some influence. In Selinsgrove, Pennsylvania as well as many smaller communities, a street tree's care and maintenance is primarily the responsibility of the landowner. However, due to the importance of the street tree's contribution to environmental services, public aesthetics, and "curb appeal" which supports higher property values (Donovan and Butry, 2010), many communities have established a "Shade Tree Commission" to enact ordinances that protect trees from removal or certain forms of potentially harmful pruning practices. In Selinsgrove, a landowner must request a permit before a tree can be removed or severely pruned. Smiley and Baker (1988) gave rationale for conducting inventories, consisting of (1) determining the need for a tree management program, (2) determining tree values, (3) identifying and prioritizing tree work to be done, (4) increasing work efficiency, and (5) providing public information and education. Numerous digital tools have been developed to manage tree information including Street Tree Resource Assessment Tool for Urban Forest Managers (STRATUM, Maco and McPherson 2003) and the U.S. Forest Services' i-Tree (USFS), and have helped communities understand the value of street trees (McPherson et al. 2005, Millward and Sabir, 2011). Inventories also establish the ecological character of street trees so the resource can be assessed with respect to continued threats like invasive species, disease, or climate change vulnerability. Species diversity in street tree communities is important to prevent a single disturbance from wiping out an entire population. Important examples of street tree disturbances would be the Dutch elm disease which killed millions of trees worldwide (Sinclair and Campana 1978) and the American chestnut blight (Anagnostakis 1987). More recently, the Asian Long-Horned Beetle (LHB) and the Emerald Ash Borer (EAB) are poised to further decimate natural and street trees as they burrow under the bark of a range of susceptible trees (Haack et al. 2010, Nowak et al. 2001). Size diversity is also an important metric in street trees to assure the tree community is composed of members that span all ranges of tree size (most notably trees of small caliper) as street trees require intentional replacement because the natural recruitment from seedlings in the wild is not generally operative in a

[1]Submitted for publication July 2012; accepted December 2012.

managed environment.

Selinsgrove is a small borough located on the western bank of the Susquehanna River in Snyder County, Pennsylvania. The borough was once part of the National Arbor Day Foundation's Tree City USA Program and contained many tree lined streets. Street widening, underground infrastructure upgrades, and sidewalk replacement projects in the 1990's and 2000's widely removed trees in the borough with virtually no replacements because the projects did not preserve adequate planting areas. Public dissatisfaction with the high rate of street tree loss reinvigorated an inactive Shade Tree Commission (established in 1972) to protect trees threatened by proposed projects. Numerous amendments were made to the Selinsgrove Borough Code (Selinsgrove Borough Code 2011) to strengthen the powers of the Commission, one of which was to make the Shade Tree Commission the body with sole authority to approve the removal of trees (§42-8. A). The Shade Tree Commission members had little information about their street trees and proposed an inventory to quantify the street trees for the work of the Commission. This report documents the 2009 inventory, provides analysis of the geographic distribution and ecological diversity of the street tree community, and identifies threats to and vulnerabilities of the trees in Selinsgrove, PA.

INVENTORY METHODOLOGY

Study Area

Selinsgrove Borough is located in Eastern Snyder County, Pennsylvania in the USDA plant hardiness zone 6. Geographic coordinates are 40° 47'N, 76° 51'W. The borough covers 490 ha and contains approximately 38 named streets that may contain street trees (alleys were excluded during this inventory). These streets encompass approximately 18.5 km of roads. Selinsgrove's Shade Tree Commission has jurisdiction over trees that are planted on public land such as parks and trees that are between the street curb and the sidewalk. On streets with no sidewalk, the Commission has jurisdiction over trees in the right-of way along the street.

Field Work

Digital records of roads and buildings were provided by the Selinsgrove Borough for use in ESRI, Inc. ArcMAP software (ESRI, Inc. Redlands, CA). Because this project was part of an educational project that was to span four years, street sampling was conducted at a slower pace than many inventories which are collected in a short time by a large volunteer force. Each street was visited from 2006 to 2009 to record information about the planting bed between the sidewalk and the street curb: namely, planting width and height to overhead wires. These dimensions were provided to the Shade Tree Commission to plan for future plantings. Trees were identified by comparing leaves with diagrams in a tree identification guide (Martine 2003) or using a diagrammatically illustrated field key (Petrides 1972). Where tree identification was unsuccessful using field guides, a volunteer in the Shade Tree Commission who is employed by the state's forestry service was consulted for assistance with the identification. If these procedures failed to produce identification, the tree was recorded as "unknown". At each tree, the location (geographic coordinates) and street address, species, height, crown radius, circumference of each trunk, number of trunks, distance from the ground to the bottom of the crown, the presence or absence of a weak fork, dead wood, structural cavities, damage to sidewalks, and insect damage were noted. Tree height was estimated with a clinometer and planting width, circumference and other dimensions were measured with a tape measure. Digital records were entered on a handheld computer (Compaq iPAQ 5550, Hewlett Packard Co. Palo Alto, CA) running mobile GIS software (ArcPad 6.0, ESRI Inc., Redlands CA) that recorded locations from a connected GPS (Garmin GPS III+, Garmin Ltd. Olathe, KS).

An aerial photograph from 1970 was also used to identify probable street trees for a historical comparison based on their positions in the borough. The image was originally taken on 23 x 23 cm film and enlarged to a 90 x 90 cm print for analysis. The photo was taken in July when tree canopy was fully established. Estimated scale of the photo used for digitizing is RF 1:5,150 or one cm on the photograph equals 51.5 m. Curb to curb measurements for streets on the photo were 1.9 to 2.4 mm, and large tree crowns were as large as 3.5 mm on the photograph. Where the center of a tree crown appeared to line up with the curb line, the tree was counted as a street tree. A 2006 image at the same scale was used to verify the technique. Four, four-block street sections with at least 10 trees were used for a comparison with the field-based counts. Average efficiency of the photo counting was 77% of the actual number of trees.

Statistical Techniques

Statistical analysis of the street tree community was performed to interpret ecological diversity, trends in the tree dimensions, and susceptibility to pests. Lists of susceptible trees given by Raupp et al. (2006) were used to estimate the threat of these insects in the Selinsgrove Borough. In addition to determining which trees might be susceptible to invasive pests, the percentages of the most common tree taxa were examined. Arborists recommend that communities attempt to achieve diversity in their tree community, with no more than 30% of any family, 20% of any genus, or 10% of any species. This diversity buffers against the chance of

wide-spread losses due to disease, insects (Santamour 1990) or extreme weather events.

Ecological statistics determined using the number of individuals and the number of different species (species richness, *R*) identified in the inventory. The Shannon Index (*H'*) was calculated from the number of individuals in a single species (n_i), the number of trees in the sample (*N*) and

$$H' = -\sum_{i=1}^{R} \frac{n_i}{N} \ln\left(\frac{n_i}{N}\right) \qquad \text{Eq. 1}$$

the species richness (*R*) or number of species present (Odum 1997).

The number of effective species is calculated using Jost

$$D = e^{H'} \qquad \text{Eq.2}$$

(2007) and the PARTITION software (Veech and Crist, 2009).

Major roadways and railroad tracks were used to divide the borough into eight distinct "neighborhoods" to evaluate spatial trends in ecological diversity, susceptibility to invasive pests, and increase or decrease in the number of trees.

Statistical analysis of the street trees measurements and neighborhood compositions was done with SAS v9.1 (SAS Institute, Cary, NC) using the general linear model (GLM) procedure and the linear regression (REG) procedure.

RESULTS

The inventory cataloged 346 street trees and 539 curb segments in Selinsgrove Borough. Thirty-four species were identified and eight individual trees remain unidentified (Figure 1). The most common species identified during the inventory were Norway maple (*Acer platanoides*), callery pear (*Pyrus calleryana*), pin oak (*Quercus palustris*), honey locust (*Gleditsia triacanthos*), and red maple (*Acer rubrum*) (see Table 1). Figure 1 suggests that the recent work of the Shade Tree Commission has clearly diversified the trees along the main thoroughfare in the "downtown" section (Market Street between Walnut and Snyder Streets). Street trees established decades ago show less species variation, such as 24 of 28 trees along Rhoads Ave are honey locust, and 14 of 27 trees along Susquehanna Ave. are pin oak, and all 7 trees along Tenth Ave. are Norway maple. Such local species dominance presumably reflects the home builder's preferences at the time neighborhoods were first constructed between 1940 and 1960 show little understanding of the values of species diversity. The population density was 18.7 trees per km of roadway.

Compared to the diversity recommendations by Santamour (1990), *Acer* accounts for 30.6 % of the community in Selinsgrove. This exceeds the 30% recommendation for a family and the 20% recommendation for genus. Similarly, three species have proportions that exceed the 10% recommendation for a single species (see Table 1). An alternate way of expressing diversity is the Shannon Index, which was 2.62 for this community. Although there were 34 unique species identified, the effective number is only 14 because of the high number of species that are comprised of one or two individuals. The five most common species make up 70% of the community, and their size distributions are shown in Figure 2.

The trees were also assessed for their susceptibility to pests. Trees susceptible to EAB and LHB include the *Acer* (maple), *Fraxinus* (ash), *Salix* (willow), *Platanus* (sycamore), *Aesculus* (horse chestnut), *Ulmus* (elm), and *Betula* (birch). These susceptible trees represent 38 % of Selinsgrove's street trees.

The results of the historical inventory are shown in Figure 3. The estimated number of street trees in 1970 is 708 compared to the present 346 trees, indicating that the borough lost approximately 50% of the trees during this time. Many areas in the borough are suitable for planting street

Table 1. The most common tree species in the Borough.

Species	Common Name	Number	Proportion %
Acer platanoides	Norway maple	69	19.9
Pyrus calleryana	Callery pear	67	19.3
Quercus palustris	Pin oak	57	16.5
Gleditsia triacanthos	Honey locust	28	8.1
Acer rubrum	Red maple	22	6.4
Acer saccharum	Sugar maple	8	2.3
Acer saccharinum	Silver maple	7	2.0
Platanus occidentalis	American sycamore	7	2.0
-- 26 other species had less that 2% each --		Total	75.6

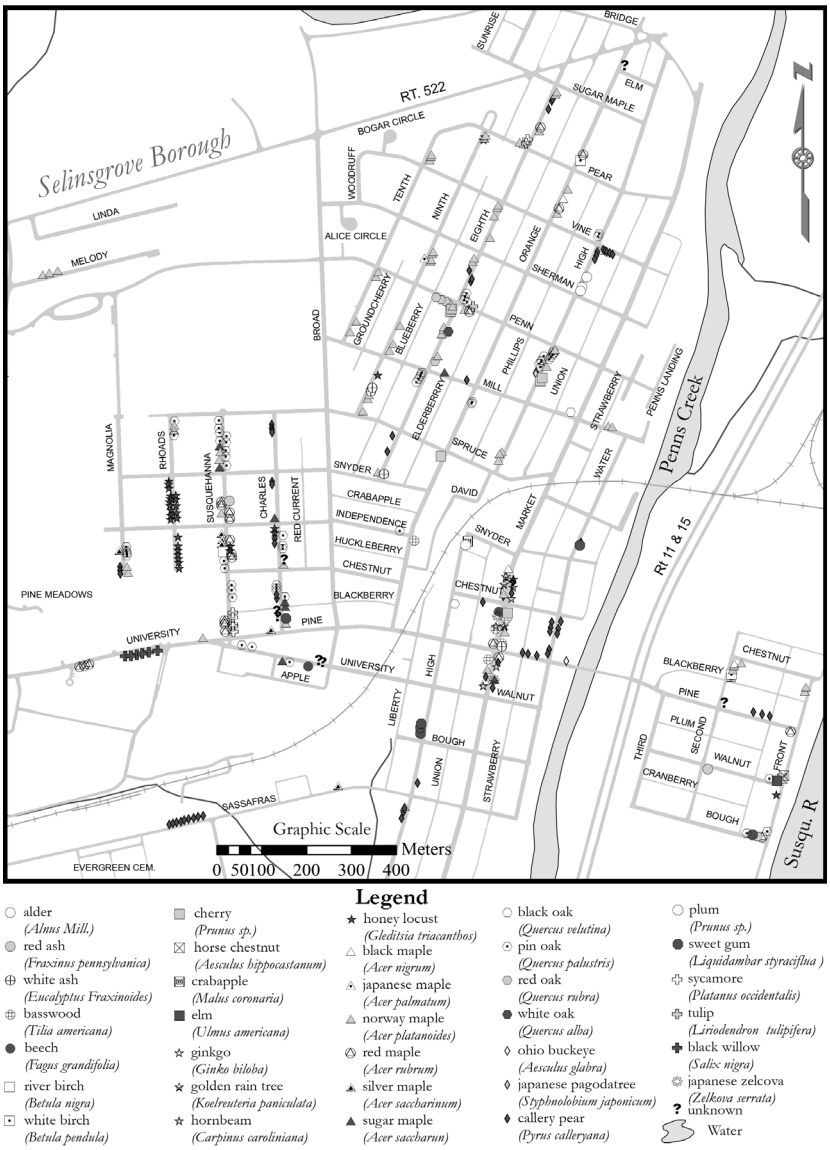

Figure 1. Distribution of street trees in Selinsgrove Borough, Pennsylvania

trees, however. The neighborhood boundaries are shown in Figure 3. With the exception of neighborhoods 4 and 7 (the south school district and the central business district), other neighborhoods lost nearly two-thirds of their trees since 1970 (see Table 2 and Figure 3). Height and diameter statistics show that the central business district (neighborhood 7) has significantly shorter and smaller diameter trees that some other neighborhoods. The neighborhoods that have had tree increases since 1970 also have lower susceptibility to invasive boring insects.

DISCUSSION

Surprisingly, there are few street trees on most major traffic routes through the borough except for the central business district (neighborhood 7, Figure 3). It has been suggested that street trees reduce driver speeds and reduce the number of crashes in urban areas (Dumbaugh 2005, Wolf and Bratton 2006).

Invasive insects are an ever-present threat and communities have lost trees to Dutch elm disease, the gypsy moth (oaks), the wooly adelgid (hemlocks), and chestnut blight. A spreading threat that is already in eleven Pennsylvania counties (including two that neighbor Snyder County: Mifflin and Juniata Counties) is the emerald ash borer (PA DCNR, 2009). This insect's larvae burrow under the bark

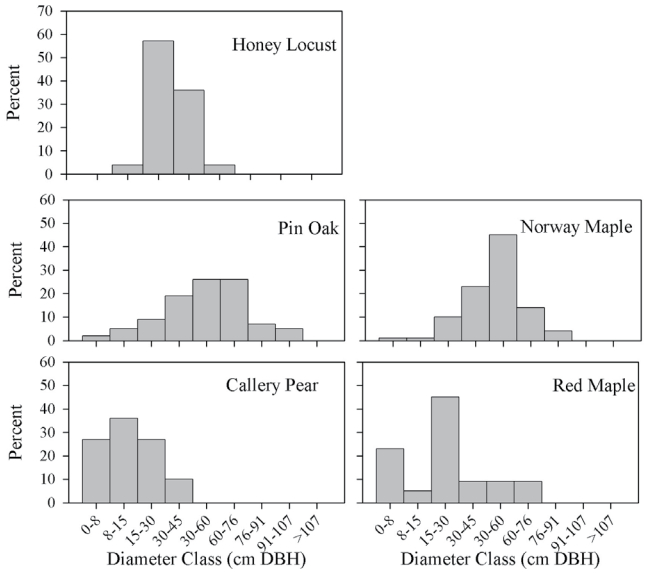

Figure 2. Size distributions of the six most common species in Selinsgrove Borough.

and can kill adult trees in three to four years. The Asian long-horned beetle is another burrowing insect that has been found in surrounding states and may become a problem in Pennsylvania communities (PA DCNR 2010). Susceptible trees represent 38% of the total community and signal the importance of maintaining species diversity in the street trees to avoid wide spread infestations and potential losses of susceptible trees.

Diversity statistics are of particular importance in the individual neighborhoods studied. The neighborhoods that exceed these recommendations are neighborhood 4 which contains nearly 30% each of honey locust and pin oak; neighborhood 6 which contains nearly 30% each of Norway maple and pin oak; and neighborhood 7 which contains 40% callery pear. The effective species for each neighborhood conveys similar information with half the neighborhoods with effective species greater than 8 (Shannon index greater than 2). While there is no "magic number" for the Shannon index, it is desirable to have species diversity to buffer against the impacts of stress and other threats. To illustrate, both neighborhoods 6 and 7 have large numbers

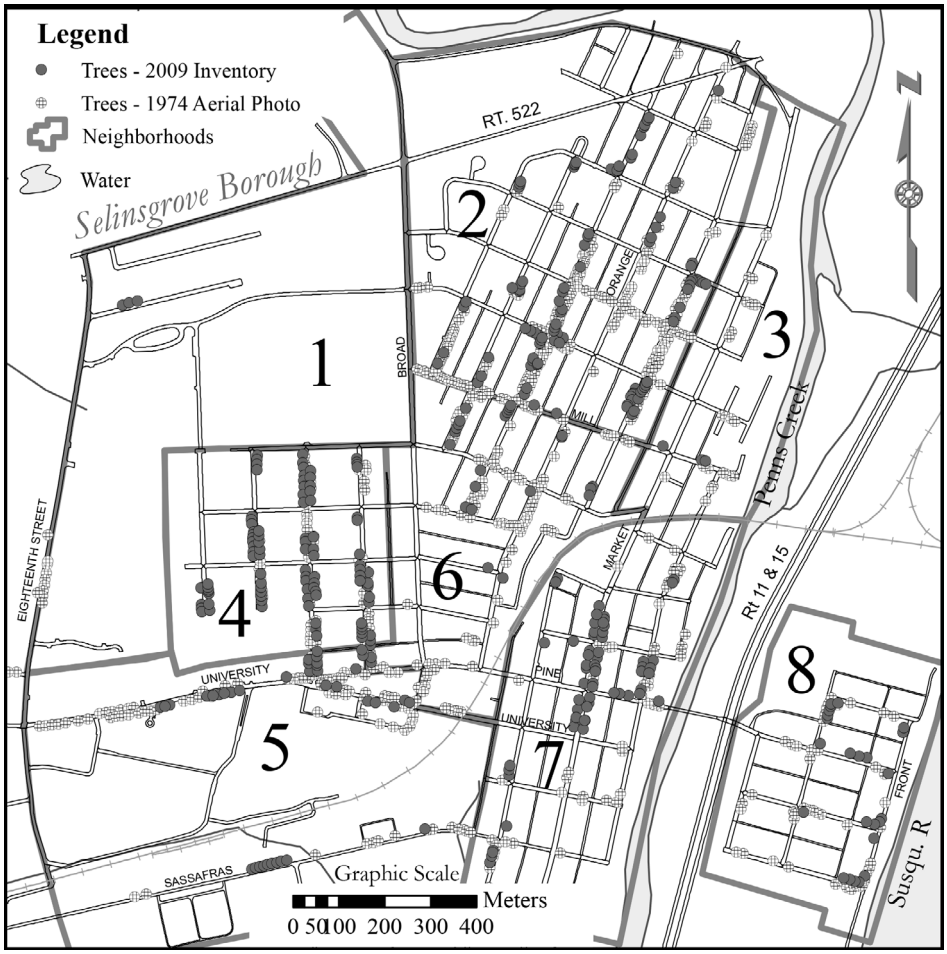

Figure 3. Street trees interpreted from a 1970 aerial photograph along with present day street trees. Neighborhood descriptions and statistics are given in Table 2.

Table 2. Ecological and tree geometry statistics for each neighborhood.

		No.	Species Richness	Shannon Index	No. of Effective Species	% susceptible to EAB or LHB[1]	Height (m)	Diameter (cm)	Tree Increase since 1970[2] (%)
1	Bluff and Schools	3	1	0.00	1	100.0	9.8±0.6 ab[3]	29 ±2.5 cd	-62.5
2	North Residential	98	17	2.05	8	49.0	10.5±4.8 ab	43±2.0 abc	-62.5
3	North Commercial	3	2	0.64	2	66.7	10.3±4.9 ab	45 ±18.5 abc	-87.5
4	South School District	93	10	1.82	6	26.9	10.8±5.2 ab	43±2.3 abc	14.8
5	University/ Industrial	38	10	2.07	8	55.3	11.8±7.3 a	33±4.3 bcd	-64.2
6	Central Residential	26	2	1.8	6	46.2	12.0±5.6 a	50 ±4.6 ab	-75.7
7	Central Business District	61	19	2.26	10	13.1	7.2±3.2 b	22 ±2.0 d	5.2
8	Isle of Que	24	14	2.45	12	54.2	8.6±3.2 ab	53 ±5.3a	-55.6

[1]EAB is Emerald Ash Borer, and LHB is Asian Long Horned Beetle
[2]Percent of trees that was lost between the 2009 inventory and the estimate from the 1970 aerial photo
[3]Values are mean ± standard error of all trees in a neighborhood. Column values with different letters are significantly different at p=0.05.

of trees and numbers of unique species, but in each case, the effective number of species in each neighborhood is only about half of the measured species richness, indicating that though there are many different species present, many of these species occur singularly (see Table 2). Gavin (1999) cautioned against making unwise species selections in order to diversify street trees because many trees are incapable of withstanding urban stresses. Selinsgrove contains 34 different street tree species, but 29 of those species comprise less than 5% of the total community, which equates to 14 effective species. While recommended tree lists have been proposed for specific communities (for example, see Gavin 1999) decisions made about planting species in the future could be made based on how well underrepresented species are faring in a community, increasing the populations of these taxa rather than continuing to plant the same common species. These calculations also provide the managers of this resource with a snapshot of the present diversity and will be able to use these measures to evaluate the progress of attempts to diversify the street tree community in the future.

We compared the trees identified in the inventory with trees we interpreted from a 1970 aerial photograph. Approximately 350 trees have been lost in the borough since the inception of the borough's Shade Tree Commission. Clearly, this was a disturbing loss and reflects the dynamic nature of street trees. Elmendorf et al. (2003) and Stevenson et al. (2008) revealed the attitudes of community leaders in communities like Selinsgrove throughout Pennsylvania. They reported that often even the efforts and opinions of shade tree organizations, such as the borough's Shade Tree Commission, do not translate into the maintenance or development of shade tree projects due to community politics and the changing priorities of community residents. These organizations and concerned citizens are encumbered by a variety of issues including insufficient financial, administrative, or popular support.

Age distribution diagrams are a useful way to evaluate whether the community has sufficient younger trees to maintain the community as trees age and eventually die or otherwise need to be removed because of size or damage to their constructed surroundings. For most communities, it is too costly to supplement the street trees by planting large-caliper trees, so having a significant number of small diameter trees assures that there will be a collection of larger trees in the future. Because determining the diameter at breast height (DBH) is faster, easier, and safer than determining actual age by tree ring borings, we discuss size distribution rather than age distribution. The five most common species make up 70% of the community, and their size distributions are shown in Figure 2. Of particular concern is the shape of the distribution curve for honey locust, Norway maple, and pin oak. These species have average diameters of nearly 60

cm, and have virtually no trees in the 15 cm DBH group, the younger trees which will eventually replace these large trees as they die or are replaced. Callery pear and red maple have more appropriate age distribution because there is a significant percent of the community which is young (small diameter) and will eventually replace the older trees.

The tree diameter classes were evaluated by neighborhood to identify areas in inappropriate size distributions. Neighborhoods 5 and 7, the university zone and the central business district, are the best poised to sustain their numbers as they age because the majority of these trees have diameters less than 30 cm. All other neighborhoods have average diameters in the 45-75 cm range (see also Table 2). This observation is also expressed in the statistically significant differences between the diameter and the height of trees. Most notably, the trees in the central business district are significantly shorter than those in the university zone and the central residential district. Similarly, the central business district trees are narrower than trees in five of the seven other neighborhoods. The differences in tree size between neighborhoods suggest that the Shade Tree Commission has disproportionately used resources to plant young trees in areas of public commerce but not in residential areas.

CONCLUSIONS

The inventory documented 346 trees in the Borough Selinsgrove, PA; approximately half the trees that were present when the Shade Tree Commission was established in 1972. Of the trees that remain, 38% are susceptible to boring insects. The existing forest has few young trees that will replace older trees that will eventually die or be removed. The Selinsgrove shade tree forest suffers from three pressing deficiencies: 1) the forest has been in numerical decline over the last 40 years as trees have been removed much faster than they have been replaced; 2) the trees that remain are not ecologically diverse in that only three species make up more than one-half of the entire forest; and 3) the age structure of the forest suggests there are insufficient young trees to sustain the numbers into the next several decades. These deficiencies put the trees at risk of continued decline as natural aging, street projects, and potential spread of invasive boring insects all act to weaken and kill trees. Since street trees do not naturally replace themselves through seedlings, intentional efforts will be required to sustain the community. Assuming a street tree might live 40 years, the current forest will require that 8 replacement trees be planted each year to sustain the tree numbers at current levels.

ACKNOWLEDGEMENTS

We thank Karl Mull and the Selinsgrove Shade Tree Commission for their guidance and feedback throughout the survey. Susquehanna University and the Susquehanna University Assistantship Program supported this project financially.

LITERATURE CITED

Anagnostakis, SA. 1987. Chestnut blight: the classical problem of an introduced pathogen. Mycologia. 79: 23–37.

Akbari, H., S. Davis, S. Dorsano, J. Huang, and S.Winnett. 1992. Cooling our communities: a guidebook on tree planting and light–colored surfacing. Government Printing Office, Washington, D.C. 217 pp.

Brack, C.L. 2002. Pollution mitigation and carbon sequestration by an urban forest. Environmental Pollution, 116:S195–S200.

Donovan, G. H., and D.T. Butry. 2009. The value of shade: Estimating the effect of urban trees on summertime electricity use. Energy and Buildings. 41:662-668.

Donovan, G. H., and D.T. Butry. 2010. Trees in the city: Valuing street trees in Portland, Oregon. Landscape and Urban Planning. 94:77-83.

Dumbaugh, E. 2005. Safe streets, livable streets. Journal of the American Planning Association, 71(3):283–300.

Elmendorf, W.F., V.J. Cotrone, and J.T. Mullen. 2003. Trends in urban forestry practices, programs and sustainability: Contrasting a Pennsylvania, U.S. study. Journal of Arboriculture 29:237–247.

Gavin, M.F. 1999. A methodology for assessing and managing biodiversity in street tree populations: A Case Study. Journal of Arboriculture, 25(3):124-128.

Georgi, N.J. andK. Zafiriadis. 2006. The impact of park trees on microclimate in urban areas. Urban Ecosyst. 9:195-209.

Haack, H.A, F. Hérard, J Sun, J.J. Turgeon. 2010. Managing invasive population of Asian longhorned beetle and citrus longhorned beetle: a worldwide perspective. Annual. Rev. Enomol. 55:521-46

Jost, L. 2007. Partitioning diversity into independent alpha and beta components. Ecology, 88:2427-2439

Maco, S.E., and E.G McPherson. 2003. A practical approach to assessing structure, function and value of street tree populations in small communities. Journal of Arboriculture. 29:84-97

Martine, C.T. 2003. Trees of New Jersy and the Mid-Altlantic States 5th ed.. J.E. Kuser, J. Benton, D.W. MacFarlane, and T. O'Learly, eds. New Jersey Forest Service. Jackson, NJ. 116 pp.

McHale,M.R, I.C. Burke, M.A. Lefshy, P.J. Peper, and E.G. McPherson. 2009. Urban Forest Biomass estimates: Is it important to use allometric relationships developed specifically for urban trees? Urban Ecosyst. 12:95-113.

McPherson, E.G., J.R. Simpson, P.J. Peper, S.E. Maco, and Q. Xiao. 2005. Municipal forest benefits and costs in five US cities. Journal of Forestry. 103:411-416.

McPherson, E.G. and J. Muchnick. 2005.Effects of street tree shade on asphalt concrete pavement performance. Journal of Arboriculture, 31:303-310.

Millward, A.A. and S Sabir, 2011. Benefits of a forested urban park: What is the value of Allan Gardens to the city of Toronto, Canada? Landscape and Urban Planning 100:177-188

Nowak, D.J., J.E. Pasek, R A. Sequeira, D.E. Crane and V.C. Mastro. 2001. Potential Effect of *Anoplophora glabripennis* (Coleoptera: Cerambycidae) on urban trees in the United States. J. Econ. Entomol. 94:116-122.

Odum, E.P. 1997 Ecology: A bridge between science and society. Sunderland, MA: Sinauer Associates, Inc., 331 pp.

PA. Dept. Conservation and Natural Resources. 2010. Asian Longhorned Beetle. http://www.dcnr.state.pa.us/forestry/fpm_invasives_ALB.aspx (accessed 8 1, 2010).

PA. Dept. Conservation and Natural Resources 2009. Emerald Ash Borer. http://www.dcnr.state.pa.us/forestry/fpm_invasives_eab.aspx (Accessed 8 1, 2010).

Petrides, G.A. 1972. A field guide to trees and shrubs, Northeastern and north-central United States and southeastern and south-central Canada. 2nd ed. Peterson Field Guides Series. Houghton Mifflin Co. Boston. 428 pp.

Raupp, M.J., A.B. Cumming, and E.C. Raupp. 2006. Street tree diversity in eastern North America and its potential for tree loss to exotic borers. Arbiculture and Urban Forestry, 32(6):297-304.

Santamour, F.S. 1990. Trees for urban planting: Diversity, uniformity, and common sense. Proc. 7th Conf. Metropolitan Tree Improvement Alliance (METRIA). 7:57-65.

Schwaab, E.C., L. Alban, J. Riley, R. Rabaglia, and K.E. Miller. 1995. "Maryland's forests: A health report." Maryland Department of Natural Resources–Forest Service, MD, 48 pp.

Selinsgrove Borough Code. http://selinsgrove.org/Documents/Selinsgrove%20Code%20Book-%20through%20October%202011.pdf." Verified 6/25/2012.

Sinclair, W.A. and R.J. Campana. 1978. Dutch elm disease: Perspectives after 60 years. Northeast Regional Research Publication, 8(5):52 pp.

Smiley, E.T, and F.A Baker. 1988. Options in street tree inventories. Journal of Arboriculture 11:210-213.

Stevenson, T.R., H.D. Gerhold, and W.F. Elmendorf. 2008. Attitudes of municipal officials toward street tree programs in Pennsylvania, U.S. Arboriculture & Urban Forestry, 34(3):144-151.

U.S. Forest Service. i-Tree. http://www.itreetools.org/about.php. Verified 6/18/ 2010.

Veech, J.A. and T.O. Crist. 2009. PARTITION: software for hierarchical partitioning of species diversity, version 3.0. http://www.users.muohio.edu/cristto/partition.htm

Wolf, K.L. and N. Bratton. 2006.Urban trees and traffic safety: Considering U.S. roadside policy and crash data. Arboriculture & Urban Forestry, 32(4):170-179.

Journal of the Pennsylvania Academy of Science 86(1): 54-60, 2012

DETECTION OF MERCURY IN NATURAL WATERS IN BERKS COUNTY, PENNSYLVANIA, USING COLD VAPOR ATOMIC ABSORPTION SPECTROSCOPY[1]

AMANDA MCGETTIGAN, DANIEL KWASNIEWSKI, AND ROSEMARIE C. CHINNI[2]

Alvernia University, Department of Math and Sciences, 400 Saint Bernardine St., Reading, PA 19607

ABSTRACT

Cold Vapor Atomic Absorption Spectroscopy (CVAAS) was used to detect potential mercury contamination in sixteen natural waterways in Berks County, Pennsylvania. Four samples were collected from each site in mercury-free Nalgene containers. After collection, the samples were brought back to the lab, acidified, and refrigerated until analysis could proceed. For analysis, each sample was prepared by adding various reagents and by digesting each in a 95°C water bath for approximately two hours. The digested samples were analyzed using tin (II) chloride and the maximum absorbance of each sample was recorded. Calibration curves were developed using serial dilutions of the mercury standard; these curves allowed for calculation of detection limits for mercury and were also used to calculate the mercury concentration in the samples if any was present. The results showed that none of the waterways tested had significant amounts of mercury present. [J PA Acad Sci 86(1): 54-60, 2012]

INTRODUCTION

Methylmercury is found in some concentration in almost all aquatic life due to the global cycling of mercury (Clarkson and Magos, 2006). This cycling begins when mercury vapor is released into the atmosphere through natural and anthropogenic sources. Natural sources consist of volcanoes, fossil fuels, and forest fires. Anthropogenic sources are broken down into four main categories: (1) area sources from landfills and laboratory release, (2) combustion processes from medical and municipal waste incinerators and coal power plants, (3) manufacturers of cement and metals, and (4) other unaccounted for industrial processes such as power plants (Clarkson and Magos, 2006; Kelter et al., 2009; Mercury in the Environment and Water Supply website).

[1]Submitted for publication July 2012; accepted December 2012
[2]Corresponding author: Rosemarie C. Chinni, Alvernia University, Department of Math and Sciences, 400 Saint Bernardine St., Reading, PA 19607, rosemarie.chinni@alvernia.edu, 610-568-1492

Once mercury vapor is released into the atmosphere, it can remain there for months possibly years at a time because of its low volatility and stability. This vapor can undergo a photochemical oxidation process to an inorganic mercuric mercury. In this form, it can be deposited back to the earth through rainwater. A fraction of this mercury can be reduced back into its vapor form in order to complete this cycle and the other fraction remains present in the aquatic environment. This inorganic mercury can settle into the aquatic environment and be converted to methylmercury by sulfide-reducing bacteria. If inorganic mercury is not readily converted to methylmercury as soon as it enters the water system, it will settle into the natural sediments of the earth; once here, it can be converted into methylmercury by microorganisms. Methylmercury is the most toxic form and has the greatest bioavailability of all the mercury compounds (Clarkson and Magos, 2006; Kelter et al., 2009; Mercury in the Environment and Water Supply website).

Methylmercury is the form of mercury that is present in water and can contaminate water supplies along with the aquatic species, primarily fish (Chan et al., 2003). In order to determine the amount the mercury present in the water, a digestion process needs to be performed on the water samples; this digestion process will produce free mercury atoms that can easily be detected by cold vapor atomic absorption spectroscopy (CVAAS).

CVAAS is utilized specifically for the detection of mercury in samples because free mercury atoms are able to exist at room temperature; therefore, there is no need for a heated cell. In this technique, mercury is reduced to its free atomic state using of a strong reducing agent in a closed system. The free mercury is pushed out of the sample container with argon gas. An absorption cell is placed in the path of the light from the spectrophotometer. This cell is connected to a tube which delivers the free mercury atoms after the atoms are expelled from the sample container. The absorbance is measured as the mercury atoms pass into the sample cell and into the light's path. The highest absorbance observed will be recorded as the analytical signal (Skoog et al., 2007; Atomic Absorption Spectroscopy website, Galbraith Laboratories, Inc.).

This project was designed for undergraduate students to learn valuable analytical techniques that included 1) using proper sampling procedures, 2) making and preparing reagents and calibration standard solutions, 3) preparing

samples for analysis by using a method of digestion, 4) using the CVAA spectrometer, 5) making and using calibration curves properly, and 6) performing data analysis and reporting the results. The main focus of the project was to determine if there were any environmental impacts from the presence of mercury in natural waterways in Berks County, PA, considering the proximity of coal mines and a nuclear power plant.

MATERIALS AND METHODS

Reagents and Standards Preparation:

Several different reagents were made for this analysis. A 1:1 nitric acid (HNO_3): water (H_2O) solution was made by adding 500 mL of concentrated nitric acid (Fisher Scientific, Fairlawn, NJ) to 400 mL water and diluting this solution to 1 L with distilled water. 0.5 N sulfuric acid (H_2SO_4) solution was made by adding 14 mL concentrated sulfuric acid (Fisher Scientific, Fairlawn, NJ) to 500 mL of distilled water and then diluted up to the 1 L mark on a volumetric flask with distilled water. A potassium permanganate ($KMnO_4$) solution was made by measuring 5 g potassium permanganate (Fisher Scientific, Fairlawn, NJ) and dissolving it in 100 mL of distilled water. A potassium persulfate ($K_2S_2O_8$) solution was made by measuring out 5 g of stock potassium persulfate (Fisher Scientific, Fairlawn, NJ) and dissolving it in 100 mL of distilled water. A sodium chloride-hydroxylammonium chloride solution was made by dissolving 12 g of sodium chloride (NaCl; Fisher Scientific, Fairlawn, NJ) and 12 g hydroxylamine hydrochloride ($NH_2OH{\bullet}HCl$; Fisher Scientific, Fairlawn, NJ) in 100 mL of distilled water. A stannous chloride solution was made by adding 25 g $SnCl_2{\bullet}2H_2O$ (Fisher Scientific, Fairlawn, NJ) to 250 mL of 0.5 N H_2SO_4.

A set of calibration standards was made by diluting a 1000 ppb mercury (Hg) AAS standard solution (Perkin Elmer, Shelton, CT). A total of five calibration standards were made that ranged in concentration from 0.5 ppb to 10.0 ppb. These solutions were all diluted using distilled water to prevent ion contamination.

Sample Collection:

Samples were collected from sixteen different lakes or streams throughout Berks County. The sample sites were spread out across Berks County in order to give a broad range of samples. The sample sites are shown in Figure 1 and marked with an "X" (Map Reference, BridgeHunter.com). The sixteen sample sites were as follows: Blue Marsh Lake, Christman Lake, Lake Ontelaunee, Hopewell Lake, Daniel Boone Lake, Hay Creek, Manor Creek, Maiden Creek, Furnace Creek, Moseleum Creek, Sacony Creek, Wolf Creek, Owatin Creek, Angelica Creek, Allegheny Creek, and Little Muddy Creek.

From each site, four water samples were collected. The water samples were collected in mercury-free 125 mL plastic Nalgene bottles (Fisher Scientific, Fairlawn, NJ). The sample collectors wore personal protective equipment on their hands, long pants, and closed toed shoes to eliminate the risk of sample contamination. Water was collected by dipping the sample bottle into the creek, lake, or stream two to three feet away from the shore line and three to six inches in depth depending on the terrain of the particular sample site. The sample bottles were then dried off and the time, date, GPS location, sample number, location name, and researcher initials were recorded on each bottle in permanent marker; this information is provided in Table 1. The water samples were brought back to the lab in ice chests to preserve the samples until the acidification process could occur. After being brought back to the laboratory, their pH was checked. For mercury determination, the water samples need to be acidified to a pH less than two. If the pH was greater than two, as was our case, the 1:1 nitric acid:water solution was added until the pH measured less than two. After acidification, the samples were preserved and placed into a refrigerator until analysis. Analysis was completed within the 28 day preservation time (O'Dell et al., 1994).

Method for Standard and Sample Analysis:

EPA Method 245.1 was used for this analysis; this method was first developed in 1972 and has been revised several times (O'Dell et al., 1994). A brief synopsis of the method is included in this section.

The calibration standards were made fresh each day of analysis. Afterwards, the standards were prepared for CVAAS analysis by taking 100 mL of each standard and placing each in separate 250 mL Erlenmeyer flasks. To each 100 mLs of standard, the following amounts of reagents were added: 5 mL of sulfuric acid, 2.5 mL nitric acid, 15 mL of potassium permanganate solution; after waiting for 15 minutes, 8 mL of potassium persulfate and finally 6 mL of sodium chloride hydroxylammonium chloride were added. Each of the standards was placed in the reaction vessel and 5 mL of tin (II) chloride was added. After the addition of the tin (II) chloride, the reaction vessel was attached to the Mercury Hydride System (MHS); the MHS was used in conjunction with the Atomic Absorption Spectrometer (AA) (MHS 15 and AAnalyst 800, Perkin Elmer, Shelton, CT). Argon gas (Air Liquide America L.P., Houston, TX) was used to carry the sample from the MHS to the absorbance cell which is placed in the path of the mercury lamp. The absorbance was monitored until a maximum reading was obtained; this usually occurred approximately 30 seconds after the reaction vessel was attached. A diagram for the

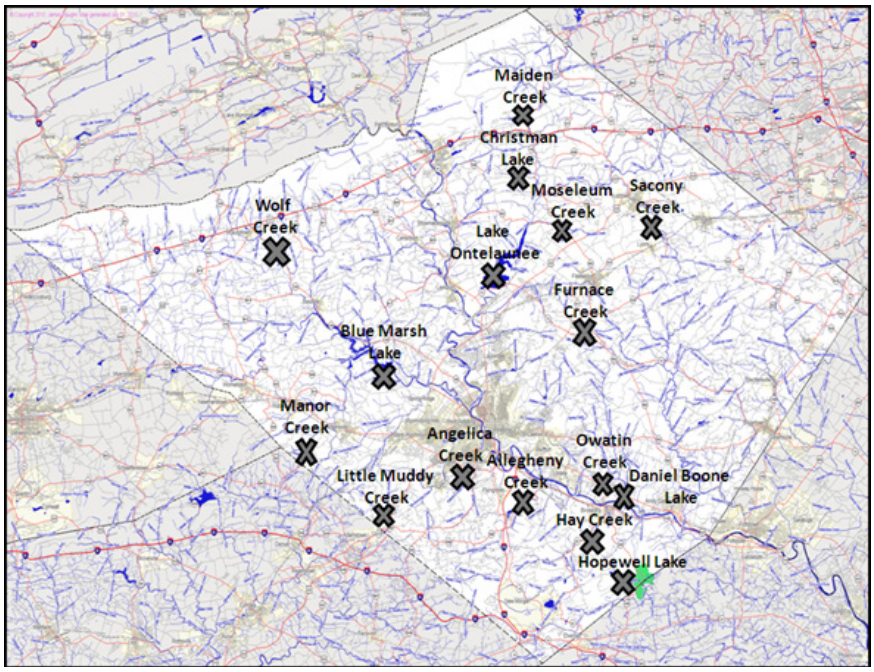

Figure 1. Map of Berks County Pennsylvania with markers ("X") to indicate the sixteen different waterways sampled during the experiment.

MHS and AA are shown in Figure 2. Three trials were run per each standard (O'Dell et al., 1994).

The water samples were prepped for CVAAS analysis in the same manner as the calibration standards with one exception; after the addition of the potassium persulfate solution, the water samples were placed in a 95˚C water bath for two hours. The purpose of this water bath was to convert the methyl mercury to elemental mercury. After the two hour digestion was complete, the water samples were taken out of the water bath and allowed to cool to room temperature. Once the samples were cooled, 6 mL of sodium chloride hydroxlyammonium chloride was added to each of the samples. One at a time, the samples were placed into the reaction vessel, 5 mL of tin(II) chloride was added and the reaction vessel was attached to the mercury hydride system for analysis. Like each calibration standard, each of the water samples was analyzed three times (O'Dell et al., 1994).

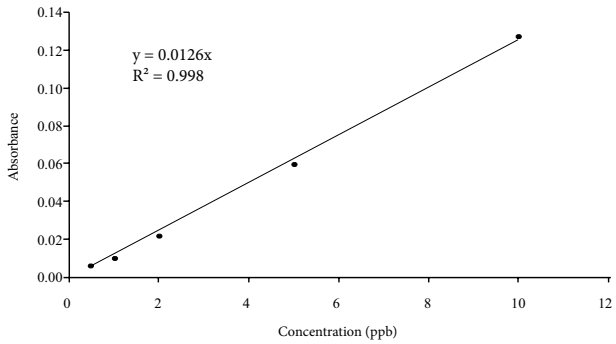

Figure 3: Example of a typical mercury calibration curve with the absorbance plotted against the concentration of the calibration standards. Each point represents an average of three trials.

Data Analysis:

After the standard data was gathered, an average absorbance was calculated for each reading using Microsoft Excel. All of the average absorbance results were background corrected using average absorbance of the blank sample; afterwards, a standard deviation and percent relative standard deviation were calculated using Microsoft Excel. In order to create the background corrected calibration curve, the background corrected average absorbance of the standards was plotted against their corresponding concentrations. A typical background corrected calibration curve is shown in Figure 3. A linear trendline was fitted to the graph. Detection limits were calculated based on a 3σ detection (Compendium of Chemical Terminology). For each sample analyzed, the linear trendline of the calibration curve was used to calculate the concentration of mercury present, if any.

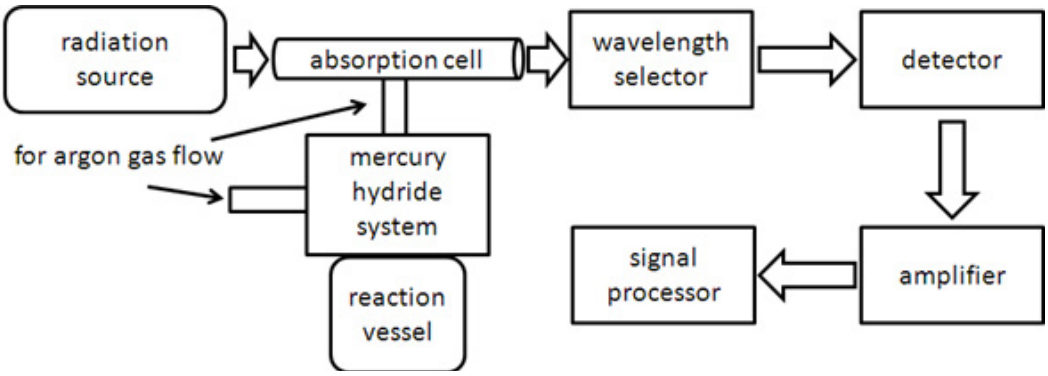

Figure 2. A diagram of the CVAAS which shows the MHS and the AA.

RESULTS AND DISCUSSION

The EPA has defined a maximum contaminant level (MCL) of 2.00 ppb of mercury in drinking water sources; the MCL provides a maximum allowable concentration in the source (Water: Drinking Water Contaminants, 2009). Approximately, four sites were analyzed each day. A new calibration curve was made each day of analysis to account for instrument instabilities like variation in the light source output, argon flow, etc. From each calibration curve, a detection limit was calculated. The detection limit represents the lowest readable concentration. The linear trendline was used to calculate the mercury concentration in each sample; therefore, if a sample produced a mercury reading below the detection limit for that day, it was labeled as "not detected or ND."

Four water samples were taken from each site at different locations in the creek or lake. There were two instances where sampling from different locations in the creek proved difficult. Little Muddy Creek was surrounded mainly by private property and farming fields limiting the researchers to a small sampling region; the samples labeled as 1, 2, and 3 were taken a few inches apart, but the GPS did not have a high enough resolution to differentiate between the three locations. Wolf Creek also ran through private properties, heavily wooded areas, and dense brush, which could not be accessed by the researchers at the time of sampling; these samples were also taken a few inches apart with the safety of the investigators in mind.

Typically four water samples were analyzed from each of the sampling sites and each water sample was analyzed three times. There were three instances where only three of the four water samples taken were analyzed; this pertained to the analysis of Little Muddy, Maiden Creek, and Furnace Creek. There was human error during the reduction process of methyl mercury to mercury. While the samples were in water baths for over two hours, condensation collected on the exterior of the Erlenmeyer flasks; leading to three broken samples (one from the three different sites) in the water baths and/or countertops. The chemicals were quickly cleaned up using the appropriate counter reagents. The three remaining samples that were analyzed from each site still provided enough replicates for sufficient mercury analysis; therefore, no new samples were taken from each of the above sites to replace the contaminated/damaged sample.

Table 1. List of the water ways which were sampled, along with the sample number, GPS coordinates and short description of the area where the water was collected.

Site	Sample	GPS Coordinates	Description
Allegheny Creek	1	N 40^0 15.987' W 75^0 53.770'	Creek flowing out of private lake surrounded by residential homes in heavily wooded area.
	2	N 40^0 15.990' W 75^0 53.787'	
	3	N 40^0 16.002' W 75^0 53.776'	
	4	N 40^0 15.953' W 75^0 53.832'	
Angelica Creek	1	N 40^0 18' 37" W 75^0 55' 20"	Creek that passes through City Park in Reading, PA. No Swimming, due to bacterial culture. Suburban.
	2	N 40^0 18' 14" W 75^0 56' 5"	
	3	N 40^0 18' 45" W 75^0 55' 41"	
	4	N 40^0 18' 43" W 75^0 55' 32"	

Blue Marsh Lake	1	N 40^0 24' 43" W 76^0 5' 18"	Freshwater Reservoir, with recreational fishing, boating, and swimming. Rural.
	2	N 40^0 24' 24" W 76^0 4' 43"	
	3	N 40^0 23' 6" W 76^0 1' 59"	
	4	N 40^0 23' 5" W 76^0 2' 2"	
Christman Lake	1	N 40^0 32.612' W 75^0 53.228'	Lake surrounded by residential community. Boating area. Suburban.
	2	N 40^0 32.612' W 75^0 53.232'	
	3	N 40^0 32.615' W 75^0 53.195'	
	4	N 40^0 32.591' W 75^0 53.689'	
Daniel Boone Lake	1	N 40^0 17' 30" W 75^0 47' 8"	Historical Homestead, site of blacksmithing and metal forge. Rural Area.
	2	N 40^0 17' 42" W 75^0 47' 43"	
	3	N 40^0 17' 42" W 75^0 47' 55"	
	4	N 40^0 17' 44" W 75^0 47' 48"	
Furnace Creek	1	N 40^0 25.153' W 75^0 49.422'	Small Creek surrounded by farm land and cattle farms. Rural.
	2	N 40^0 25.146' W 75^0 49.425'	
	3	N 40^0 25.146' W 75^0 49.422'	
	4	N 40^0 25.137' W 75^0 49.428'	
Hay Creek	1	N 40^0 15' 58" W 75^0 48' 15"	Creek filled with pollutants that runs through the town of Birdsboro, site of old steel mill. Urban.
	2	N 40^0 15' 49" W 75^0 47' 34"	
	3	N 40^0 15' 56" W 75^0 47' 17"	
	4	N 40^0 15' 56" W 75^0 48' 16"	
Hopewell Lake	1	N 40^0 12' 2" W 75^0 47' 22"	State Park, Heavily Wooded Area. Heavy fishing and boating area.
	2	N 40^0 12' 1" W 75^0 47' 34"	
	3	N 40^0 12' 1" W 75^0 47' 17"	
	4	N 40^0 15' 56" W 75^0 48' 16"	
Lake Ontelaunee	1	N 40^0 26.944' W 75^0 54.878'	Large Freshwater Reservoir provides freshwater to the city of Reading, PA.
	2	N 40^0 26.911' W 75^0 55.104'	
	3	N 40^0 28.194' W 75^0 55.205'	
	4	N 40^0 28.222'W 75^0 55.217'	
Little Muddy Creek	1	N 40^0 16' 29" W 76^0 3' 15"	Rural Creek occupied by wildlife, surrounded by cattle farms and cornfields.
	2	N 40^0 16' 29" W 76^0 3' 15"	
	3	N 40^0 16' 29" W 76^0 3' 15"	
	4	N 40^0 16' 30" W 76^0 3' 15"	
Maiden Creek	1	N 40^0 35.175' W 75^0 53.684'	Large Creek that flows through Northern Berks County and under old train crossings and bridges.
	2	N 40^0 35.170' W 75^0 53.674'	
	3	N 40^0 35.167' W 75^0 53.681'	
	4	N 40^0 35.163' W 75^0 53.689'	
Manor Creek	1	N 40^0 18.772' W 76^0 5.933'	Creek that flowed out of local private lake next to rural federal property.
	2	N 40^0 18.718' W 76^0 5.942'	
	3	N 40^0 18.709' W 76^0 5.942'	
	4	N 40^0 18.712' W 76^0 5.945	

Moseleum Creek	1	N 40^0 29.615' W 75^0 49.644'	Small Creek surrounded by farm land and cattle farms. Rural.
	2	N 40^0 29.609' W 75^0 49.729'	
	3	N 40^0 29.609' W 75^0 49.726'	
	4	N 40^0 29.609' W 75^0 739'	
Owatin Creek	1	N 40^0 17' 42" W 75^0 47' 58"	Small Creek in heavily wooded area flows into Daniel Boone Lake. Rural.
	2	N 40^0 17' 43" W 75^0 47' 57"	
	3	N 40^0 17' 30" W 75^0 47' 8"	
	4	N 40^0 17' 52" W 75^0 47' 15"	
Sacony Creek	1	N 40^0 31.961' W 75^0 51.271'	Creek that flows through Kutztown, PA. Surrounded by farms and wooded areas. Suburban/Rural.
	2	N 40^0 32.233' W 75^0 50.317'	
	3	N 40^0 32.103' W 75^0 47.261'	
	4	N 40^0 32.099' W 75^0 47.354'	
Wolf Creek	1	N 40^0 28' 2" W 76^0 6' 43"	Surrounded by local farms and farming equipment. Rural.
	2	N 40^0 29' 31" W 76^0 6' 43"	
	3	N 40^0 29' 31" W 76^0 6' 43"	
	4	N 40^0 29' 31" W 76^0 6' 43"	

The average absorbance values from each of the water samples were background corrected using the average absorbance value from the blank sample analyzed. The corrected absorbance values were used to determine the average concentration of mercury in the sample using the linear trendline from the background corrected calibration curve. From this, standard deviations and percent relative standard deviations (%RSDs) could be calculated for each water sample. Ten of the sixteen sites showed no mercury contamination in any of the samples analyzed. The other sites recorded mercury concentrations below 0.56 ppb; this is below the MCL of 2.0 ppb mercury. The range of mercury concentrations in each water source can be seen in Table 2. Table 3 shows the individual water samples from each site that produced a mercury concentration along with their %RSDs. It should be noted that the %RSDs were all below 1.2% showing the precision of CVAAS.

CONCLUSION

Throughout this project, the students learned how to use proper sampling procedures for water, store the water for future analysis, make and prepare reagents for the mercury analysis, and make calibration standards through dilutions. Furthermore, the students learned how to properly digest

Table 2. Summary of the overall mercury concentrations in all waterways sampled.

Site	Range of mercury concentrations (ppb)
Allegheny Creek	0.43 to 0.56
Angelica Creek	ND
Blue Marsh Lake	0.15 to 0.23
Christman Lake	ND 3 of the 4 samples; one sample contained 0.15 ppb
Daniel Boone	ND
Furnace Creek	ND
Hay Creek	ND
Hopewell Lake	ND
Lake Ontelaunee	ND
Little Muddy Creek	ND
Maiden Creek	0.11 to 0.12 (range from 2 samples; ND in one sample)
Manor Creek	0.38 to 0.53
Moseleum Creek	ND
Owatin Creek	ND
Sacony Creek	ND
Wolf Creek	0.18 to 0.34 (range from 3 samples; ND in one sample)

Table 3. Individual sample information for the sites that showed mercury present.

Site	Sample	Avg. Conc. (ppb)	%RSD
Allegheny Creek	1	0.56	0.30
	2	0.43	0.40
	3	0.56	0.33
	4	0.49	0.34
Blue Marsh Lake	1	0.20	0.85
	2	0.16	1.0
	3	0.23	0.72
	4	0.15	1.1
Christman Lake	1	0.15	0.62
	2	ND	
	3	ND	
	4	ND	
Maiden Creek	1	0.12	0.13
	2	ND	
	3	0.11	0.23
	4	ND	
Manor Creek	1	0.53	0.32
	2	0.43	0.43
	3	0.48	0.35
	4	0.38	0.45
Wolf Creek	1	0.34	0.64
	2	ND	
	3	0.18	0.93
	4	0.18	1.0

the water samples; this was the most time-consuming part of the experiment. The students developed a thorough understanding of the operation of the CVAA spectrometer and used calibration curves to determine detection limits and predict the amount of mercury in their samples. As a result, all of the learning objectives were fulfilled throughout this experiment.

The data presented here demonstrates the capabilities of CVAAS to determine the presence of methylmercury contaminants in fresh water samples. The average detection limit was 0.084 ppb. The sites that showed mercury present were below the MCL. Therefore, none of the waterways sampled in Berks County, PA, contained enough mercury to be considered unsafe to society and the surrounding wildlife.

Future research includes testing the same water sample sites during different seasons to determine if there is any change in the mercury concentration from one season to another. Other research options include analyzing different waterways in Berks County, PA, and testing the water samples for other contaminants such as arsenic and lead.

ACKNOWLEDMENTS

This work was funded by U.S. Department of Energy.

LITERATURE CITED

Atomic Absorption Spectroscopy. Galbraith Laboratories, Inc. http://www.galbraith.com/spectroscopy.htm

Chan, H.M., A.M. Scheuhammer, A. Ferran, C. Loupelle, J. Holloway, and S. Weech. 2003. Impacts of Mercury on Freshwater Fish-Eating Wildlife and Humans. Human and Ecological Risk Assessment. 9: 867-883.

Clarkson, T.W. and L. Magos. 2006. The Toxicology of Mercury and Its Chemical Compounds. Critical Reviews in Toxicology. 36:609-662.

Compendium of Chemical Terminology, 2nd ed., IUPAC, Research Triangle Park, NC.

Kelter, P., A. Scott, and M. Mosher. 2009. Chemistry: The Practical Science, Media Enhanced Edition. Houghton Mifflin Harcourt. Boston, MS.

Map Reference: BridgeHunter.com, Historic Bridges of the United States. http://bridgehunter.com/pa/berks/big-map

Mercury in the Environment and Water Supply. http://people.uwec.edu/piercech/Hg/mercury_water/cycling.htm

O'Dell, J.W., B.B. Potter, L.B. Lobring, and T.D. Martin. 1994. EPA Method 245.1; Determination of Mercury in Water by Cold Vapor Atomic Absorption Spectrometry, Revision 3.0.

Skoog, D.A., F.J. Holler, and S.A. Crouch. 2007. Principles of Instrumental Analysis. 6th ed. Thomson Brooks Cole. Belmont, CA. 236-37.

Water: Drinking Water Contaminants. 2009. EPA 816-F-09-0004. http://water.epa.gov/drink/contaminants/index.cfm

Journal of the Pennsylvania Academy of Science 86(1): 61-68, 2012

LIGHT AND SCANNING ELECTRON MICROSCOPIC OBSERVATIONS OF THE LARVAL STAGES AND ADULT OF SPHAERIDIOTREMA GLOBULUS (TREMATODA: PSILOSTOMIDAE)[1]

JANE E. HUFFMAN[2], PATRICIA STEVENS[2], AND BERNARD FRIED[3]

[2]*Northeast Wildlife DNA Laboratory, Department of Biological Sciences, East Stroudsburg University, East Stroudsburg, PA 18301*

[3]*Department of Biology, Lafayette College, Easton, PA 18042*

ABSTRACT

Sphaeridiotrema globulus **(Rudolphi, 1814) is a digenetic trematode occurring in river and lentic aquatic systems in North America and has been identified as the cause of ulcerative hemorrhagic enteritis in waterfowl. The purpose of this study was to describe the stages of *S. globulus* using light (LM) and scanning electron microscopy (SEM). *Elimia virginica* snails infected with *S. globulus* were collected from Lake Musconetcong, NJ. Daughter rediae and cercariae were collected from the infected snails and LM and SEM microscopy were used to describe these stages with particular emphasis on the tegumentary surface. The tegument of *S. globulus* daughter rediae and cercariae is aspinose. The daughter rediae and cercariae showed simpler tegumentary structures than similar stages described in several species of echinostomids. [J PA Acad Sci 86(1): 61-68, 2012]**

INTRODUCTION

Sphaeridiotrema globulus (Rudolphi, 1814) (Psilostomidae) is a cosmopolitan digenean that infects the digestive tract of waterfowl. It causes severe hemorrhagic enteritis that may be fatal to the host. Price (1934) reported three fatal outbreaks of *S. globulus* in the lesser scaup (Marila affinis) on the Potamac River in Washington, DC. Huffman and Roscoe (1989) and Mucha and Huffman (1991) studied the pathogenic effects of this fluke in experimentally infected mute swans (*Cygnus olor*), Canada geese (*Branta canadensis*), and mallard ducks (*Anas platyrhynchos*). Sauer et al. (2007) investigated waterfowl die-offs from *S. globulus* in the Upper Mississippi River National Wildlife and Fish Refuge. The larval stages of *S. globulus* occur in *Elimia virginica* (Pleuroceridae) snails (Huffman and Fried 1983).

Huffman (1986) examined the structure and composition of the metacercarial cyst wall of *S. globulus* by light and transmission electron microscopy. McLaughlin et al. (1993) reported on the scanning electron microscopy (SEM) of adult of *S. pseudoglobulus.* The purpose of this study was to describe the stages of *S. globulus* using light (LM) and scanning electron microscopy (SEM).

[1]Submitted for publication June 2012; accepted November 2012.

MATERIALS AND METHODS

Elimia virginica snails were collected from Lake Musconetcong (40045'N, 74042'W) located in Morris County, New Jersey. Snails were collected by hand and transported to the laboratory in coolers. Infected snails were identified and cercariae collected following previously described methods within 24 hr of collection (Huffman and Fried 1983). All cercariae were examined using a compound microscope at 100x and 400x. Cercariae of *S. globulus* were identified based on the specific characteristics given in Macy and Ford (1964).

Four adult Pekin ducks were each infected with 500 *S. globulus* metacercariae. The ducks were necropsied on days 4 and 6 postinfection. Intestinal tissue with worms attached, and isolated worms were collected, washed in phosphate buffered saline (PBS), fixed in cold 3% gluteraldehyde in 0.2 M phosphate buffer (pH 7.0) and used for SEM. Some adult worms were teased with needles to collect eggs. Some of the eggs were fixed in 3% gluteraldehyde, and others were placed in spring water and incubated at 250C to study development. Eggs were randomly selected, and observed for development, at 4 day intervals for the first 16 days postembryonation, and daily after day 16.

Sphaeridiotrema globulus metacercariae, cercariae and daughter rediae were fixed in 10% neutral buffered formalin for 1-2 hr for observations by LM. Fixed cercariae and rediae were mounted on slides in a drop of water, covered with a coverslip, and measured under a compound microscope with the aid of a calibrated ocular micrometer. For the rediae, the total length, total width, and the pharyngeal width were measured, and the number of cercariae in the daughter rediae was recorded. For the cercariae, the body length, body width, and tail length, were measured. The mean, standard deviation (SD), and range were determined for each measurement using Microsoft Excel.

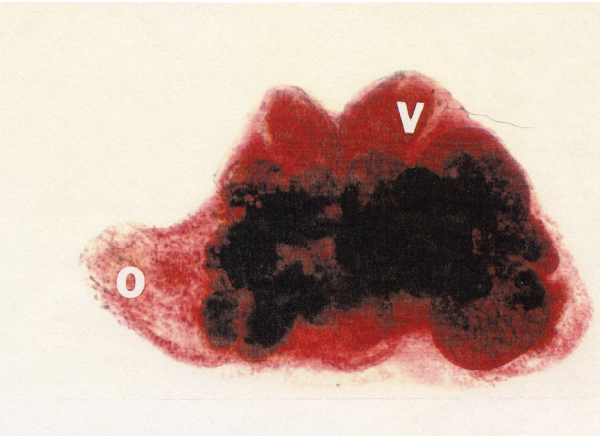

A

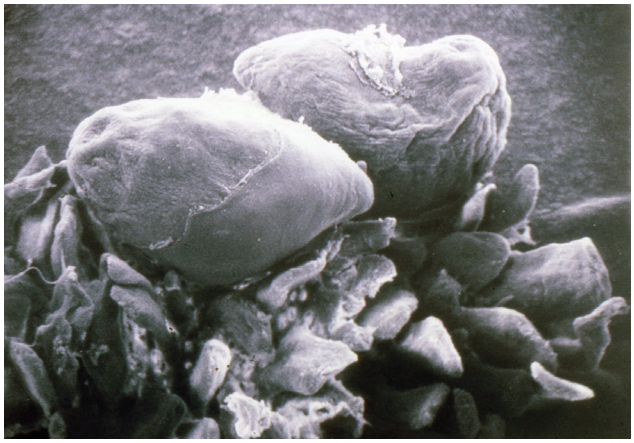

B

Figure 1. A. Light micrograph of a whole mount of *Sphaeridiotrema globulus* adult fixed in AFA and stained with Gower's acetic carmine. Ventral sucker (V), oral sucker (O). B. Scanning electron micrograph of two adult *S. globulus* attached to the intestine of a duck and the area of erosion of the intestinal villi produced by the worms.

Free swimming *S. globulus* cercariae released from snails, and daughter rediae dissected from snails were fixed in 3% gluteraldehyde in 0.2 M phosphate buffer (pH 7) for 24 hr for SEM. The samples were dehydrated in a graded ethanol series (70%, 85%, 90%, and 100%) and post fixed with 1% osmium tetraoxide for 1-2 hr. The samples were again dehydrated in a graded ethanol series (70%, 85%, 90%, and 100%), and placed in examethyldisilazane (HMDS) (Polysciences, Inc, Warrington, PA) for 15 min and then allowed to air dry. Samples were attached to stainless steel stubs using double sided tape and sputter coated with gold palladium. All samples were examined with an Amray 1810 Scanning Electron Microscope at an acceleration of 20kV at varying magnifications.

RESULTS

The length of the adult worm (Figure 1A) ranged from 850 to 940 µm with a mean ± SD of 900.4 ± 4.5 µm. The width ranged from 350 to 560 µm with a mean ± SD of 487 ± 7.3 µm. The oral sucker length ranged from 56 to 81 µm with a mean ± SD of 73.3 ± 0.7 µm. The width ranged from 46 to 60 µm with a mean ± SD of 53.5 ± 0.5 µm. The length of the acetabulum ranged from 361 to 402 µm with a mean ± SD of 379 ± 1.2 µm. The width ranged from 79 to 90 µm with a mean ± SD of 84.9 ± 0.5 µm. The length of the tegumentary spines ranged from 27 to 31 µm with a mean ± SD of 28.4 ± 0.13 µm. The aciliate papillae diameter ranged from 7 to 10 µm with a mean ± SD of 8.2 ± 0.09 µm. The ciliate papillae length ranged from 2 to 5 µm with a mean ± SD of 2.75 ± 0.09 µm.

SEM of two adult *S. globulus* (Figure 1B) attached to the intestine illustrates the erosion of the intestinal villi. The outer surface of the adult *S. globulus* was covered with tegumental proturbences with both deep and shallow irregular transverse grooves that encircled the body (Figure 2 A & B). Numerous aciliate papillae surrounded the oral sucker (Figure 3A). The diameter of the papillae was 8.2 ± 0.09 µm (Figure 3B). The lip of the ventral sucker was comprised of rows of spines in an alternating pattern (Figure 3C). The acetabular spines were 2.84 ± 0.13 µm long (Figure 3D). The excretory pore was located dorso-posteriorly (Figure 4A). Protuberances with transverse grooves appeared more compact in this area than elsewhere on the tegument. Papillae were present on the dorsal surface measuring 2.75 ± 0.09 µm in diameter (Figure 4B).

Fifty eggs dissected from worms were measured (Figure 5A & B). The egg shell length ranged from 77 to 99 µm with a mean ± SD of 89 ± 0.7 µm. The width ranged from 70 to 79 µm with a mean ± SD of 73.1 ± 0.28 µm. The opercular diameter ranged from 24 to 31 µm with an average of 26.4 ± 0.2 µm. The abopercular knob diameter ranged from 24 to 32 µm with a mean ± SD of 26.4 ± 0.23 µm. The topography of the egg shell and operculum was smooth (Figure 6A). The abopercular knob was uneven with an apparent ring (Figure 6B & C), and had no folds.

Fifty daughter rediae (Figure 7A) of *S. globulus* dissected from *E. virginica* snails were measured. The total length of the daughter rediae ranged from 672 to 976 µm with a mean ± SD of 810.8 ± 10 µm. The width of the daughter rediae ranged from 288 to 400 µm with a mean ± SD of 366.8 ± 3.6 µm. The pharyngeal diameter of the rediae ranged from 9 to 13 µm with a mean ± SD of 10.5 ± 1.2 µm. The number of cercariae within the redia was 6-8 with a mean ± SD of 6.4 ± 0.1 per redia.

The SEM of daughter rediae of *S. globulus* had a papilliform process located at the posterior end of the redia (Figure 7B & C), and two ambulatory buds located on the


A

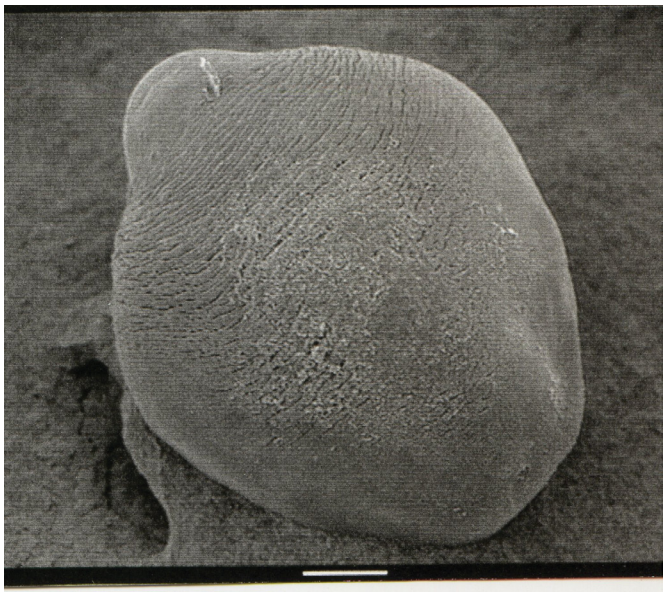
B

Figure 2. A. Adult *S. globulus* showing the ventral and oral suckers. Bar = 100 µm. B. Dorsal view showing protuberances and transverse grooves. Bar = 100 µm.

posterior third of the redia (Figure 7D). An excretory pore (Figure 8A) was located centrally on the redia; a mouth containing a muscular pharynx was located at the anterior end (Figure 8B), and a birth papilla was located just posterior to the mouth (Figure 8C).

Figure 9A shows the numerous microvilli and uniciliate papillae of the daughter redia of *S. globulus*. Figure 9B shows a uniciliate papillae. The mouth of the daughter redia was surrounded by a collar containing numerous concentric tegumental folds (Figure 9C). The birth pore was 15 ± 2.0 µm in length, and 4 ± 0.25 µm in width. The papilliform process had irregular tegumental folds (Figure 9D). The tegument was covered with protuberances (Figure 10A). Deep or shallow transverse grooves encircled the redia (Figure 10B).

Fifty *S. globulus* cercariae obtained following isolation of *E. virginica* were measured by LM. The body length of the cercariae (Figure 11) ranged from 158 to 212 µm with a mean ± SD of 190.8 ± 1.8 µm. The body width ranged from 106 to 172 µm with a mean ± SD of 136.1 ± 2.3 µm. The tail length ranged from 272 to 380 µm with a mean ± SD of 328.8 ± 4.2 µm. The length of the ventral sucker ranged from 48 to 72 µm with a mean ± SD of 60.8 ± 0.8 µm. The width of the ventral sucker ranged from 64 to 84 µm with a mean ± SD of 73.8 ± 1.3 µm. The spines on the ventral sucker ranged in length from 0.7 to 1.3 µm with a mean ± SD of 1.04 ± 0.05 µm. The aciliate papillae were 0.50 µm in length and the unicilliate papillae were 1.0 µm in length.

SEM of the cercariae (Figure 12A) showed the cup - shaped structure of the cercarial body. The cercarial tail


A

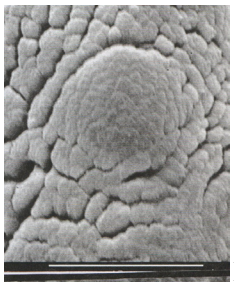
B

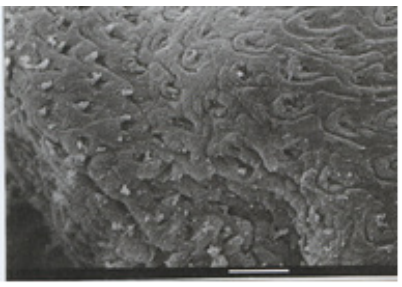
C

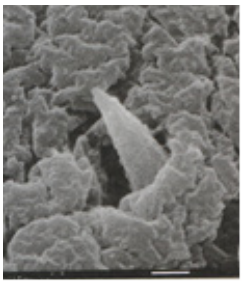
D

Figure 3. A. *S. globulus* oral sucker with aciliate papillae. Bar = 10 µm, B. Aciliate papillae. Bar = 10 µm. C. Alternating rows of acetabular spines. Bar = 10 µm. D. Acetabular spine. Bar = 1 µm.

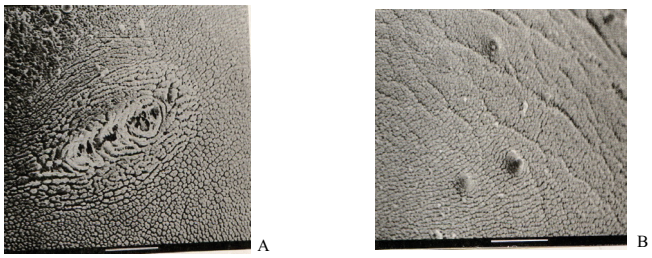

Figure 4. A. *S. globulus* excretory pore surrounded by protuberances, dorsal surface. Bar = 10 µm. B. Aciliate papillae on dorsal surface. Bar = 10 µm.

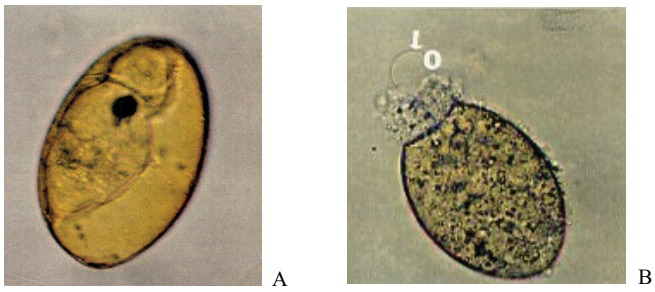

Figure 5. A. Whole mounts of *S. globulus* eggs A – 26 days-old. B. An empty egg showing the operculum (O) 40x.

lacked fin folds (Figure 12A). A lateral groove extended the length of the tail. The tail tegument consisted of numerous protuberances that occurred in a repeated rectangular pattern (Figure 12B).

The tegument of the body was surrounded by protuberances and shallow or deep transverse grooves which were covered with minute spines (Figure 12C). Dispersed randomly among the spines were uniciliate papillae. The uniciliate papillae were short and extended just above the tegument; the diameter of the papillae was 0.50 µm (Figure 12C). The sensory papillae varied in size. The cercarial acetabulum was located medially (Figure 13A). Small spines were present on the tegument of the acetabular lip, pointing away from the ventral opening (Figure 13B). The spines measured 1.04 ± 0.05 µm in length. Inside the acetabular lip, surrounding the opening, was a ring of tightly packed knob-like tubercles with smooth surfaces (Figure 13C).

The interior of the oral sucker (Figure 14A) was surrounded by aciliate papillae and uniciliate papillae (Figure 14B). Six aciliate papillae appeared to form a crown close to the oral opening. These papillae contained cilia of varying lengths, and were scattered throughout the tegument. The aciliate papillae measured 1 µm in diameter, and showed a pattern of circular rows surrounding the body.

The metacercariae of *S. globulus* are spherical in shape, with a diameter that ranged from 119 to 137 µm with a mean ± SD of 125.4 ± 0.7 µm (Figure 15A). SEM of the cysts indicated that the outer layer is smooth with a wrinkled surface (Figure 15B & C).

DISCUSSION

In the adult the oral sucker is surrounded by numerous aciliate papillae. These papillae occur without a distinct pattern and may serve a sensory function, aiding the adult worm in locating highly vascularized areas in the host gut. A second type of papilla (ciliate) was observed on the adult *S. globulus*. It occurred on both the dorsal and ventral surfaces, and did not have any regular pattern. It had a dome-like region located close to the tegumentary surface with a short cilium extending just above the tegument; this type of papillae may have a sensory function as noted in studies on various echinostomatids (Fried and Fujino 1987).

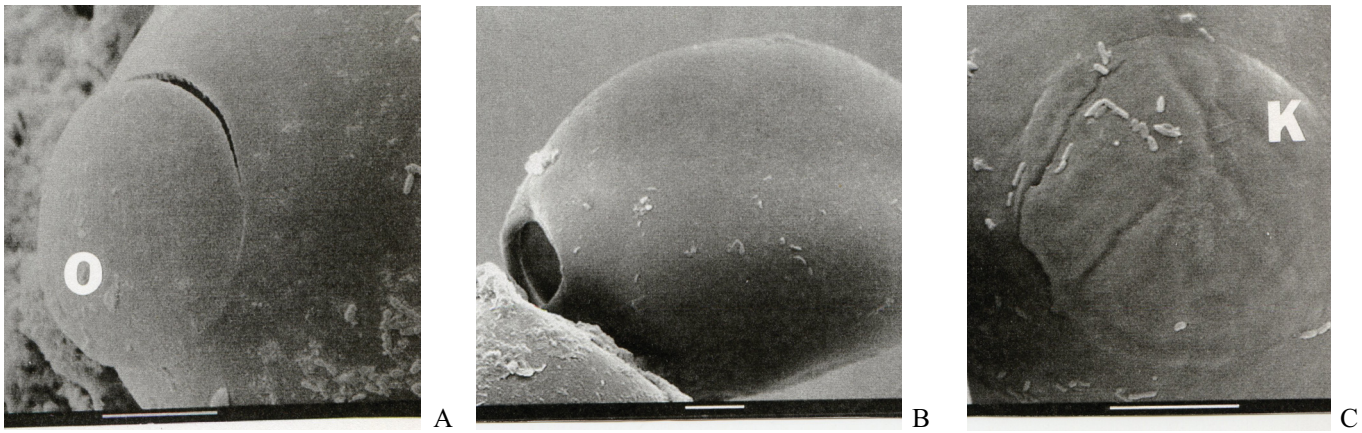

Figure 6. SEM of *S. globulus* egg. A. Operculum (O) Bar = 10 µm. B. Opercular opening. Bar = 10 µm. C. Abopercular knob (K). Bar = 10 µm.

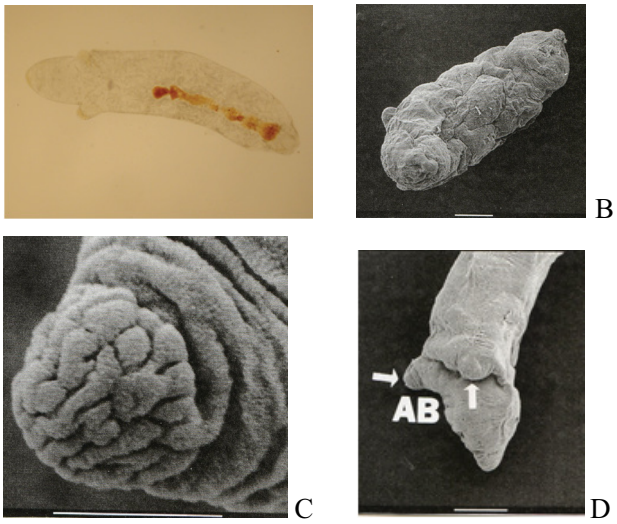

Figure 7. A. Light micrograph of daughter redia of S. globulus. B. *S. globulus* redia. Bar = 100 µm. C. Papiliform process. Bar = 10 µm. D. Ventral view of the redia showing the ambulatory buds (AB). Bar = 100 µm.

The acetabulum of *S. globulus* is surrounded by spines which occur in rows extending in an alternating pattern. The spines point away from the acetabulum as described by Barber and Caira (1995) for *Austrobilharzia variglandis*. The excretory pore of the *S. globulus* adult was oval in shape, and numerous protuberances surrounded the pore.

McLaughlin et al. (1993) compared the morphology and morphometrics of adult *S. globulus* and *S. pseudoglobulus* grown experimentally in domestic ducklings from metacercariae obtained from *E. virginica* from Lake Musconetcong in Netcong, NJ and from *Bithynia tentaculatum* collected from the Riviere du Sud, near Lacolle, Quebec. Differences in morphologic measurements of the worms were noted between the McLaughlin et al. (1993) study and this one. The McLaughlin et al. (1993) study made measurements using LM and this study used SEM.

Many redial measurements based on LM and SEM have been done on various species of the family Echinostomatidae. By comparison the redial length of *S. globulus* is smaller than that reported for *Echinostoma trivolvis* and *E. caproni* (Fried and Awatramani, 1992; Krejei and Fried, 1994). The redial width of *E. trivolvis* and *E. caproni* is larger than that of *S. globulus* (Fried and Awatramani, 1992; Krejei and Fried, 1994). The pharyngeal diameter of *S. globulus* was smaller (10.5 ± 1.2 µm) than measurements obtained for *E. caproni* (56 ± 10 µm) and for *E. trivolvis* (40.2 ± 1.1 µm) (Fried and Awatramani, 1992; Krejei and Fried, 1994). The number of mature cercariae for *E. caproni* was 4.8 ± 1.4, and for *E. trivolvis* it was 3.2 ± 1.1 (Fried and Awatramani, 1992; Krejei and Fried, 1994). The number of cercariae for *S. globulus* was greater with a mean of 6.4 ± 0.1.

The tegumentary structure of the rediae of *S. globulus* has not been previously described. Transverse folds were seen along the length of the daughter rediae of *S. globulus* as seen in various other trematodes (Fujino and Ichikawa, 2000). Numerous uniciliated papillae were seen surrounding the mouth of the rediae of *S. globulus*. The uniciliated papillae are probably sensory structures and have been seen in several other trematode species (Valkounova et al. 1989; Fujino and Ichikawa, 2000). The distal portion of the lobed collars and the ambulatory buds were observed to have a ridged tegumentary structure, which was devoid of other structural features. The lack of transverse folds at the distal portion of these structures may relate to use of these structures for locomotion and positioning within the snail.

Spines did occur around the margin of the ventral sucker of *S. globulus*. Transverse ridges or folds were observed along the body of the cercariae. Uniciliated papillae were observed over the entire cercarial body. The cilia observed on the cercariae were longer than those observed around the mouth of the rediae. The uniciliated papillae probably have a sensory function and aid the cercariae in its search of a second intermediate host and possibly an encystment site in that host. Small spherical bodies were also

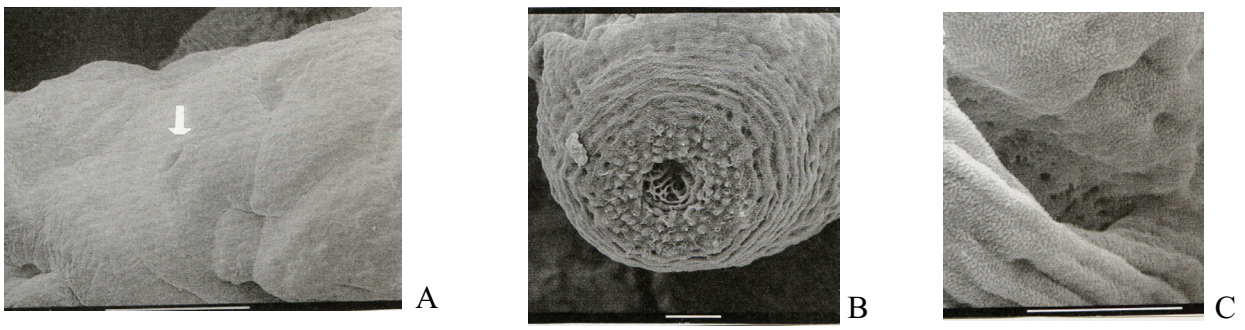

Figure 8. A. *S. globulus* redia, excretory pore (arrow). Bar = 100 µm. B. Mouth of redia. Bar = 10 µm. C. Birth papilla. Bar = 10 µm.

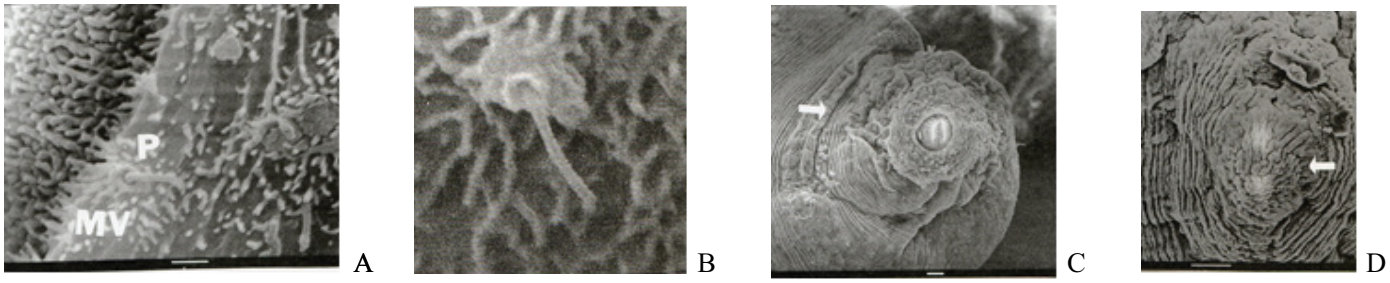

Figure 9. A. *S. globulus* redia illustrating microvilli (MV) and uniciliate papillae (P). Bar = 1 µm. B. uniciliate papilla. Bar 1 µm. C. Redial collar with concentric folds. Bar = 10 µm. D. Irregular folds of papilliform process. Bar = 10 µm.

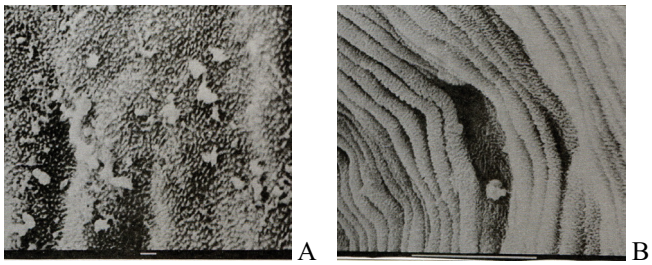

Figure 10. A. Protuberances on the surface of the redia. Bar = 1 µm. B. Deep transverse grooves of the redial tegument. Bar = 10 µm.

Figure 11. Light micrograph of *S. globulus* cercaria. Stained with Mayer's carmine.

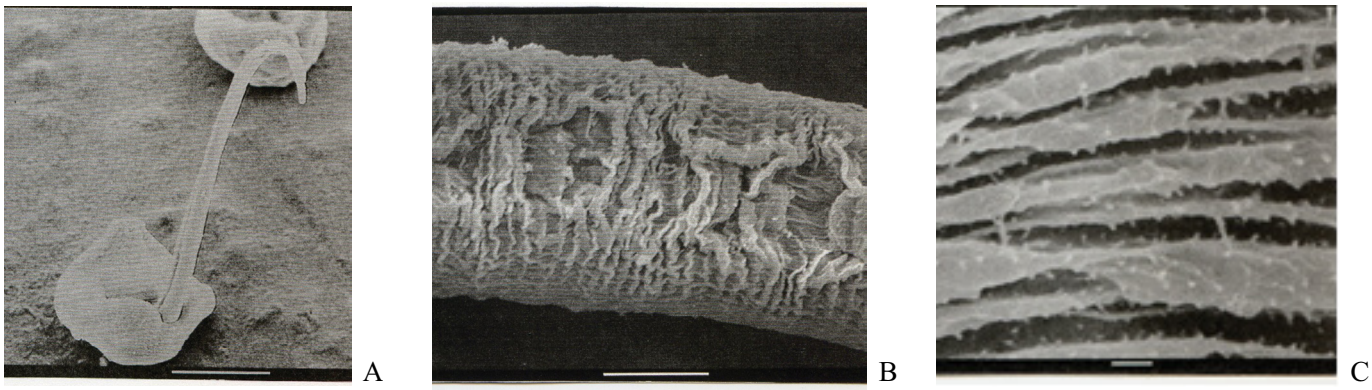

Figure 12. A. Cercarial tail lacking fin fold. Bar = 100 µm. B. Lateral groove and rectangular protuberences. Bar = 10 µm. C. Protuberances and minute spines on the cercarial tegument. Bar = 1 µm.

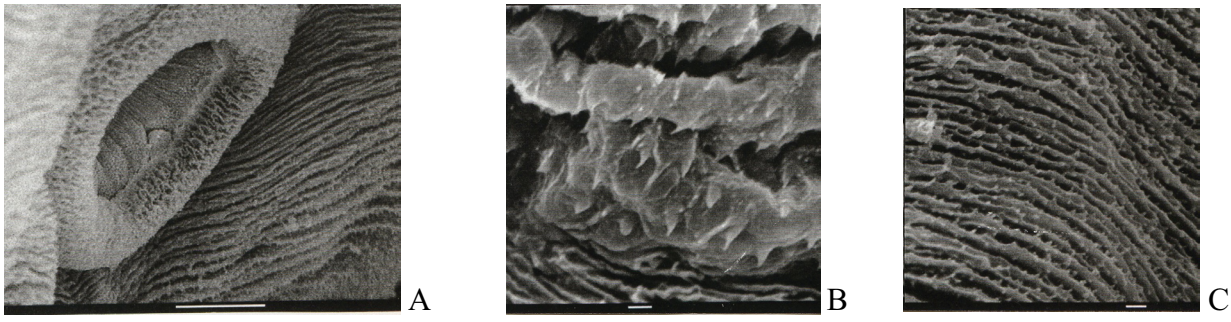

Figure 13. A. Cercarial acetabulum. Bar = 10 µm. B. Acetabular lip with spines and uniciliate papillae. Bar = 1 µm. C. Uniciliate papillae. Bar = 1 µm.

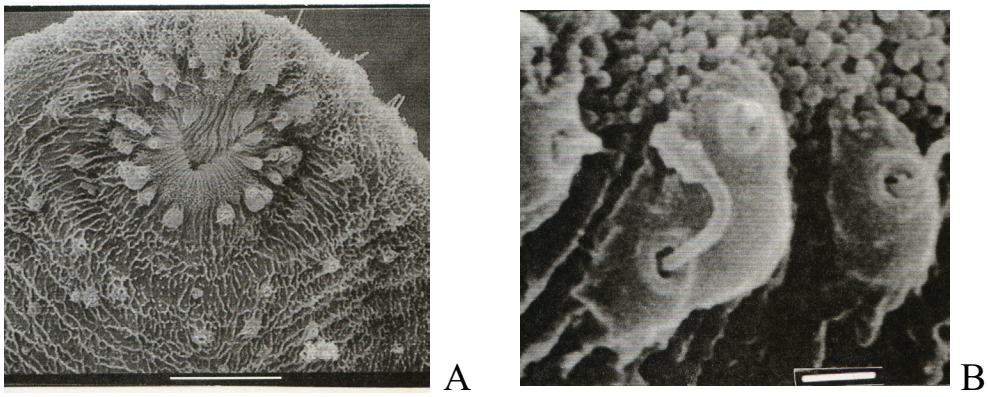

Figure 14. A. Oral sucker of cercaria. Bar = 10 µm. B. Uniciliate and aciliate papillae. Bar = 1 µm.

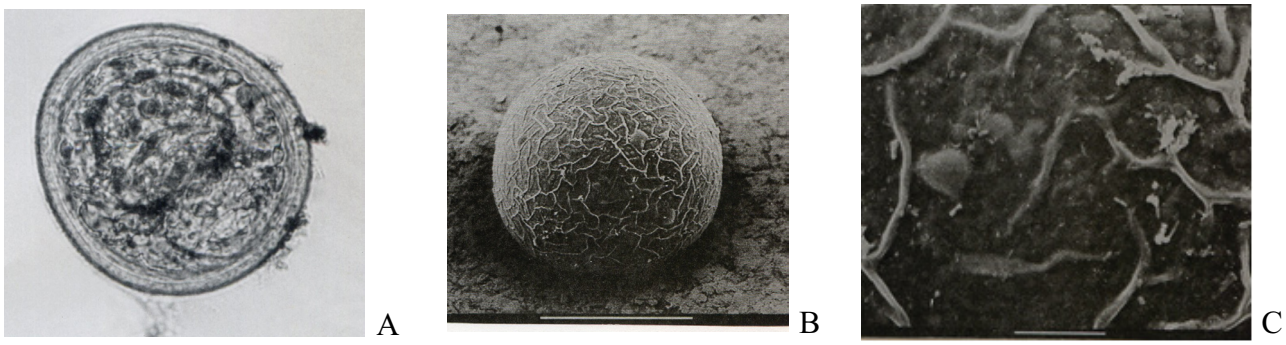

Figure 15. A. Light micrograph of *S. globulus* metacercaria. B. SEM of metacercaria with wrinkled surface. Bar = 100 µm. C. Wrinkled surface. Bar = 10 µm.

observed on the tegument of the cercariae. These spherical bodies have been observed in several other species of trematodes but the exact function is unknown (Fujino and Ichikawa, 2000).

Although McLaughlin et al. (1993) did not find acetabular spines in the *S. globulus* specimens he examined, we report the presence of spines in worms of this species. Reasons for this difference are not apparent at this time.

The measurements of the rediae and cercariae presented here represent the average values for *S. globulus* found in *E. virginica* snails in Lake Musconetcong. These measurements should aid in a better understanding of distinguishing characteristics of species of the genus *Sphaerdiotrema* or for identifying potential geographic differences where closely related species of *Sphaeridiotrema* occur.

LITERATURE CITED

Barber, K.E., and J.N. Caira. 1995. Investigation of the life cycle and adult morphology of the avian blood fluke *Austrobilharzia variglandis* (Trematoda: Schistosomatidae) from Connecticut. Journal of Parasitology 81:584-592.

Fried, B., and T. Fujino. 1987. Argentophilic and scanning electron microscopic observations of the tegumentary papillae of *Echinostoma revolutum* (Trematoda) cercariae. Journal of Parasitology 73: 1169-1174.

Fried, B., and R. Awatramani. 1992. Light and scanning electron microscopical observations of the daughter rediae of *Echinostoma trivolvis* (Trematoda). Parasitology Research 78: 257-259.

Fujino, T., H. Ichikawa. 2000. Ultrastructural studies on echinostomes. In: Fried B, Graczyk, TK (eds). Echinstomes as Experimental Models for Biological Research. Springer, New York. pp. 119-136.

Huffman, J.E. 1986. Structure and composition of the metacercarial cyst wall of *Sphaeridiotrema globulus* (Trematoda). International Journal for Parasitology 16: 647-653.

Huffman, J. E., and B. Fried. 1983. Trematodes from *Goniobasis virginica* (Gastropoda: Pleuroceridae) in Lake Musconetcong, New Jersey. Journal of Parasitology 69:429.

Huffman, J. E., and D. E. Roscoe. 1989. Experimental infections of waterfowl with *Sphaeridiotrema globulus* (Digenea). Journal of Wildlife Diseases 25:143–146.

Krejei, K.G., and B. Fried. 1994. Light and scanning electron microscopic observations of the eggs, daughter rediae, cercariae, and encysted metacercariae of *Echinostoma trivolvis* and *Echinostoma caproni*. Parasitology Research 80:42-47.

Macy, R. W., and J. R. Ford. 1964. The psilostome trematode *Sphaeridiotrema globulus* (Rud.) in Oregon. Journal of Parasitology 50: 93.

McLaughlin, J.D., M.E. Scott, and J.E. Huffman. 1993. *Sphaeridiotrema globulus* (Rudolphi, 1814) (Digenea): evidence for two species known under a single name and a description of *Sphaeridiotrema pseudoglobulus* n.sp. Canadian Journal of Zoology 71: 700-707.

Mucha, K. H. and J. E. Huffman. 1991. Inflammatory cell stimulation and wound healing in *Sphaeridiotrema globulus* experimentally infected mallard ducks (Anas platyrhynchos). Journal of Wildlife Diseases 27: 428–434.

Price, E. W. 1934. Losses among wild ducks due to infestation with *Sphaeridiotrema globulus* (Rudolphi) (Trematoda; Psilostomidae). Proceedings of the Helminthological Society of Washington 1:31–34.

Sauer, J. S., R. A. Cole, and J. M. Nissen. 2007. Finding the exotic faucet snail (Bithynia tentaculata): Investigation of waterbird die-offs on the Upper Mississippi River National Wildlife and Fish Refuge. U.S. Geological Survey Open-File Report 2007-1065:1–3.

Valkounova, J., Z. Zdarska, and V. Nasincova. 1989. Ultrastructural observations on the redia of *Echinostoma revolutum*. Folia Parasitology 36:25-30.

Journal of the Pennsylvania Academy of Science 86(1): 69-74, 2012

WOODEN VERSUS INSULATED METAL NESTBOXES: A COMPARISON OF REPRODUCTIVE SUCCESS AND USE BY SONGBIRDS[1]

MARGARET E. RUSHMORE, TODD J. UNDERWOOD[2], AND WILLIAM P. BROWN[3]

Department of Biology, Kutztown University, Kutztown, PA 19530

ABSTRACT

We compared reproductive success of Tree Swallow (*Tachycineta bicolor*) and House Wren (*Troglodytes aedon*) nests in wooden nestboxes to insulated metal nestboxes to determine if a new insulated metal nestbox design is a safe alternative to wooden nestboxes. We also examined the preference of four species of cavity-nesting birds to nest in wooden versus metal nestboxes. No significant differences were found among clutch size, hatching success, and the number of fledglings produced in Tree Swallow and House Wren nests between the two types of nestboxes. Therefore, insulated metal nestboxes appear to be a safe alternative to wooden nestboxes. Metal nestboxes were preferred by Tree Swallows to wooden nestboxes ($\chi 2 = 6.5$, $n = 25$, $p = 0.01$). However, wooden nestboxes were preferred to metal nestboxes as a first choice for nesting 77.1% of the time for all four species. House Wrens, Eastern Bluebirds (*Sialia sialis*), and House Sparrows (*Passer domesticus*) all preferred wooden to metal nestboxes (Fisher's Exact Tests, all $p < 0.001$). Thus, insulated metal boxes are safe, but may not attract desirable species, such as Eastern Bluebirds, when compared to traditional wooden Peterson-style boxes. [J PA Acad Sci 86(1): 69-74, 2012]

INTRODUCTION

Cavity nesting birds have an increased likelihood of nest success compared to birds nesting in open cups (Pinkowski 1979, Brawn 1988). The success of a cavity nester is dependent on whether it uses an artificial nesting structure, such as a nestbox, or a natural cavity in a tree (Pinkowski 1979). Purcell et al. (1997) found that birds nesting in nestboxes had lower predation rates, larger clutch sizes, and fledged more young compared to birds nesting in natural cavities. Thus, artificial nestboxes can be used as a safe and effective supplement to nests in natural cavities.

The extensive use of nestboxes has led to major advances in our knowledge of the ecology, behavior and physiology of many species of cavity-nesting birds (Lambrechts et al. 2010). Nestboxes are commonly used because they increase the nesting opportunities for native species, allow for easy observation and monitoring of nests, are long lasting, and allow bird enthusiasts the ability to increase local biodiversity. Artificial nestboxes help to reduce the competition for nest sites between native and non-native species and may help local populations of native species recover by increasing the number of possible nesting sites (Zeleny 1976). However, nestbox design may influence reproductive success (Radunzel et al. 1997).

Many different types of nestbox designs have been used, but overall the Peterson-style nestbox appears to be favored among cavity-nesting bird species, especially Eastern Bluebirds (*Sialia sialis*), and by bird enthusiasts (Berner and Pleines 1993, Somershoe and Zegers 2000). Most nestboxes are made of wood but they can also be made of artificial products, such as PVC pipe, plastics, and metal (Kern et al. 2009). One problem faced when using some types of metal is the lack of insulation for the developing eggs and young (Zeleny 1976). Internal nestbox temperature is an important determining factor of a bird's reproductive success due to the potential threat of nest failure (Black 1999). Metal nestboxes can potentially be harmful to the developing eggs because the embryos will not survive if temperatures inside the box exceed 42°C (Zeleny 1980). The issue of harmful internal temperatures can be avoided by use of proper aluminum paint or insulation in the nestbox (Zeleny 1976). Kern et al. (2009) recently examined nestbox preference and temperature differences between insulated metal nestboxes and wooden nestboxes and found that temperature was not significantly different between the two nestbox types, likely due to the foam insulation in the walls of the metal nestbox and the light external color. Kern et al. (2009) also found that wooden nestboxes were significantly preferred to metal boxes by five species of cavity-nesting birds overall, but this conclusion was based on only a single year of data with small sample sizes for each species.

In this study, we further examined the value of a new insulated metal Peterson-style nestbox compared to a traditional wooden Peterson-style nestbox. Our first objective was to determine whether measures of reproductive success

[1]Submitted for publication June 2012; accepted August 2012.
[2]Corresponding Author. E-mail: underwoo@kutztown.edu, (610) 683 – 4323
[3]Current Address: Division of Natural Sciences, Keuka College, Penn Yan, NY 14478

Figure 1: The Peterson-style nestboxes compared in this study. Nestboxes were placed in a paired design of one wooden (left) and one insulated metal (right) nestbox approximately 3 meters apart

differed between nests in the two types of nestboxes. Our second objective was to examine bird preference for using the two nestbox types over three breeding seasons.

MATERIALS AND METHODS

In March 2008, sixty Peterson-style nestboxes, half made of wood and half made of metal, were set up on Kutztown University property in Maxatawny Township, Berks County, Pennsylvania. Wooden nestboxes were made of 1 inch cedar with the oval entrance hole of a Peterson box. These nestboxes were unpainted and weathered to a light gray appearance after about one year. By comparison, metal nestboxes were commercially produced "Trendsetter Bluebird Boxes" made of aluminum and lined with ¼ inch foam board insulation. Metal nestboxes had the basic Peterson design but differed from wooden boxes by having a round entrance hole lined with a black plastic insert and were painted white (Figure 1). Forty nestboxes were located at the Pennsylvania German Cultural Heritage Center, which consists of a small wetland habitat surrounded by agricultural fields and hedgerows of trees. The other twenty nestboxes were located along a mowed trail at the Ronald Rhein Environmental Study Area, which consists of a deciduous forest surrounded by a small wetland and agricultural fields. Nestboxes were placed in pairs, with one metal and one wooden nestbox located about 3 meters apart from each other (Figure 1). The entrance holes of nestboxes in each pair were oriented in the same direction, except for two pairs where the nestbox entrances were slightly off due to logistical constraints of the landscape. This paired design placed each pair of nestboxes in the same orientation and microhabitat. Each nestbox pair was at least 60 meters away from any other nestbox pair.

From late April through August of 2008-2010, we checked nestboxes approximately every one to three days to document the occupancy of each nest and to record nest contents. To compare reproductive success between wooden and metal nestboxes, we examined three variables: clutch size, hatching success, and number of fledglings produced. Clutch size was the total number of eggs laid in a completed clutch (i.e., nest failures prior to clutch completion were excluded). Hatching success was calculated as the percentage of eggs present at the start of incubation that successfully hatched. This allowed for a more reliable examination of hatching success

by eliminating any losses due to predation or nest failure before clutch completion. The number of fledglings produced was defined as the number of nestlings successfully leaving the nest. Nestbox preference was determined by checking which box in each pair (wooden or metal) eggs were laid in first for each year. First nesting in a pair of boxes was used as a measure of preference instead of overall nestbox usage because this eliminated the potential influence of another species that was already using one of the pair of nestboxes. Overall, nestbox preferences were recorded over three years for Tree Swallows (*Tachycineta bicolor*), Eastern Bluebirds, House Sparrows (*Passer domesticus*), and House Wrens (*Troglodytes aedon*).

We combined data from all three years of our study for analyses of reproductive success and used t-tests to compare means for each reproductive variable for wooden to metal nestboxes. Before analyzing hatching success, we transformed these data using an arcsine square root transformation because hatching success was expressed as a percentage. However, original percentage data were used in tables to illustrate trends. Although several species of cavity nesting birds used our boxes, we only compared reproductive success of Tree Swallows and House Wrens due to sample size limitations. Nestbox preference data between wooden or metal nestboxes were analyzed with Chi-Squared tests or, when observed or expected values were less than five, Fisher's exact tests. We used a significance level of $p = 0.05$ and discussed non-significant trends with a $p < 0.1$.

RESULTS

Hatching success was not significantly different for Tree Swallow nests in wooden compared to metal nestboxes, although there was a trend toward lower hatching success of nests in metal nestboxes (Table 1). The mean clutch size and mean number of fledglings were not significantly different for Tree Swallow nests in wooden nestboxes compared to metal nestboxes (Table 1). By comparison, hatching success of House Wren nests in metal nestboxes compared to wooden nestboxes was not significantly different, although there was a trend toward lower hatching success in wooden nestboxes (Table 1). The mean clutch size and number of fledglings were not significantly different for House Wren nests in wooden compared to metal nestboxes (Table 1).

Tree Swallows preferred to nest in metal rather than wooden nestboxes ($\chi 2 = 6.5$, $n = 25$, $p = 0.01$; Table 2). By comparison House Wrens, Eastern Bluebirds, and House Sparrows all preferred to nest in wooden rather than metal nestboxes (Fisher's Exact Tests, all $p < 0.001$; Table 2). Overall, species using our nestboxes chose to nest first in wooden nestboxes 77.1% of the time compared to the 22.9% in metal nestboxes.

DISCUSSION

We examined the reproductive success of songbirds nesting in wooden compared to metal nestboxes and found no significant difference in any of three reproductive variables. However, there were two opposite and non-significant trends in hatching success. Interestingly, hatching success was slightly lower for Tree Swallow nests in metal nestboxes, but for House Wren nests hatching success was slightly lower in wooden nestboxes. We also found that wooden nestboxes were preferred to metal nestboxes for three of the four species. Overall, metal nestboxes appeared to have no direct impact on the reproductive success of species in this study, although our sample of Tree Swallow nests in wooden nestboxes was small.

Clutch size in cavity-nesting birds, such as Tree Swallows and Eastern Bluebirds, is influenced by nestbox type (Radunzel et al. 1997) and size (Stewart and Robinson 1999). However, we found no difference in clutch size between nests in wooden and metal nestboxes for Tree Swallows or House Wrens. The floor area of nestboxes and natural cavities can influence Tree Swallow clutch sizes, with larger clutches produced in larger floor areas (Rendell and Robertson 1989, Stewart and Robinson 1999). In bluebirds, Radunzel et al. (1997) found that nests in open-topped nestboxes had slightly larger clutches than those in standard nestboxes with a roof. The main difference in our two nestboxes was the material used in construction not the overall design and dimensions. Our nestbox types had similar floor dimensions (8.3 x 8.9 cm wooden vs. 8.9 x 8.9 cm metal), but metal boxes had a slightly larger floor area (73.9 cm^2 wooden vs. 79.2 cm^2 metal). Because our nestboxes were similar in design and floor size, we conclude that the metal nestboxes had no influence on clutch size in Tree Swallow or House Wren nests.

Hatching success can be used as a way to compare reproduction between different cavity-nesting species as well as to indicate possible nestbox overheating (Nolan 1963). Internal temperature of a nestbox can have a direct effect on both the success of the clutch and the development of the eggs. For example, bluebird eggs and nestlings cannot survive in temperatures above 41ºC (Black 1999). High temperatures can cause impaired development of eggs (Marking et al. 2010). Although we found no significant difference in hatching success of nests in wooden versus metal nestboxes, there were strong trends but in opposite directions for Tree Swallows compared to House Wrens. Tree Swallow nests had lower hatching success in metal nestboxes, whereas House Wren nests had lower hatching success in wooden nestboxes. The opposing direction of these trends suggests that some other factor besides temperature may have influenced hatching success. The main causes of egg failure in both species were partial nest predation and nest competition or nest usurpation. We found punctured eggs in nests and on the ground at several nestboxes, which

Table 1. A comparison of the mean clutch size, hatching success, and number of fledglings (± SE) in Tree Swallow and House Wren nests in wooden nestboxes compared to those in metal nestboxes. Data were collected from 30 pairs of nestboxes in Kutztown, PA from 2008-2010.

	Tree Swallow			House Wren		
	Metal	Wood	t-Test	Metal	Wood	t-test
Clutch Size	4.87 ± 0.21 (n = 30)	4.88 ± 0.35 (n = 8)	t = 0.0 p = 0.99	5.53 ± 0.15 (n = 17)	5.58 ± 0.19 (n = 51)	t = 0.2 p = 0.81
Hatching Success (%)	87.07 ± 3.50 (n = 27)	96.88 ± 3.13 (n = 8)	t = 2.0 p = 0.06	92.22 ± 3.76 n = 15	81.17 ± 4.67 (n = 49)	t = 1.7 p = 0.09
Number of Fledglings	2.81 ± 0.38 (n = 36)	4.11 ± 0.61 (n = 9)	t = 1.6 p = 0.12	4.20 ± 0.61 (n = 15)	3.53 ± 0.34 (n = 57)	t = 0.9 p = 0.36

were sometimes followed by new nests of House Wrens or House Sparrows. House Wrens and House Sparrows are well known for destroying nests and taking over nestboxes (Davis and Roca 1995). For unknown reasons, these egg losses were greater in different types of nestboxes for the two species. Overall, metal nestboxes did not appear to have a negative impact on hatching success due to a higher internal temperature.

We did not find significant differences in the number of fledglings produced from nests in wooden compared to metal nestboxes for both Tree Swallows and House Wrens. A slightly lower mean number of fledglings from Tree Swallow nests in metal nestboxes was found, however, this was likely influenced by the lower hatching success of these nests. House Wren nests in wooden nestboxes had a noticeably lower mean number of fledglings compared to those in metal, but also appeared to be influenced by the lower hatching success of these nests. No evidence was found that overheating had a direct impact on the number of fledglings produced from nests in either wooden or metal nestboxes. This is important because the number of fledglings produced is the ultimate measure of a bird's reproductive success.

Three out of the four main species using our nestboxes chose wooden nestboxes to metal nestboxes. Only Tree Swallows showed a preference for metal nestboxes. Because our two nestbox types differed in a few ways, these preferences might be due to one or more factors. The shape or diameter of the entrance hole of the nestboxes may have played a role in these preferences. The metal nestboxes had a circular entrance hole compared to the oval entrance hole of the wooden nestbox, a typical Peterson-Style box. Both Eastern Bluebirds and House Wrens show a strong preference for oval entrance holes to round ones (Lumsden 1986, Davis 1995, Somershoe and Zegers 2000). By comparison, Tree Swallows show no preference between oval and circular sized entrance holes (Lumsden 1986, Somershoe and Zegers 2000). These different preferences for entrance hole shapes among species may explain the strong overall preference for wooden nestboxes to metal nestboxes.

Nestbox entrance orientation can directly affect nest temperature and microclimate, thus, directly influencing nest preference in some species (Ardia et al. 2006). Both Tree Swallows and Eastern Bluebirds show preferences for nestboxes facing certain directions (Lumsden 1986). However, the paired design of our nestbox placement should have controlled for any influence of entrance orientation.

External color of the nestbox can also play a role in nestbox preference. House Wrens show a preference for nestboxes with a red or green exterior to those that are white, yellow, or blue (McCabe 1961). Kibler (1969) suggested that Eastern Bluebirds prefer darker colored nestboxes to white nestboxes, but we know of no definitive study of nestbox color preference among Eastern Bluebirds. Nevertheless, the white paint on the exterior of our metal nestboxes may have deterred some birds from nesting in them. However, our study was not designed to test for the influence of color and we cannot make any conclusions based on color.

Kern et al. (2009) found no internal temperature differences between wooden and insulated metal nestboxes and suggested that insulated metal nestboxes were safe for birds to nest in. Our results support this conclusion because we found no significant differences in three reproductive variables from nests in wooden compared to metal nestboxes and found no

Table 2. The preferences of four species of birds to nest in wooden versus metal nestboxes in Kutztown, PA from 2008 to 2010. Nestboxes were arranged in pairs of one wooden and one metal nestbox. Each preference indicated the first nest occurring in a wooden or metal nestbox pair when both nestboxes were unoccupied.

	Preference	
Species	Wooden	Metal
Tree Swallow	8	17
House Wren	28	3
Eastern Bluebird	24	0
House Sparrow	14	2
Total:	74	22

evidence that overheating impacted reproductive success in general. Tree Swallows more readily nested in metal nestboxes, whereas Eastern Bluebirds, House Sparrows, and House Wrens were more likely to nest in wooden nestboxes. Overall, wooden nestboxes were chosen to metal nestboxes, possibly due to the shape of their entrance hole as well as a potential avoidance of a white exterior color. However, we cannot be sure which factor or factors were responsible for the strong preference for wooden nestboxes because we were unable to properly control for the differences in the two types of nestboxes. The lack of differences in reproductive success shows that insulated metal nestboxes can be used as a safe alternative to wooden nestboxes. Although insulated metal nestboxes are safe, they may not attract the desired species for nests due to the strong preference to nest in wooden Peterson-style nestboxes. Future tests should be conducted where the insulated metal nestboxes are offered without other nestbox choices to determine their ability to attract bluebirds. We also found that mice nesting in the metal nestboxes chewed and removed the rigid foam insulation. Thus, metal nestboxes may last longer than wooden nestboxes, but will require maintenance over time.

ACKNOWLEDGMENTS

We thank T. Kern, R. Underwood, and M. Zuefle for field assistance, the Pennsylvania German Cultural Heritage Center for allowing us to use their property for our nestboxes, and two anonymous reviewers for helpful comments on our manuscript. This project was funded by the Kutztown University Research Committee.

LITERATURE CITED

Ardia, D.R., J.H. Perez, and E.D. Clotfelter. 2006. Nest box orientation affects internal temperature and nest site selection by Tree Swallows. J. Field Ornithol. 77:339-344.

Berner, K.L., and V.A. Pleines. 1993. Field tests of several styles of bluebird nest boxes. Sialia 15:3-11.

Black, C.C. 1999. Wooden nest boxes found cooler. Bluebird 21(4):4-5.

Brawn, J.D. 1988. Selectivity and ecological consequences of cavity nesters using natural vs. artificial nest sites. Auk 105:789-791.

Davis, W.H. 1995. Testing the features of the Peterson box. Sialia 17:135-136.

Davis, W.H, and P. Roca. 1995. Bluebirds and Their Survival. The University Press of Kentucky. Lexington, KY.

Kern, T.T., T.J. Underwood, and W.P. Brown. 2009. Field comparisons of insulated metal nestboxes to wood nestboxes: temperature differences and bird preferences. Bluebird 32(4):6-10.

Kibler, L.F. 1969. The establishment and maintenance of a bluebird nest-box project. A review and commentary. Bird-Banding. 40:114-129.

Lambrechts, M.M, F. Adriaensen, D.R. Ardia, A.V. Artemyev, F. Atiénzar, J. Bańbura, E. Barba, J.C. Bouvier, J. Camprodon, C.B. Cooper, R.D. Dawson, M. Eens, T. Eeva, B. Faivre, L.Z. Garamszegi, A.E. Goodenough, A.G. Gosler, A. Grégoire, S.C. Griffith, L. Gustafsson, L. Scott Johnson, W. Kania, O. Keišs, P.E. Llambias, M.C. Mainwaring, R. Mänd, B. Massa, T.D. Mazgajski, A. Pape Møller, J. Moreno, B. Naef-Daenzer, J. Nilsson, A.C. Norte, M. Orell, K.A. Otter, C. Ryul Park, C.M. Perrins, J. Pinowski, J. Porkert, J. Potti, V. Remes, H. Richner, S. Rytkönen, M. Shiao, B. Silverin, T. Slagsvold, H.G. Smith, A. Sorace, M.J. Stenning, I. Stewart, C.F. Thompson, P. Tryjanowski, J. Török, A.J. Van Noordwijk, D.W. Winkler, and N. Ziane. 2010. The design of artificial nestboxes for the study of secondary hole-nesting birds: a review of methodological inconsistencies and potential biases. Acta Ornithol. 45:1-26.

Lumsden, H.G. 1986. Choice of nest boxes by Tree Swallows, *Tachycineta bicolor*, House Wrens, *Troglodytes aedon*, Eastern Bluebirds, *Sialia sialis*, and European Starlings, *Sturnus vulgaris*. Can. Field-Nat. 100:343-349.

Marking, L., F. Carig, and C. Koperski. 2010. Effects of occupancy and venting on temperatures inside bluebird nestboxes. Bluebird 33(1):18-22.

McCabe, R.A. 1961. The selection of colored nest boxes by House Wrens. Condor 63:322-329.

Nolan, V., Jr. 1963. Reproductive success of birds in a deciduous scrub habitat. Ecology 44:305-313

Pinkowski, B.C. 1979. Nest site selection in Eastern Bluebirds. Condor 81:435-436.

Purcell, K.L., J. Verner, and L.W. Oring. 1997. A comparison of the breeding ecology of birds nesting in boxes and tree cavities. Auk 114:646-656.

Radunzel, L.A., D.M. Muschitz, V. M. Bauldry, and P. Arcese. 1997. A long-term study of the breeding success of Eastern Bluebirds by year and cavity type. J. Field Ornithol. 68:7-18.

Rendell, W.B., and R.J. Robertson. 1989. Nest-site characteristics, reproductive success and cavity availability for Tree Swallows breeding in natural cavities. Condor. 91: 875–885.

Stewart, L.M., and R.J. Robertson. 1999. The role of cavity size in the evolution of clutch size in Tree Swallows. Auk. 116: 553-556.

Somershoe, S.G., and D.A. Zegers. 2000. Nest-box preference and productivity by Eastern Bluebirds, Tree Swallows studied. Bluebird 22(2):14-17.

Zeleny, L. 1976. The Bluebird: How You Can Help Its Fight for Survival. Indiana University Press. Bloomington, IN.

Zeleny, L. 1980. Bluebird nesting box temperatures. *Sialia* 2:10-15.

Journal of the Pennsylvania Academy of Science 86(1): 75-78, 2012

CASE REPORT: *STAPHYLOCOCCUS INTERMEDIUS* DERMATITIS IN DENNING NEW JERSEY BLACK BEARS (*URSUS AMERICANUS*)[1]

SHAMUS P. KEELER[2], KELCEY I. BURGUESS[3], HEATHER LEMASTER[3], AND JANE E. HUFFMAN[4]

[2]Southeastern Cooperative Wildlife Disease Study (SCWDS), Department of Population Health, 589 D.W. Brooks Drive, College of Veterinary Medicine, University of Georgia, Athens, GA 30602
[3]New Jersey Division of Fish and Wildlife, Hampton, NJ 09927
[4]Department of Biological Sciences, Northeast Wildlife DNA Laboratory, East Stroudsburg University, East Stroudsburg, PA 18301

ABSTRACT

On 18 March 2006, during annual den research, personnel from the New Jersey Division of Fish and Wildlife Black Bear Project examined a 5-yr-old female and three yearling black bears (*Ursus americanus*) with severe dermatitis. The female and three yearlings all exhibited weight loss. Deep skin scrapings were taken and examined under a stereomicroscope. The skin of each bear was swabbed with BBL CultureSwabs. No mites were found in the skin scrapings. *Staphylococcus intermedius* was the only bacterial species isolated from the four bears. To our knowledge this is the first report of non-mange related dermatitis caused by *S. intermedius* in black bears.

New Jersey black bears (*Ursus americanus*) are found primarily in the northern portion of the state but the population has been steadily moving south. The average New Jersey black bear litter size is 2.7 cubs. They den in rock cavities, brush piles, felled trees, and open nests (Carr and Burguess, 2004).
[J PA Acad Sci 86(1): 75-78, 2012]

A number of diseases have been reported in black bears including infestations by ectoparasites. Cases of mange in black bears have been documented throughout their range including New Jersey. Black bears have been found to be hosts to four species of mites, *Eutrombicula splendens*, *Sarcoptes scabei*, *Demodex ursi*, and *Ursicotes americanus* (Burguess and Huffman, 2005). Cases of denning-related dermatitis have been reported from black bears in New Mexico and Colorado but the causative agents were not identified. In both instances, mange was considered as a possible cause, but no mites were found in skin scrapings (Costello et al., 2006; Beck, 1991). *Staphylococcus intermedius* was cultured from a captive red wolf (*Canis rufus*) which was reported to have a dermatosis related to zinc deficiency (Kearns et al., 2000).

Staphylococcus dermatitis is a very common skin disease in domestic animals (Scott et al., 2001). Cutaneous staphylococcal infections have been reported in numerous free ranging wildlife species including sea lions, ground squirrels and minks (Sweeney and Gilmartin, 1974, Campbell et al 1981, Crandell et al., 1971). In dogs and cats, the most common causative agent is *Staphylococcus intermedius* (Phillips and Kloos, 1981, Igimi et al., 1994). *Staphylococcus intermedius* has also been identified as the causative agent in numerous wildlife cases (Biberstein et al., 1984). *Staphylococcus intermedius* was first reported by Hajek (1976) and commonly inhabits the skin of most mammals (Scott et al., 2001). *Staphylococcus spp.* were among the most common bacterial species isolated from oral, nasal, and rectal swabs of black bears in Alberta, Canada (Goatcher et al., 1987). In New Jersey, *Staphylococcus spp.* were isolated from 28% (36/129) of sampled black bears (Keeler et al., 2005). *Staphylococcus intermedius* was isolated from pustules on a Florida black bear with trombiculiasis (Cunningham et al., 2001).

On 18 March 2006, during annual den research, personnel from the New Jersey Division of Fish and Wildlife Black Bear Project found a 5-yr-old female and three yearlings with severe dermatitis. The female and yearlings were denning in a rock cavity in Sussex County, New Jersey (41° 6 19 N, 74° 29 50 W). The sow had been monitored yearly since October 2004.

The sow was anesthetized with 3 cc of ketamine hydrochloride (KH) (200 mg/kg) and 0.66 cc of xylazine hydrochloride (XH) (450 mg/kg) (Congaree Veterinary Pharmacy, Cayce, SC). All 3 yearlings were anesthetized with 2 cc of KH (200 mg/kg) and

[1]Submitted for publication May 2012; accepted July 2012.

0.44 cc of XH (450 mg/kg). The drugs were administered using explosive discharging darts (Pneudart, Williamsport, PA) from a hand held air pistol. Venous blood was drawn into whole blood tubes with 7.5% EDTA (Daigger & Co., Vernon Hills, IL). Each bear was weighed and the overall length, head and body girth, and shoulder height were measured. Deep skin scrapings were taken as described by Bornstein et al. (2001). The skin of each bear was swabbed with BBL CultureSwab EZ (Fisher Scientific). Soil samples were taken from the den site.

All four bears had patches of hair loss, crustiness, scaling, and reddening of their skin (Figure 1). The skin scrapings were examined under a stereomicroscope for the presence of mites. The BBL Culture Swabs and soil samples were plated onto MacConkey agar (MAC), Columbia Colistin-Nalidixic Acid Agar (CNA), Trypticase Soy Agar (TSA) and Blood Agar (BA) (5% sheep red blood cells) and incubated at 37 °C for 18-24 hours. Analytical Profile Index (API) (bioMerieux Vitek, Inc. Durham, North Carolina) strips were used for biochemical identification of bacterial isolates. The NJDFW Black Bear Project database contains data on NJ black bears from 1981 to 2006 and was used to calculate the average weights for sows, yearlings, and cubs.

The sow weighed 107 lbs. The average weight for 5-yr-old sows with yearlings during denning is 191.7 ± 33.5 lbs. The sow had 2 female and one male yearling. The male weighed 32 lbs and the two females weighed 33.5 and 31.0 lbs. In New Jersey, the average weight for male yearlings during denning is 95.2 ± 31.3 and for female yearlings the average weight is 72 ± 19.5. The length, head girth, and shoulder measurements of the female and the three yearlings were consistent with other black bears examined during the 2006 denning season. The body girth of the female and yearlings with bacterial dermatitis however, was smaller compared to the average of the other bears examined. No mites were seen in the skin scrapings from the black bears. Only *Staphylococcus intermedius* was isolated from the sow and yearlings. Numerous species of Gram negative rods, gram positive rods, and gram positive cocci were cultured from the soil including *Staphylococcus intermedius.*

The sow had been initially collared in October 2004 during annual fall research trapping. At that time, she weighed 196 lbs. and

Figure 1. A 5-yr-old female NJ black bear (Tag Number: 3932-4501) with patches of hair loss, crustiness, scaling and reddening of the skin caused by a cutaneous infection with *Staphylococcus intermedius.*

was 3.5 -yrs-old. In New Jersey, the average weight for 3.5-yr-old sows in October is 176.9± 25.7. On 23 March 2005, the female was examined along with her three cubs. At that time the sow weighed 116 lbs. In New Jersey, the average weight for 4-yr-old sows with cubs during denning is 189.7 ± 32.4. All three cubs (one male and two females) weighed 4 lbs. The average weight for male cubs is 5.1± 1.4 lbs. and the average weight for female cubs is 4.8± 1.2 lbs in New Jersey. From October 2004 to March 2005, the female dropped 40.8% of her body weight. Based on data from New Jersey black bears for 2001 to 2006, the average percentage of weight loss for denning females with cubs is 12.6+ 4.1%.

Examination of the sow during the 2007 denning season indicated that she had recovered from the dermatitis and was reproductively successful. The sow weighed 134.5 lbs., average weight for 6-yr-olds with cubs during denning is 191.7 ± 43.5. She had 3 cubs, one male and 2 females, and weights were consistent with the average weight for cubs. BBL culture swabs were used to take samples from the abdomen of the sow and the soil in the den. Several species of Gram negative bacteria and *S. intermedius* was cultured from the skin of the sow. No sign of dermatitis was detected. A variety of bacterial species were cultured from the soil but not *S. intermedius*.

Staphylococcus intermedius is an opportunistic pathogen and often causes secondary infections in animals (Scott et al., 2001). A secondary infection of S. intermedius was documented in a Florida black bear with trombiculic mange (Cunningham et al., 2001). In our study, the sow and yearlings were thought to be suffering from mange but no mites were detected in the skin scrapings. In the previous year, the sow and her three cubs showed no signs of mange or dermatitis but the sow had dropped 40.8% of her weight during the three months of denning, which put her weight below the average for females of her age for that denning season.

Staphylococcus intermedius was the only bacterial species isolated from the skin of the four bears on 18 March, 2006. Personnel from the New Jersey Division of Fish and Wildlife Black Bear Project have handled over 1200 black bears since 2000 (Carr and Burguess, 2004). During that time, no bear has ever been documented with dermatitis during denning. To our knowledge this is the first report of non-mange related dermatitis caused by *S. intermedius* in black bears. The lower den weights of the bears may indicate that they were under weight when they entered the den. The sow has had a history of low den weights. It is unknown whether the bears were suffering from the dermatitis before entering the den or if they acquired the infection during the denning period. Bears are known to have reduced immune function during denning (Hellegren, 1998). The combination of reduced weight and immune function may have contributed to susceptibility to infection with *S. intermedius*

ACKNOWLEDGEMENTS

We would like to thank New Jersey Division of Fish & Wildlife personnel for assistance in collection of all samples.

LITERATURE CITED

Beck,T.D.I. 1991. Black bears of west-central Colorado. Colorado Division of Wildlife Technical Publication No. 39.

Biberstein, E.L., Jang, S.S., and D.C. Hirsh. 1984. Species distribution of coagulase-positive Staphylococci in animals. Journal of Clinical Microbiology 19: 610-615.

Bornstein, S., T. Morner, and W.M. Samual. 2001. *Sarcoptes scabiei* and sarcoptic mange. Pages 107–119 in W.M. Samual, M.J. Pybus, and A.A. Kocan, editors. Parasitic diseases of wild mammals. Iowa State University, Ames, Iowa, USA.

Burguess, K.I. and J.E. Huffman. 2005. Diseases of Bears. In Wildlife Diseases: Landscape Epidemiology, Spatial Distribution, and Utilization of Remote Sensing Technology S.K Mujumdar, J.E. Huffman, F.J. Brenner, and A.I. Panah (eds.), Pennsylvania Academy of Sciences, Easton, PA, , pp. 298-322.

Campbell, G.A., S.D. Kosanke, D.M. Toth, and G.L. White. 1981. Disseminated staphylococcal infection in a colony of captive ground squirrels (*Citellus lateralis*). Journal of Wildlife Diseases 17: 177-181.

Carr, P.C. and K. Burguess. 2004. Black bear in New Jersey Status Report. New Jersey Division of Fish and Wildlife. Trenton, NJ.

Costello, C.M., K.S. Quigley, D.E. Jones, R.M. Inman, and K.H. Inman. 2006. Observations of a denning-related dermatitis in American black bears. Ursus 17: 186-190.

Crandell R.A., G.A. Huttenhauer, and H.W. Casey. 1971. Staphylococcic dermatitis in mink. Journal of American Veterinary Medical Association 159: 638-639.

Cunningham, M.W., L.A Phillips, and C. Welbourn. 2001. Trombiculiasis in the Florida black bear. Journal of Wildlife Diseases 37: 634-639.

Goatcher, L.J., M.W. Barrett, R.N. Coleman, A.W.L. Hawley, and A.A. Qureshi. 1987. A study of predominant aerobic microflora of black bears (*Ursus americanus*) and grizzly bears (*Ursus arctos*) in northwestern Alberta. Canadian Journal of Microbiology 33: 949-954.

Hájek, V. 1976. *Staphylococcus intermedius*, a new species isolated from animals. International Journal of Systematic Bacteriology 26:401-408.

Hellgren E.C. 1998. Physiology of hibernation in bears. Ursus 10:467–477.

Igimi,v.S., H. Atobe, Y. Tohya, A. Inoue, E.Takahashi, and S. Konishi, 1994. Characterization of the most frequently encountered *Staphylococcus sp.* in cats. Veterinary Microbiology 39:255-260.

Kearns K.S., J. Sleeman, L. Frank, and L. Munson. 2000. Zinc-responsive dermatosis in a red wolf (*Canis rufus*). Journal of Zoo and Wildlife Medicine. 31:255–258.

Keeler, S.P., J.E. Huffman, K.I. Burguess, and P. Carr. 2005. A study of bacterial assemblages of New Jersey black bears (*Ursus americanus*). In Proceedings: 18th Eastern Black Bear Workshop 2005, Florida Fish and Wildlife Conservation Commission, Black Bear Management and Research Program (ed.). Florida Fish and Wildlife Conservation Commission, Black Bear Management and Research Program, Tallahassee, Florida, p. 274.

Phillips, W.E., Jr and W.e. Kloos. 1981. Identification of coagulase-positive *Staphylococcus intermedius* and S*taphylococcus hyicus* subsp. *hyicus* isolates from veterinary clinical specimens. Journal of Clinical Microbiology 14:671–673.

Scott D.W., W.H. Miller, and C.G. Griffin. 2001. Small Animal Dermatology. 6th ed. W. B. Saunders Co., Philadelphia, Pennsylvania.

Sweeney, J.C. and W.G. Gilmartin. 1974. Survey of diseases in free-living California sea lions. Journal of Wildlife Diseases 10: 370-376.